Search for bottom-squark pair production with the ATLAS detector in final states containing Higgs bosons, *b*-jets and missing transverse momentum

Aad, G., Abbott, B., Abbott, D. C., Abdinbov, O., Abed Abud, A., Abeling, K., … Zwalinksi, L.

2019.

Published for SISSA by Springer

Received: August 9, 2019
Revised: October 17, 2019
Accepted: November 17, 2019
Published: December 9, 2019

Search for bottom-squark pair production with the ATLAS detector in final states containing Higgs bosons, b-jets and missing transverse momentum

The ATLAS collaboration

E-mail: atlas.publications@cern.ch

Abstract: The result of a search for the pair production of the lightest supersymmetric partner of the bottom quark ($\tilde{b}_1$) using 139 fb^{-1} of proton-proton data collected at $\sqrt{s} =$ 13 TeV by the ATLAS detector is reported. In the supersymmetric scenarios considered both of the bottom-squarks decay into a b-quark and the second-lightest neutralino, $\tilde{b}_1 \to b + \tilde{\chi}_2^0$. Each $\tilde{\chi}_2^0$ is assumed to subsequently decay with 100% branching ratio into a Higgs boson (h) like the one in the Standard Model and the lightest neutralino: $\tilde{\chi}_2^0 \to h + \tilde{\chi}_1^0$. The $\tilde{\chi}_1^0$ is assumed to be the lightest supersymmetric particle (LSP) and is stable. Two signal mass configurations are targeted: the first has a constant LSP mass of 60 GeV; and the second has a constant mass difference between the $\tilde{\chi}_2^0$ and $\tilde{\chi}_1^0$ of 130 GeV. The final states considered contain no charged leptons, three or more b-jets, and large missing transverse momentum. No significant excess of events over the Standard Model background expectation is observed in any of the signal regions considered. Limits at the 95% confidence level are placed in the supersymmetric models considered, and bottom-squarks with mass up to 1.5 TeV are excluded.

Keywords: Hadron-Hadron scattering (experiments), Supersymmetry

ArXiv ePrint: 1908.03122

https://doi.org/10.1007/JHEP12(2019)060

JHEP12(2019)060

Contents

JHEP12(2019)060

1 Introduction

Supersymmetry (SUSY) [1–6] provides an extension to the Standard Model (SM) that solves the hierarchy problem [7–10] by introducing partners of the known bosons and fermions. In R-parity-conserving models [11], SUSY particles are produced in pairs and the lightest supersymmetric particle (LSP) is stable and provides a candidate for dark matter [12, 13]. The superpartners of the SM bosons (the wino, bino and higgsinos) mix to form the neutralinos ($\tilde{\chi}^0_{1,2,3,4}$) and charginos ($\tilde{\chi}^\pm_{1,2}$) physical states. For a large selection of models, the LSP is the lightest neutralino ($\tilde{\chi}^0_1$). Naturalness considerations suggest that the supersymmetric partners of the third-generation quarks are light [14, 15]. If this is assumed, the lightest bottom-squark ($\tilde{b}_1$) and lightest top-squark ($\tilde{t}_1$) mass eigenstates[1]

[1]The scalar partners of the left-handed and right-handed chiral components of the bottom quark ($\tilde{b}_{\mathrm{L,R}}$) or top quark ($\tilde{t}_{\mathrm{L,R}}$) mix to form mass eigenstates for which $\tilde{b}_1$ and $\tilde{t}_1$ are defined as the lighter of the two states.

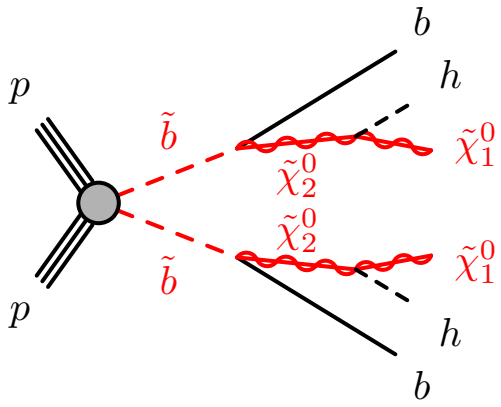

Figure 1. Graphical representation of the SUSY signal targeted by this analysis. Bottom squarks are produced in pairs and subsequently decay into $b\tilde{\chi}_2^0$ with $\mathcal{B} = 100\%$. The two $\tilde{\chi}_2^0$ particles decay into $h\tilde{\chi}_1^0$ also with $\mathcal{B} = 100\%$.

could be significantly lighter than the other squarks and the gluinos. As a consequence, $\tilde{b}_1$ and $\tilde{t}_1$ could be pair-produced with relatively large cross-sections at the Large Hadron Collider (LHC). Depending on the mass hierarchy considered, it is possible that the $\tilde{b}_1$ and $\tilde{t}_1$ could decay into final states with Higgs bosons, h, like the one in the SM, and this allows the Higgs boson to be used as a probe for new physics.

This article presents a search for the pair production of bottom squarks decaying into the LSP via a complex decay chain containing the second-lightest neutralino ($\tilde{\chi}_2^0$) and the Higgs boson: $\tilde{b}_1 \to b + \tilde{\chi}_2^0$ and subsequently $\tilde{\chi}_2^0 \to h + \tilde{\chi}_1^0$. Such a decay hierarchy is predicted in minimal supersymmetric extensions to the SM (MSSM) [16, 17], with h assumed to be the lightest of the neutral bosons introduced in the MSSM. The bottom squark decaying through a next-to-lightest neutralino is one of the possible modes within the MSSM. Dedicated searches for direct decays into the lightest neutralino ($\tilde{b}_1 \to b\tilde{\chi}_1^0$) or a chargino ($\tilde{b}_1 \to t\tilde{\chi}_1^\pm$) have been reported by the ATLAS and CMS collaborations (see for example [18, 19] and [20–22]).

When the LSP is bino-like and the $\tilde{\chi}_2^0$ is a wino-higgsino mixture, the branching ratio ($\mathcal{B}$) of $\tilde{\chi}_2^0 \to h + \tilde{\chi}_1^0$ is enhanced relative to the other possible $\tilde{\chi}_2^0$ decays. The Higgs boson mass is taken to be 125 GeV, and the decay into a pair of bottom quarks is assumed to be the same as in the SM ($\mathcal{B} = 58\%$ [23, 24]), although it could be enhanced or reduced in the MSSM.

This search is interpreted within simplified model scenarios [25, 26] and figure 1 illustrates the targeted model. In the first set of models, already considered by the ATLAS Collaboration using 8 TeV data [27], the mass of the $\tilde{\chi}_1^0$ is fixed at 60 GeV. The bottom-squark and $\tilde{\chi}_2^0$ masses vary in the ranges 250–1600 GeV and 200–1500 GeV, respectively. The assumption about the $\tilde{\chi}_1^0$ mass is motivated by dark-matter relic density measurements and might be favoured in Higgs-pole annihilation scenarios [28] where $m_{\tilde{\chi}_1^0} \simeq m_h/2$. The previous search performed by ATLAS using 8 TeV data excluded bottom-squark masses up to 750 GeV in this scenario [27].

JHEP12(2019)060

The second set of SUSY models assumes a fixed mass difference between the $\tilde{\chi}_2^0$ and $\tilde{\chi}_1^0$, sufficient to produce an on-shell Higgs boson. The mass difference, $\Delta m(\tilde{\chi}_2^0, \tilde{\chi}_1^0)$, is set to 130 GeV, whilst bottom-squark and $\tilde{\chi}_1^0$ masses vary in the ranges 400–1500 GeV and 1–800 GeV, respectively. A similar scenario is considered by the CMS Collaboration in ref. [29], where the $h \to \gamma\gamma$ decay mode is exploited to exclude bottom-squark masses up to 530 GeV; no prior ATLAS searches have targeted these models.

The final states are characterised by a unique signature, which contains many jets, of which up to six can be identified as originating from the fragmentation of b-quarks (referred to as b-jets), missing transverse momentum ($\mathbf{p}_{\mathrm{T}}^{\mathrm{miss}}$, the magnitude thereof referred to as $E_{\mathrm{T}}^{\mathrm{miss}}$), and no charged leptons (referred to as leptons). New selections and dedicated procedures aiming to maximise the efficiency of reconstructing the Higgs boson candidates decaying into a b-quark pair are employed in this article. Section 2 presents a brief overview of the ATLAS detector, with section 3 describing the data and simulated samples used in the analysis. The event reconstruction methods are explained in section 4. An overview of the analysis strategy is presented in section 5, with the background estimation strategy discussed in section 6. The systematic uncertainties considered in the analysis are described in section 7. Section 8 presents the results and interpretation thereof, with the conclusions presented in section 9.

2 ATLAS detector

The ATLAS detector [30] is a multipurpose particle physics detector with a forward-backward symmetric cylindrical geometry and nearly 4π coverage in solid angle.[2] The inner tracking detector consists of pixel and silicon microstrip detectors covering the pseudorapidity region $|\eta| < 2.5$, surrounded by a transition radiation tracker which enhances electron identification in the region $|\eta| < 2.0$. Between Run 1 and Run 2, a new inner pixel layer, the insertable B-layer [31, 32], was added at a mean sensor radius of 3.3 cm. The inner detector is surrounded by a thin superconducting solenoid providing an axial 2 T magnetic field and by a fine-granularity lead/liquid-argon (LAr) electromagnetic calorimeter covering $|\eta| < 3.2$. A steel/scintillator-tile calorimeter provides hadronic coverage in the central pseudorapidity range ($|\eta| < 1.7$). The endcap and forward regions ($1.5 < |\eta| < 4.9$) of the hadronic calorimeter are made of LAr active layers with either copper or tungsten as the absorber material. An extensive muon spectrometer with an air-core toroidal magnet system surrounds the calorimeters. Three layers of high-precision tracking chambers provide coverage in the range $|\eta| < 2.7$, while dedicated fast chambers allow triggering in the

[2] ATLAS uses a right-handed coordinate system with its origin at the nominal interaction point in the centre of the detector. The positive x-axis is defined by the direction from the interaction point to the centre of the LHC ring, with the positive y-axis pointing upwards, while the beam direction defines the z-axis. Cylindrical coordinates (r, ϕ) are used in the transverse plane, ϕ being the azimuthal angle around the z-axis. The component of momentum in the transverse plane is denoted by p_{T}. The pseudorapidity η is defined in terms of the polar angle θ by $\eta = -\ln\tan(\theta/2)$. Rapidity is defined as $y = 0.5\ln[(E+p_z)/(E-p_z)]$ where E denotes the energy, and p_z is the component of the momentum along the beam direction. The separation of two objects in η–ϕ space is given by $\Delta R = \sqrt{(\Delta\eta)^2 + (\Delta\phi)^2}$.

JHEP12(2019)060

region $|\eta| < 2.4$. The ATLAS trigger system consists of a hardware-based level-1 trigger followed by a software-based high-level trigger [33].

3 Data and simulated event samples

The data analysed in this study correspond to a total of 139 fb^{-1} of proton-proton (pp) collision data collected by the ATLAS detector with a centre-of-mass energy of 13 TeV and a 25 ns proton bunch crossing interval in the period between 2015 and 2018. All detector subsystems were required to be operational during data taking. The average number of interactions per bunch crossing (pile-up) increased from $\langle\mu\rangle = 20$ (2015–2016 dataset) to $\langle\mu\rangle = 37$ (2018 dataset), with a highest $\langle\mu\rangle = 38$ (2017 dataset). The uncertainty in the combined 2015–2018 integrated luminosity is 1.7 % [34], obtained using the LUCID-2 detector [35] for the primary luminosity measurements.

Events are required to pass an $E_{\mathrm{T}}^{\mathrm{miss}}$ trigger [36] which is fully efficient for events with reconstructed $E_{\mathrm{T}}^{\mathrm{miss}} > 250$ GeV. Additional single-lepton triggers requiring electrons or muons are used to estimate the SM backgrounds, with an offline selection of $p_{\mathrm{T}}(\ell) > 27$ GeV used to ensure the trigger is fully efficient ($\ell = e, \mu$).

Dedicated Monte Carlo (MC) simulated samples are used to model SM processes and estimate the expected signal yields. All samples were produced using the ATLAS simulation infrastructure [37] and GEANT4 [38], or a faster simulation based on a parameterisation of the calorimeter response and GEANT4 for the other detector systems [37].

The SUSY signal samples were generated with MadGraph5_aMC@NLO v2.6.2 [39] at leading order (LO) and interfaced to PYTHIA v8.230 [40] for the modelling of the parton showering (PS), hadronisation and the underlying event with the A14 [41] set of tuned parameters (tune). The matrix element (ME) calculation was performed at tree level and includes the emission of up to two additional partons. The ME-PS matching was done using the CKKW-L [42] prescription, with a matching scale set to one quarter of the bottom-squark mass. The NNPDF2.3 LO [43] parton distribution function (PDF) set was used. Signal cross-sections were calculated to approximate next-to-next-to-leading order in the strong coupling constant, adding the resummation of soft gluon emission at next-to-next-to-leading-logarithm (approximate NNLO+NNLL) [44–47] accuracy. The nominal cross-section and its uncertainty were derived using the PDF4LHC15_mc PDF set, following the recommendations of ref. [48]. For $\tilde{b}_1$ masses between 400 GeV and 1.5 TeV, the cross-sections range from 2.1 pb to 0.26 fb, with uncertainties from 6% to 17%.

The SM backgrounds considered in this analysis are: $t\bar{t}$ pair production; single-top-quark production; Z + jets; W + jets; $t\bar{t}$ production with an electroweak (ttV) or Higgs (ttH) boson; and diboson production. The samples were simulated using different MC generator programs depending on the process. Pair production of top quarks, $t\bar{t}$, was generated using POWHEG-BOX v2 [49–52] interfaced with PYTHIA v8.230 and the A14 tune with the NNPDF2.3 LO PDF set for the ME calculations. The h_{damp} parameter in POWHEG-BOX, which controls the p_{T} of the first additional emission beyond the Born level and thus regulates the p_{T} of the recoil emission against the $t\bar{t}$ system, was set to 1.5 times the top-quark mass ($m_t = 172.5$ GeV) as a result of studies documented in ref. [53].

JHEP12(2019)060

The generation of single top quarks in the Wt-channel, s-channel and t-channel production modes was performed by POWHEG-BOX v2 [50–52, 54] similarly to the $t\bar{t}$ samples. For all processes involving top quarks, top-quark spin correlations were preserved. All events with at least one leptonically decaying W boson were retained; fully hadronic $t\bar{t}$ and single-top events do not contain sufficient $E_{\mathrm{T}}^{\mathrm{miss}}$ to contribute significantly to the background. The production of $t\bar{t}$ pairs in association with electroweak vector bosons (W, Z) or Higgs bosons was modelled by samples generated at NLO using MadGraph5_aMC@NLO v2.2.3 and showered with PYTHIA v8.212. Events containing W or Z bosons with associated jets, including jets from the fragmentation of heavy-flavour quarks, were simulated using the SHERPA v2.2.1 [55] generator. Matrix elements were calculated for up to two additional partons at NLO and four partons at LO using the Comix [56] and OpenLoops [57] ME generators and were merged with the SHERPA PS [58] using the ME+PS@NLO prescription [59]. The NNPDF3.0 NNLO [43] PDF set was used in conjunction with a dedicated PS tune developed by the SHERPA authors. Diboson processes were also simulated using the SHERPA generator using the NNPDF3.0 NNLO PDF set. They were calculated for up to one (ZZ) or zero (WW, WZ) additional partons at NLO and up to three additional partons at LO. Other potential sources of backgrounds, such as the production of three or four top quarks or three gauge bosons, are found to be negligible. Finally, contributions from multijet background are estimated from data using a jet smearing procedure described in ref. [60] and are found to be negligible in all regions.

All background processes are normalised to the best available theoretical calculation for their respective cross-sections. The NLO $t\bar{t}$ inclusive production cross-section is corrected to the theory prediction at NNLO in QCD including the resummation of NNLL soft-gluon terms calculated using Top++2.0 [61–67]. Samples of single-top events are normalised to the NLO cross-sections reported in refs. [68–70].

For all samples, except those generated using SHERPA, the EvtGen v1.2.0 [71] program was used to simulate the properties of the bottom- and charm-hadron decays. All simulated events include a modelling of contributions from pile-up by overlaying minimum-bias pp interactions from the same (in-time pile-up) and nearby (out-of-time pile-up) bunch crossings simulated in PYTHIA v8.186 and EvtGen v1.2.0 with the A3 [72] tune and the NNPDF2.3 LO set [43].

4 Event reconstruction

This search is based upon a selection of events with many b-jets, large missing transverse momentum and no charged leptons (electrons and muons) in the final state. All events are required to have a reconstructed primary vertex which is consistent with the beamspot envelope and consists of at least two associated tracks in the inner detector with $p_{\mathrm{T}} > 500\,\mathrm{MeV}$. If more than one vertex passing the above requirements is found, the one with the largest sum of the squares of transverse momenta of associated tracks [73] is chosen.

Jet candidates are reconstructed from three-dimensional clusters of energy in the calorimeter [74] with the anti-k_t jet algorithm [75, 76] using a radius parameter of 0.4. The application of a jet energy scale (JES) correction derived from data and simulation [77]

JHEP12(2019)060

is used to calibrate the reconstructed jets. A set of quality criteria is applied to identify jets which arise from non-collision sources or detector noise [78] and any event which contains a jet failing to satisfy these criteria is removed. Additional jets that arise from pile-up interactions are rejected by applying additional track-based selections to jets with $p_{\mathrm{T}} < 120$ GeV and $|\eta| < 2.4$ [79], and the jet momentum is corrected by subtracting the expected average energy contribution from pile-up using the jet area method [80]. Jets are classified as either 'baseline' or 'signal'; baseline jets are required to have $p_{\mathrm{T}} > 20$ GeV and $|\eta| < 4.8$ whilst signal jets are selected after resolving overlaps with electrons and muons, as described below, and must pass tighter requirements of $p_{\mathrm{T}} > 30$ GeV and $|\eta| < 2.8$.

Signal jets are identified as b-jets if they are within $|\eta| < 2.5$ and are tagged by a multivariate algorithm which uses a selection of inputs including information about the impact parameters of inner-detector tracks, the presence of displaced secondary vertices and the reconstructed flight paths of b- and c-hadrons inside the jet [81]. The b-tagging algorithm used has an efficiency of 77%, determined in a sample of simulated $t\bar{t}$ events. It was chosen as part of the optimisation procedure and the corresponding misidentification rate is 20% for c-jets and 0.9% for light-flavour jets. To compensate for differences between data and MC simulation in the b-tagging efficiencies and mis-tag rates, correction factors are derived from data and applied to the samples of simulated events; details are found in ref. [81].

Electron candidates are reconstructed from energy clusters in the electromagnetic calorimeter matched to a track in the inner detector and are required to satisfy a set of 'loose' quality criteria [82]. They are also required to lie within the fiducial volume $|\eta| < 2.47$ and have $p_{\mathrm{T}} > 4.5$ GeV. Muon candidates are reconstructed by matching tracks in the inner detector with tracks in the muon spectrometer. Muon candidates which have a transverse (longitudinal) impact parameter relative to the primary vertex larger than 0.2 mm (1 mm) are rejected to suppress muons from cosmic rays. Muon candidates are also required to satisfy 'medium' quality criteria [83] and have $|\eta| < 2.5$ and $p_{\mathrm{T}} > 4$ GeV. Electron (muon) candidates are matched to the primary vertex by requiring the transverse impact parameter (d_0) to satisfy $|d_0|/\sigma(d_0) < 5$ (3), and the longitudinal impact parameter (z_0) to satisfy $|z_0 \sin\theta| < 0.5$ mm. Lepton candidates remaining after resolving overlaps with baseline jets are called 'baseline' leptons. In the control regions where tighter lepton identification is required, 'signal' leptons are chosen from the baseline set with $p_{\mathrm{T}} > 20$ GeV and are required to be isolated from other activity in the detector using a criterion designed to accept at least 95% of leptons from Z boson decays; details are found in ref. [84]. In the dilepton control region where the single-lepton triggers are used, the leading lepton is required to have $p_{\mathrm{T}} > 27$ GeV; which ensures full efficiency of the single-lepton triggers. Signal electrons are further required to satisfy 'tight' quality criteria [82]. The MC events are corrected to account for differences in the lepton trigger, reconstruction and identification efficiencies between data and MC simulation.

Possible reconstruction ambiguities between baseline electrons, muons and jets are resolved by firstly removing electron candidates which share an inner detector track with a muon candidate. Jet candidates are then removed if they are within $\Delta R = \sqrt{(\Delta y)^2 + (\Delta\phi)^2} = 0.2$ of an electron candidate; next, electron candidates are discarded if they are within $\Delta R = 0.4$ of a jet. Muons are discarded if they lie within $\Delta R = 0.4$ of

JHEP12(2019)060

any remaining jet, except for the case where the number of tracks associated with the jet is less than three, where the muon is kept and the jet is discarded.

Identified τ leptons decaying hadronically are not considered but the following τ-veto procedure is applied to reject events which contain τ-like objects. Candidates (τ_{cand}) are identified as jets which have $|\eta| < 2.5$ and less than five inner detector tracks of $p_{\text{T}} > 500$ MeV. If an event contains a tau candidate with a small azimuthal distance to the $\mathbf{p}_{\text{T}}^{\text{miss}}$ ($\Delta\phi(E_{\text{T}}^{\text{miss}}, \tau_{\text{cand}}) < \pi/3$), then the event is vetoed.

The missing transverse momentum $\mathbf{p}_{\text{T}}^{\text{miss}}$ is defined as the negative vector sum of the p_{T} of all selected and calibrated physics objects (electrons, muons, photons [82] and jets) in the event, with an extra term added to account for soft energy in the event which is not associated with any of the selected objects [85]. This soft term is calculated from inner-detector tracks with p_{T} above 500 MeV matched to the PV, thus ensuring it is robust against pile-up contamination [86, 87].

5 Analysis strategy

Three sets of non-orthogonal signal regions (SRs) are defined to target different mass hierarchies of the SUSY particles involved. These definitions exploit various discriminating observables and algorithms developed to explicitly reconstruct Higgs boson candidates in the decay chain. Events with charged leptons are vetoed in all SRs. Events with one or two charged leptons are used to define control regions (CRs) to aid in the estimation of the main SM backgrounds. Additionally, events with zero charged leptons are utilised to define validation regions (VRs) to ensure the background estimation method, described in section 6, is robust. The optimisation procedure for the event selection aims to maximise the yield of bottom-squark pair production events while reducing SM background contributions. It is performed for the two simplified model scenarios introduced in section 1. Since the $h \to bb$ decay mode is considered, the final state contains a large jet multiplicity, with many of these jets originating from b-quarks, and large $E_{\text{T}}^{\text{miss}}$ from the neutralinos.

The event selection criteria are defined on the basis of kinematic requirements for the objects described in the previous section and the event variables described below. For these definitions, signal jets are used and are ordered according to decreasing p_{T}.

- N_{jets}: the number of signal jets.

- $N_{b\text{-jets}}$: the number of b-jets.

- $\min \Delta\phi(\text{jet}_{1-4}, \mathbf{p}_{\text{T}}^{\text{miss}})$: the minimum azimuthal distance between the four highest-p_{T} jets and the $\mathbf{p}_{\text{T}}^{\text{miss}}$. This is a powerful discriminating variable against multijet background events containing a large amount of $E_{\text{T}}^{\text{miss}}$ due to mismeasured jets. Typically, multijet background events exhibit low values of this variable and studies using data-driven multijet estimates indicate that a selection of $\min \Delta\phi(\text{jet}_{1-4}, \mathbf{p}_{\text{T}}^{\text{miss}}) > 0.4$ is sufficient to reduce the multijet background to a negligible level.

JHEP12(2019)060

- $\Delta\phi(j_1, \mathbf{p}_{\mathrm{T}}^{\mathrm{miss}})$: the azimuthal distance between the highest-p_{T} jet and the $\mathbf{p}_{\mathrm{T}}^{\mathrm{miss}}$. This variable is used to select events where the $\mathbf{p}_{\mathrm{T}}^{\mathrm{miss}}$ is expected to be recoiling against the leading jet.

- m_{eff}: the effective mass [88] of an event is defined as the scalar sum of the p_{T} of all signal jets and the $E_{\mathrm{T}}^{\mathrm{miss}}$, i.e.:

$$m_{\mathrm{eff}} = \sum_{i \leq N_{\mathrm{jets}}} (p_{\mathrm{T}}^{\mathrm{jet}})_i + E_{\mathrm{T}}^{\mathrm{miss}}.$$

- $\mathcal{S}$: referred to as the "object-based $E_{\mathrm{T}}^{\mathrm{miss}}$-significance" [89] is defined as follows:

$$\mathcal{S} = \sqrt{\frac{|\mathbf{p}_{\mathrm{T}}^{\mathrm{miss}}|^2}{\sigma_{\mathrm{L}}^2(1-\rho_{\mathrm{LT}}^2)}}.$$

  The total momentum resolution of all jets and leptons, at a given p_{T} and $|\eta|$, is determined from parameterised Monte Carlo simulation which well reproduces the resolution measured in data. σ_{L} is the total momentum resolution after being rotated into the longitudinal (parallel to the $\mathbf{p}_{\mathrm{T}}^{\mathrm{miss}}$) plane. The quantity ρ_{LT} is a correlation factor between the longitudinal and transverse momentum resolution (again with respect to the $\mathbf{p}_{\mathrm{T}}^{\mathrm{miss}}$) of each jet or lepton. The significance $\mathcal{S}$ is used to discriminate events where the $E_{\mathrm{T}}^{\mathrm{miss}}$ arises from invisible particles in the final state from events where the $E_{\mathrm{T}}^{\mathrm{miss}}$ arises from poorly measured particles (and jets). Additionally, it is useful in discriminating between signal events with large $E_{\mathrm{T}}^{\mathrm{miss}}$ and Z+jets events with medium-to-low $E_{\mathrm{T}}^{\mathrm{miss}}$.

Additional selections on the p_{T} of the leading jet and of the leading b-jet are also applied as detailed in the following subsections. In all signal regions, events containing baseline leptons with $p_{\mathrm{T}} > 10$ GeV are vetoed, as well as events containing τ-lepton candidates that align with the $\mathbf{p}_{\mathrm{T}}^{\mathrm{miss}}$ within $\Delta\phi = \pi/3$. Only events with $E_{\mathrm{T}}^{\mathrm{miss}} > 250$ GeV are retained to ensure full efficiency of the trigger.

The event kinematics targeted by the three SRs are depicted in figure 2. The first signal region is SRA, designed to target the 'bulk' region of both signal models, with moderate- to high-mass splitting between the $\tilde{b}_1$ and $\tilde{\chi}_2^0$. In these scenarios all of the b-jets, from both the bottom-squark and Higgs boson decays, are at a relatively high p_{T} and can be resolved in the detector. The b-jets from the Higgs boson can be isolated by removing the ones most likely from the bottom-squark decays and checking the angular separation between the remaining b-jets.

The second region, SRB, is designed to target the phase space of the $\Delta m(\tilde{\chi}_2^0, \tilde{\chi}_1^0) = 130\,\mathrm{GeV}$ scenario with a small mass splitting between the $\tilde{b}_1$ and $\tilde{\chi}_2^0$, referred to as the "compressed" region. An initial-state radiation (ISR)-like selection is used where the small mass splitting between the bottom squark and neutralino leads to relatively soft b-jets from the bottom squark decay, which are difficult to reconstruct. In this scenario it is possible to reconstruct both Higgs bosons using angular separation methods. Finally, SRC is designed

JHEP12(2019)060

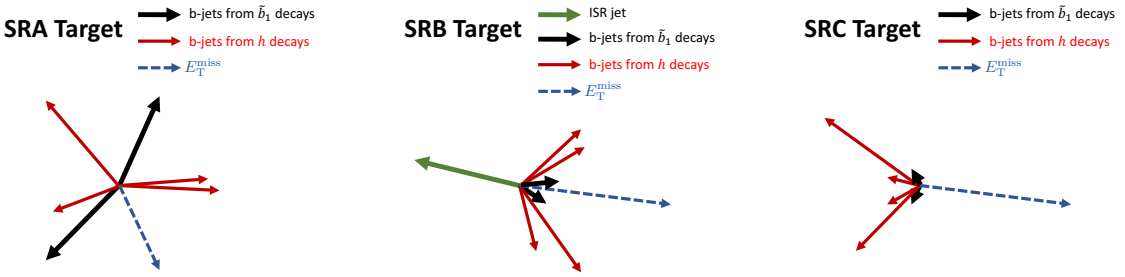

(a) SRA. **(b)** SRB. **(c)** SRC.

Figure 2. The different event kinematics, in the transverse plane, targeted by the three SRs: (a) kinematics in the bulk region, with high-p_{T} b-jets arising from the bottom-squark decay; (b) kinematics in the compressed region of the $\Delta m(\tilde{\chi}_2^0, \tilde{\chi}_1^0) = 130$ GeV scenario with soft b-jets from the bottom squark; (c) kinematics in the compressed region of the $m(\tilde{\chi}_1^0) = 60$ GeV scenario which also contains soft b-jets from the bottom squark.

to target the "compressed" region of the $m(\tilde{\chi}_1^0) = 60\,\mathrm{GeV}$ signal scenario, where the mass splitting between the $\tilde{b}_1$ and $\tilde{\chi}_2^0$ is small. The b-jets from the bottom squark decay are very soft and as such a lower b-jet multiplicity is used in this region, when compared to the A- and B-type selections. Additionally, the visible system (b-jets from the bottom squark decay and Higgs boson decay) is produced back-to-back with the reconstructed $\mathbf{p}_{\mathrm{T}}^{\mathrm{miss}}$.

5.1 The SRA selections

To exploit the kinematic properties of the signal over a large range of $\tilde{b}_1$, $\tilde{\chi}_2^0$ and $\tilde{\chi}_1^0$ masses, incremental thresholds are imposed on the main discriminating variable, m_{eff}, resulting in three mutually exclusive regions, $1.0 < m_{\mathrm{eff}} < 1.5$ TeV, $1.5 < m_{\mathrm{eff}} < 2.0$ TeV and $m_{\mathrm{eff}} > 2.0$ TeV. These are labelled as SRA-L, -M and -H, respectively, to maximise coverage across the $\tilde{b}_1$ mass range. The selection criteria for the three SRAs are summarised in table 1.

At least four b-tagged jets are required. To discriminate against multijet background, events where the $\mathbf{p}_{\mathrm{T}}^{\mathrm{miss}}$ is aligned with a jet in the transverse plane are rejected by requiring $\min \Delta\phi(\mathrm{jet}_{1-4}, \mathbf{p}_{\mathrm{T}}^{\mathrm{miss}}) > 0.4$. As a large $E_{\mathrm{T}}^{\mathrm{miss}}$ is expected from the neutralinos which escape the detector, a selection of $E_{\mathrm{T}}^{\mathrm{miss}} > 350$ GeV is used. Additionally, the leading b-jet (b_1) is expected to have a large p_{T}, hence a selection of $p_{\mathrm{T}}(b_1) > 200$ GeV is employed. At least one of the two Higgs boson candidates in the event is identified using a reconstruction algorithm referred to as *max-min*, which is a two-step procedure to remove the high-p_{T} b-jets from the bottom squark decay and then use the remaining b-jets to reconstruct a Higgs boson in the decay chain. The procedure is implemented as follows: first, pairs of b-jets are formed by iterating through all of the b-jets in the event, and the pair with the largest separation in ΔR is designated as arising from the bottom-squark decay and removed from the subsequent step; second, the pair with the smallest ΔR is identified as a

JHEP12(2019)060

Variable	SRA	SRA-L	SRA-M	SRA-H
N_{leptons} (baseline)	$= 0$		$= 0$	
N_{jets}	≥ 6		≥ 6	
$N_{b\text{-jets}}$	≥ 4		≥ 4	
$E_{\text{T}}^{\text{miss}}$ [GeV]	> 350		> 350	
$\min \Delta\phi(\text{jet}_{1-4}, \mathbf{p}_{\text{T}}^{\text{miss}})$ [rad]	> 0.4		> 0.4	
τ veto	Yes		Yes	
$p_{\text{T}}(b_1)$ [GeV]	> 200		> 200	
$\Delta R_{\text{max}}(b, b)$	> 2.5		> 2.5	
$\Delta R_{\text{max-min}}(b, b)$	< 2.5		< 2.5	
$m(h_{\text{cand}})$ [GeV]	> 80		> 80	
m_{eff} [TeV]	> 1.0	$\in [1.0, 1.5]$	$\in [1.5, 2.0]$	> 2.0

Table 1. Definitions for the SRA, alongside the three varying m_{eff} intervals used. The letter appended to the SRA label corresponds to the low (-L), medium (-M) or high (-H) m_{eff} selection. This selection is sensitive to the bulk regions of both signal scenarios. The jets and b-jets are ordered by p_{T}.

possible Higgs boson candidate and its invariant mass calculated. The following ΔR and mass quantities are defined:

- $\Delta R_{\text{max}}(b, b)$: the distance in η–ϕ between the two b-jets with the maximal angular separation which are most likely to originate from the initial decay of the $\tilde{b}_1$;
- $\Delta R_{\text{max-min}}(b, b)$: the distance in η–ϕ between the two b-jets with the minimum angular separation which are most likely to originate from the same Higgs boson decay, selected out of the remaining b-jets;
- $m(h_{\text{cand}})$: the invariant mass of the b-jet pair identified as a Higgs candidate by the *max-min* algorithm. A lower bound on $m(h_{\text{cand}})$ is used; in the majority of events the distribution peaks around the Higgs boson mass, but in scenarios where the incorrect combination of b-jets is chosen the signal can extend to higher masses.

When applied to signal, the *max-min* algorithm correctly selects a $h \to bb$ pairing in 20%–40% of cases for a single Higgs boson decay, depending upon the model. For a signal model corresponding to $m(\tilde{b}_1, \tilde{\chi}_2^0, \tilde{\chi}_1^0) = (1100, 330, 200)$ GeV, about 3% of the simulated signal events are retained by the SRA selections.

5.2 The SRB selections

The SRB region targets small mass-splitting between the $\tilde{b}_1$and $\tilde{\chi}_2^0$ (of order 5–20 GeV), in the case of the $\Delta m(\tilde{\chi}_2^0, \tilde{\chi}_1^0) = 130$ GeV scenarios. The presence of an ISR jet boosting the bottom squarks, and consequently their decay products, is exploited. To efficiently

JHEP12(2019)060

Variable	SRB
N_{leptons} (baseline)	$= 0$
N_{jets}	≥ 5
$N_{b\text{-jets}}$	≥ 4
$E_{\text{T}}^{\text{miss}}$ [GeV]	> 350
$\min \Delta\phi(\text{jet}_{1-4}, \mathbf{p}_{\text{T}}^{\text{miss}})$ [rad]	> 0.4
τ veto	Yes
$m(h_{\text{cand1}}, h_{\text{cand2}})_{\text{avg}}$ [GeV]	$\in [75, 175]$
Leading jet not b-tagged	Yes
$p_{\text{T}}(j_1)$ [GeV]	> 350
$\lvert\Delta\phi(j_1, E_{\text{T}}^{\text{miss}})\rvert$ [rad]	> 2.8
m_{eff} [TeV]	> 1

Table 2. Definitions for SRB, targeting the compressed region of the $\Delta m(\tilde{\chi}_2^0, \tilde{\chi}_1^0) = 130$ GeV scenario. The jets and b-jets are ordered by p_{T}.

suppress SM background contributions, events are selected where the highest-p_{T} jet is not b-tagged and has $p_{\text{T}} > 350$ GeV; this jet is presumed to arise from ISR in the scenario under consideration. Additional selections of $E_{\text{T}}^{\text{miss}} > 350$ GeV and $\Delta\phi(j_1, E_{\text{T}}^{\text{miss}}) > 2.8$ are applied. An m_{eff} selection of > 1 TeV is also applied. The soft p_{T} spectrum predicted for b-jets from $\tilde{b}_1$decays can cause the b-jets to be difficult to reconstruct, hence a different algorithm, aiming to reconstruct both Higgs boson candidates, is employed.

Differently from the scenarios targeted by SRA, pairs of b-jets with the largest ΔR are found to be more likely to arise from the decay of the same Higgs boson candidate. Two pairs at a time are identified following an iterative procedure, such that at first the pair of b-jets leading to the highest ΔR, ΔR_{bb1}, is defined, followed by the second highest ΔR, ΔR_{bb2}, built considering only the remaining b-jets. The average mass of the two candidates $m(h_{\text{cand1}}, h_{\text{cand2}})_{\text{avg}}$ is calculated and a requirement is placed on the average mass, corresponding to a window around the Higgs boson mass: [75, 175] GeV. For a signal model corresponding to $m(\tilde{b}_1, \tilde{\chi}_2^0, \tilde{\chi}_1^0) = (700, 680, 550)$ GeV, about 0.1% of the simulated signal events are retained by the SRB selections. The efficiency of correctly selecting the b-jets using this algorithm is in the range 15%–30%. The SRB requirements are listed in table 2.

5.3 The SRC selections

When considering the scenario with a constant $\tilde{\chi}_1^0$ mass of 60 GeV, the ΔR-based Higgs boson reconstruction algorithms are ineffective in the compressed region of phase space with a small mass splitting between the $\tilde{b}_1$ and $\tilde{\chi}_2^0$. In the inclusive SRC, the main discriminating quantity is $\mathcal{S}$; a selection of $\mathcal{S} > 22$ is employed. Events are also required to have at least three b-jets. Four non-overlapping regions (SRC22, SRC24, SRC26 and SRC28) are defined as subsets of the inclusive SRC region, with incremental thresholds placed on $\mathcal{S}$ as detailed

JHEP12(2019)060

Variable	SRC	SRC22	SRC24	SRC26	SRC28
N_{leptons} (baseline)	$= 0$	$= 0$			
N_{jets}	≥ 4	≥ 4			
$N_{b\text{-jets}}$	≥ 3	≥ 3			
$E_{\text{T}}^{\text{miss}}$ [GeV]	> 250	> 250			
$\min \Delta\phi(\text{jet}_{1-4}, \mathbf{p}_{\text{T}}^{\text{miss}})$ [rad]	> 0.4	> 0.4			
$\mathcal{S}$	> 22	$\in [22, 24]$	$\in [24, 26]$	$\in [26, 28]$	> 28

Table 3. Definitions for SRC, alongside the four varying $\mathcal{S}$ intervals used. The letter appended to the SRC label corresponds to the lower bound on the $\mathcal{S}$ interval. SRC targets small mass splittings between the $\tilde{b}_1$ and $\tilde{\chi}_2^0$, in the $m(\tilde{\chi}_1^0) = 60$ GeV signal scenario. The jets and b-jets are ordered by p_{T}.

in table 3, to ensure full coverage of the target models as a function of bottom-squark and neutralino mass. For a signal model corresponding to $m(\tilde{b}_1, \tilde{\chi}_2^0, \tilde{\chi}_1^0) = (1200, 1150, 60)$ GeV, about 11% of the simulated signal events are retained by the SRC selections. The $\mathcal{S}$ variable is effective in rejecting the SM background arising from associated production of a Z boson decaying into neutrinos and b-jets.

6 Background estimation

There are two main SM backgrounds which are expected to contribute to the yields for the SRs introduced in the previous section. For SRAs and SRB, the main background is top-quark production which, according to MC estimates, contributes between 70% and 85% of the total background, depending upon the region considered, and is dominated by top-quark pairs produced in association with two b-quarks arising from gluon splitting. In the SRCs, the main backgrounds arise from Z+jets (up to 50% of the total) and from top-quark-related processes (up to 20% of the total).

The main SM backgrounds in each SR are determined separately with a profile likelihood fit to the event yields in the associated CRs [90]. This is commonly referred to as a background-only fit which constrains and adjusts the normalisation of the background processes. The background-only fit uses the observed event yield and the expected number of MC events in the associated CRs, which are described by Poisson statistics, as a constraint to adjust the normalisation of the background processes assuming that no signal is present.

The normalisation factor is referred to as the μ factor. The CRs are designed to be enriched in specific background contributions relevant to the analysis, whilst minimising the potential signal contamination, and they are orthogonal to the SRs.

When performing the fit for SRA, a multi-bin approach is used, with a single CR divided into three bins of m_{eff}. Such an approach allows the calculation and use of a single normalisation parameter (applied to the main $t\bar{t}$ background across all bins of m_{eff}), and additionally enables the fit to take into account the modelling of the m_{eff} variable.

JHEP12(2019)060

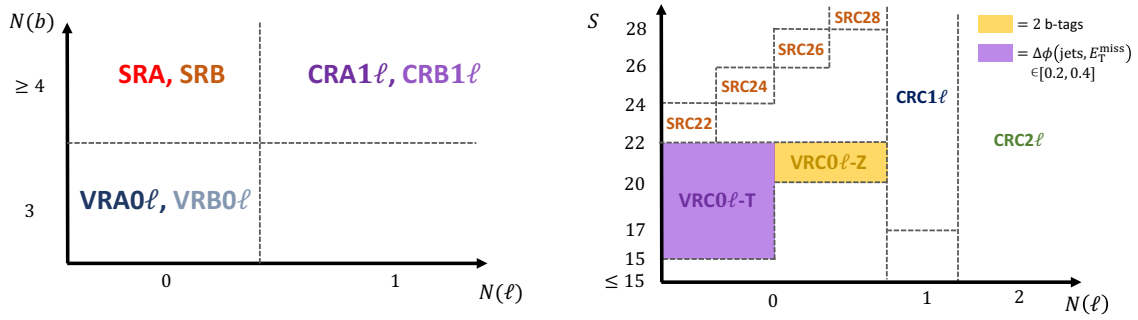

(a) (b)

Figure 3. Schematic diagrams of the fit strategies for (a) the A-, B- and (b) C-type regions. Generally the CRs require a different lepton multiplicity than the SRs. The validation regions are defined with a lower b-jet multiplicity requirement, except in the case of the VRC0ℓ-T region, which instead inverts the SR $\min\Delta\phi(\text{jet}_{1-4}, \mathbf{p}_{\text{T}}^{\text{miss}})$ selection.

The systematic uncertainties, described in section 7, are included in the fit as nuisance parameters. They are constrained by Gaussian distributions with widths corresponding to the sizes of the uncertainties and are treated as correlated, when appropriate, between the various regions. The product of the various probability density functions and the Gaussian distributions forms the likelihood function, which the fit maximises by adjusting the background normalisation and the nuisance parameters. This approach reduces the influence of systematic uncertainties on the backgrounds with dedicated CRs, as these are absorbed by the normalisation parameter.

Finally, the reliability of the MC extrapolation of the SM background estimates outside of the CRs is evaluated in dedicated VRs, orthogonal to CRs and SRs.

The fit strategies for the A- and B-type regions are very similar and are represented schematically in figure 3a. They rely on CRs with a single-lepton requirement, as the $t\bar{t}$ background in the SR is dominated by semileptonic $t\bar{t}$ decays where the lepton is not identified. The main background in both regions is $t\bar{t}$ pair production in association with heavy-flavour jets. The fit strategy for the C-type regions is presented in figure 3b. The strategy is different because the main background in these regions is Z+jets, closely followed by the top-quark backgrounds. In order to define CRs enhanced in $t\bar{t}$ and Z+jets, additional variables are used:

- m_{T}: the event transverse mass m_{T} is defined as $m_{\text{T}} = \sqrt{2p_{\text{T}}(\ell)E_{\text{T}}^{\text{miss}}(1-\cos(\Delta\phi))}$, where $\Delta\phi$ is the difference in azimuthal angle between the lepton and the $\mathbf{p}_{\text{T}}^{\text{miss}}$. This is used in the one-lepton CRs to reject multi-jet events which can be misidentified as containing a prompt lepton.

- $m_{\ell\ell}$: the invariant mass of the two leptons in the event. Since the two-lepton CR is used to constrain the Z+jets background, the $m_{\ell\ell}$ variable is required to be within the Z-mass window: [86, 106] GeV (used exclusively in the two-lepton CR).

JHEP12(2019)060

- $\tilde{E}_{\mathrm{T}}^{\mathrm{miss}}$: the 'lepton corrected' $E_{\mathrm{T}}^{\mathrm{miss}}$. For the two-lepton CR the transverse momentum vectors of the leptons are subtracted from the $E_{\mathrm{T}}^{\mathrm{miss}}$ calculation in order to mimic the neutrinos from $Z \to \nu\nu$ decays (used exclusively in the two-lepton CR).

When designing the CRs and VRs, the potential signal contamination is checked in each region to ensure that the contribution from the signal process being targeted is small in the regions. The signal contamination in the CRs and VRs is found to be negligible, at the level of $< 1\%$ of the total SM expectation, depending upon the signal mass hierarchy of the models considered in this search.

6.1 A-type CR and VR definitions

A single, $t\bar{t}$-dominated CR (CRA1ℓ) is defined for the A-type regions and is split into the same three identical m_{eff} selections as the SRAs. The CR is defined similarly to the SR selection (as documented in table 1); however, exactly one signal lepton (either e or μ) with $p_{\mathrm{T}} > 20$ GeV is required in the final state. Furthermore, the selections used to isolate the Higgs boson in the SRAs, namely the $\Delta R_{\mathrm{max}}(b,b)$, $\Delta R_{\text{max-min}}(b,b)$ and $m(h_{\mathrm{cand}})$ selections, are not applied in order to increase the number of events in the CR. The leading b-jet p_{T} selection is lowered to > 100 GeV to further increase the number of events in the region, and a selection on the transverse mass of $m_{\mathrm{T}} > 20$ GeV is applied to suppress misidentified leptons. Such selections result in pure $t\bar{t}$ CRs, with $t\bar{t}$ contributing more than 80% of the total SM contribution in each of the CRs. The fraction of top-quark pairs produced in association with b-quarks is equivalent between CRs and SRs, and accounts for about 70% of the total $t\bar{t}$ background. Figure 4a presents the distribution of $m(h_{\mathrm{cand}})$ in CRA1ℓ, and shows that this variable is well modelled.

A zero-lepton validation region (VRA0ℓ) is also defined, and split according to the same m_{eff} thresholds as the SRAs and CRAs. This VR is used to validate the modelling of the $t\bar{t}$ background when extrapolating from the one-lepton CRs to zero-lepton regions. The selections are based upon the SR selections but the VRs are orthogonal due to the b-jet multiplicity selection, which requires exactly three b-jets. Additionally, the $\Delta R_{\mathrm{max}}(b,b)$, $\Delta R_{\text{max-min}}(b,b)$ and $m(h_{\mathrm{cand}})$ selections are not applied in this region. A selection of $\mathcal{S} < 22$ is applied to ensure this region is orthogonal to the SRC regions.

6.2 B-type CR and VR definitions

For the B-type $t\bar{t}$ CR (CRB1ℓ), a similar method of using a one-lepton region enriched in $t\bar{t}$ is implemented. The SR selections (as documented in table 2) are applied, and additionally exactly one signal lepton with $p_{\mathrm{T}} > 20$ GeV is required. The $m(h_{\mathrm{cand1}}, h_{\mathrm{cand2}})_{\mathrm{avg}}$ selection is dropped to increase the number of events in the region, and the $|\Delta\phi(j_1, E_{\mathrm{T}}^{\mathrm{miss}})|$ selection is loosened to > 2.2. Similarly to the A-type CR, a selection of $m_{\mathrm{T}} > 20$ GeV is applied to suppress misidentified leptons. These selections result in a pure CR with 80% of the total expected SM background consisting of $t\bar{t}$. Figure 4b presents the $m(h_{\mathrm{cand1}}, h_{\mathrm{cand2}})_{\mathrm{avg}}$ distribution in this region; it is shown to be well modelled.

The associated VR (VRB0ℓ) is defined in a similar manner to the A-type VR, with selections similar to those of the SRB region, but an exclusive b-jet multiplicity selection

JHEP12(2019)060

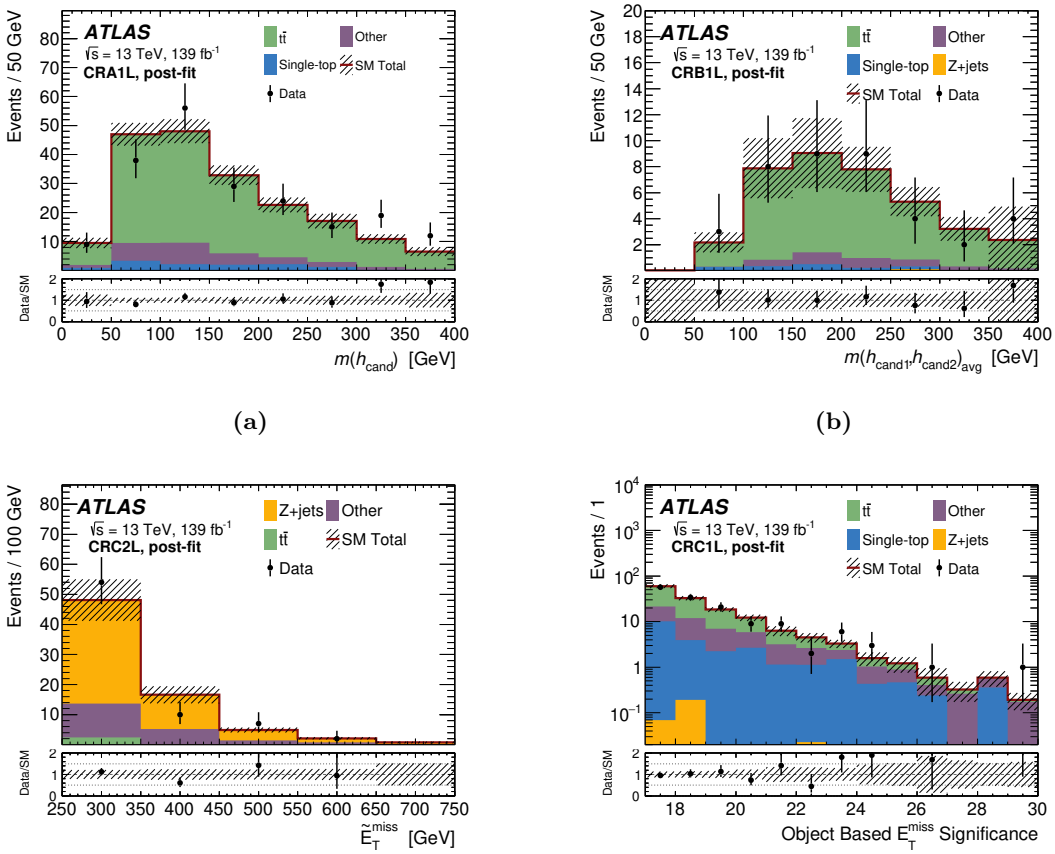

Figure 4. Distributions of (a) $m(h_{\text{cand}})$ in CRA1ℓ, (b) $m(h_{\text{cand1}}, h_{\text{cand2}})_{\text{avg}}$ in CRB1ℓ, (c) $\tilde{E}_{\text{T}}^{\text{miss}}$ in CRC2ℓ, and (d) $\mathcal{S}$ in CRC1ℓ after the background-only fit; ratios of data to SM predictions are reported in the bottom panels. All uncertainties as defined in section 7 are included in the uncertainty bands of the top and bottom panels in each plot. The backgrounds which contribute only a small amount (diboson, W+jets and $t\bar{t}$ +$W/Z/h$) are grouped and labelled as 'Other'. Overflow events which do not fall into the axis range are placed into the rightmost bin.

of exactly three b-jets. Additionally, the selections used to reconstruct the Higgs bosons in the event are dropped to enhance the number of events in the region. A selection of $\mathcal{S} < 22$ is also applied to ensure this region is orthogonal to the C-type SRs.

6.3 C-type CR and VR definitions

Two CRs are defined for the C-type SRs, one to constrain the Z+jets background (CRC2ℓ) and one to constrain the backgrounds associated with top quarks, $t\bar{t}$ and single top (CRC1ℓ). A single normalisation parameter is used to constrain both the $t\bar{t}$ and single-top backgrounds, while the Z+jets background is constrained with an additional normalisation parameter. These CRs are based upon the SR shown in table 3, but are orthogonal due to the different lepton multiplicities required.

JHEP12(2019)060

The CRC2ℓ requires two same-flavour (SF) opposite-sign (OS) leptons, with invariant mass in the Z-mass window. The leading two leptons are required to have $p_{\mathrm{T}} > 27$ GeV and $p_{\mathrm{T}} > 20$ GeV respectively. To imitate the $E_{\mathrm{T}}^{\mathrm{miss}}$ selection in the SR, a selection of $\tilde{E}_{\mathrm{T}}^{\mathrm{miss}} > 250$ GeV is utilised. For this region the selections on $\mathcal{S}$ are dropped to enhance the number of events in the region. Figure 4c shows the $\tilde{E}_{\mathrm{T}}^{\mathrm{miss}}$ distribution in this region. The CRC1ℓ region used to constrain the top-quark-related backgrounds requires one signal lepton with $p_{\mathrm{T}} > 20$ GeV. A selection of $\mathcal{S} > 17$ is applied. Similarly to the A- and B-type CRs, a selection of $m_{\mathrm{T}} > 20$ GeV is applied to remove the multi-jet contribution with fake or non-prompt leptons. Figure 4d presents the $\mathcal{S}$ distribution in this region.

Two zero-lepton VRs are defined to validate the extrapolation from CR to SR based on the SR selections. A VR with zero leptons and two b-jets (VRC0ℓ-Z) with $\mathcal{S} \in [20, 22]$ and $E_{\mathrm{T}}^{\mathrm{miss}} \in [250, 600]$ GeV ensures a region orthogonal to the SR, but with a large contribution from the Z+jets process. A second VR is used to validate the modelling of the $t\bar{t}$ and single-top backgrounds (VRC0ℓ-T); a selection of zero leptons, $\mathcal{S} \in [15, 22]$ and an inverted selection on the $\min \Delta\phi(\mathrm{jet}_{1-4}, \mathbf{p}_{\mathrm{T}}^{\mathrm{miss}}) \in [0.2, 0.4]$ is applied to ensure orthogonality.

6.4 Summary of CR and VR results

A full overview of the control and validation regions used in the analysis can be found in table 4. The control region pre-fit yields and fitted normalisation factors μ_{bkg} for the A-, B- and C-type regions are presented in figure 5a. All μ values are consistent with unity, within 2σ of the normalisation uncertainty, suggesting the modelling of the key SM background processes is already good before performing the fit. Figure 5b presents the observed yields, post-fit background estimates and significance [91] for the A-, B- and C-type validation regions. The background-only fit estimates are in good agreement with the data in these regions, and the post-fit expectation is within 1σ of the central value for all regions.

JHEP12(2019)060

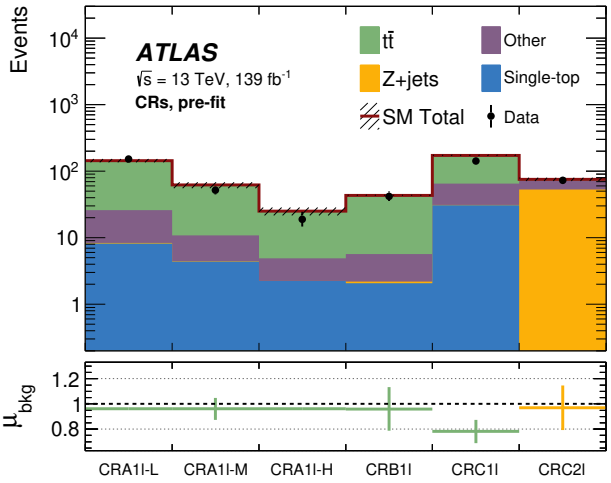

(a)

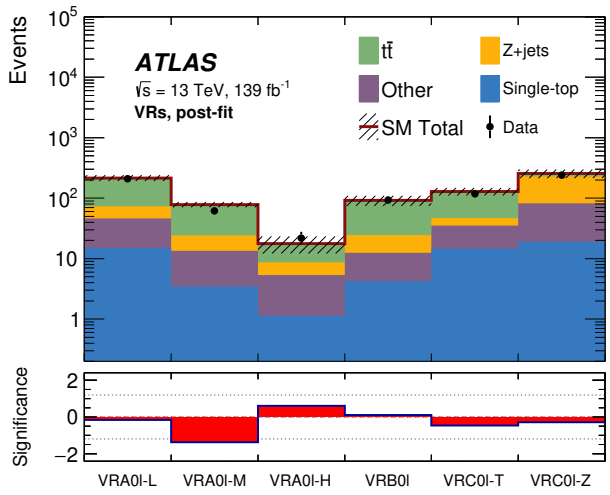

(b)

Figure 5. (a) Control region event pre-fit event yields compared with SM MC predictions (top) and post-fit μ scale factors (bottom) for the A-, B- and C-type regions. The uncertainty in the μ factors and the total expected yield include statistical and systematic uncertainties as introduced in section 7. For the A-type regions, since the fit is performed in the m_{eff} intervals, the normalisation is applied to all bins equally. (b) Results of the background-only fit extrapolated to VRs for the A-, B- and C-type regions. The normalisation of the backgrounds is obtained from the fit to the CRs. The upper panel shows the observed number of events and the predicted background yields. Statistical and systematic uncertainties as introduced in section 7 are included in the uncertainty band. The lower panel shows the significance in each VR. The significance calculation is performed as described in ref. [91]. The minor backgrounds (diboson, W+jets and $t\bar{t}$ +$W/Z/h$) are grouped and labelled as 'Other'.

JHEP12(2019)060

		Control Regions				Validation Regions			
Variable	Units	CRA1ℓ	CRB1ℓ	CRC1ℓ	CRC2ℓ	VRA0ℓ	VRB0ℓ	VRC0ℓ-T	VRC0ℓ-Z
$E_{\mathrm{T}}^{\mathrm{miss}}$ Trigger		✓	✓	✓	—	✓	✓	✓	✓
Lepton Trigger		—	—	—	✓	—	—	—	—
$E_{\mathrm{T}}^{\mathrm{miss}}$	[GeV]	> 250	> 300	> 250	< 70	> 350	> 350	> 250	$\in [250, 600]$
$\min[\Delta\phi(\mathrm{jet}_{1-4}, E_{\mathrm{T}}^{\mathrm{miss}})]$	[rad]	—	—	—	> 0.2	> 0.4	> 0.4	$\in [0.2, 0.4]$	> 1.2
N_{leptons} (baseline)		$= 1$	$= 1$	$= 1$	$= 2$	$= 0$	$= 0$	$= 0$	$= 0$
N_{leptons} (signal)		$= 1$	$= 1$	$= 1$	$= 2$(SFOS)	—	—	—	—
$p_{\mathrm{T}}(\ell_1)$	[GeV]	> 20	> 20	> 20	> 27	—	—	—	—
$p_{\mathrm{T}}(\ell_2)$	[GeV]	—	—	—	> 20	—	—	—	—
m_{T}	[GeV]	> 20	> 20	> 20	—	—	—	—	—
$m_{\ell\ell}$	[GeV]	—	—	—	$\in [86, 106]$	—	—	—	—
τ veto		—	✓	—	—	✓	✓	—	—
N_{jets}		≥ 6	≥ 4	≥ 4	≥ 4	≥ 6	≥ 4	≥ 4	≥ 4
$N_{b\text{-jets}}$		≥ 4	≥ 4	≥ 3	≥ 3	$= 3$	$= 3$	≥ 3	$= 2$
$p_{\mathrm{T}}(b_1)$	[GeV]	> 100	—	—	—	> 100	—	—	—
$p_{\mathrm{T}}(j_1)$	[GeV]	—	> 350	—	—	—	> 350	—	—
Leading jet not b-tagged		—	✓	—	—	—	✓	—	—
$\lvert\Delta\phi(j_1, E_{\mathrm{T}}^{\mathrm{miss}})\rvert$	[rad]	—	> 2.2	—	—	—	> 2.8	—	—
$\tilde{E}_{\mathrm{T}}^{\mathrm{miss}}$	[GeV]	—	—	—	> 250	—	—	—	—
$\mathcal{S}$		—	—	> 17	—	< 22	< 22	$\in [15, 22]$	$\in [20, 22]$
m_{eff}	[TeV]	> 1.0	> 1.0	—	—	> 1.0	> 1.0	—	—

Table 4. Summary of all control and validation region definitions used in the analysis.

7 Systematic uncertainties

Several sources of experimental and theoretical systematic uncertainty on the signal and background estimates are considered in this analysis. Their impact is reduced by fitting the event yields and normalising the dominant backgrounds in the CRs defined with kinematic selections resembling those of the corresponding SRs (see section 6). Uncertainties due to the numbers of events in the CRs are also introduced in the fit for each region. The magnitude of the contributions arising from detector, theoretical modelling and statistical uncertainties are summarized in table 5.

Dominant detector-related systematic uncertainties arise from the b-tagging efficiency and mis-tagging rates, and from the jet energy scale and resolution. In SRA and SRB, the contributions of these uncertainties are almost equivalent. In SRC, the b-tagging uncertainty is dominant. The systematic uncertainty on the b-tagging efficiency ranges from 4.5% for b-jets with $p_{\mathrm{T}} \in [35, 40]$ GeV up to 7.5% for b-jets with high p_{T} (> 100 GeV). The b-tagging uncertainty is estimated by varying the η-, p_{T}- and flavour-dependent scale factors applied to each jet in the simulation within a range that reflects the systematic uncertainty in the measured tagging efficiency and mis-tag rates in data [81]. The uncertainties in the jet energy scale and resolution are based on their respective measurements in data [77, 92].

The uncertainties associated with lepton reconstruction and energy measurements have a negligible impact on the final results; however, the lepton, photon and jet-related uncertainties are propagated to the calculation of the $E_{\mathrm{T}}^{\mathrm{miss}}$, and additional uncertainties due to the energy scale and resolution of the soft term are included in the $E_{\mathrm{T}}^{\mathrm{miss}}$.

The systematic uncertainties related to the modelling of the energy of jets and leptons in the simulation are propagated to $\mathcal{S}$. No additional uncertainty on the energy resolution is applied, as the resolutions are taken to be the maximum of the parameterised data and simulation resolutions when performing the calculation for both data and MC simulation.

Uncertainties in the modelling of the SM background processes from MC simulation and their theoretical cross-section uncertainties are also taken into account. The dominant uncertainties in SRA and SRB arise from theoretical and modelling uncertainties of the $t\bar{t}$ background. They are computed as the difference between the predictions from nominal samples and those from additional samples differing in hard-scattering generator and parameter settings, or by using internal weights assigned to the events depending on the choice of renormalisation and factorisation scales, initial- and final-state radiation parameters, and PDF sets. The impact of the PS and hadronisation model is evaluated by comparing the nominal generator with a POWHEG sample interfaced to HERWIG 7 [93, 94], using the H7UE set of tuned parameters [94]. To assess the uncertainty due to the choice of hard-scattering generator and matching scheme, an alternative generator setup using aMC@NLO+PYTHIA8 is employed. It uses the shower starting scale, $\mu_{\mathrm{q}} = H_{\mathrm{T}}/2$, where H_{T} is defined here as the scalar sum of the p_{T} of all outgoing partons.

The dominant uncertainties in SRC arise from the MC modelling of the Z+jets process, followed by the $t\bar{t}$ and single-top modelling. The Z+jets (as well as W+jets) modelling uncertainties are estimated by considering different merging (CKKW-L) and resummation scales using alternative samples, PDF variations from the NNPDF3.0 NNLO replicas [55], and

JHEP12(2019)060

Region	SRA		SRB		SRC	
Total background expectation	17.1		3.3		37.9	
Total background uncertainty	2.8	(16%)	0.9	(27%)	6.2	(16%)
Systematic, experimental	1.4	(8%)	0.3	(10%)	3.0	(8%)
Systematic, theoretical	2.3	(13%)	0.6	(18%)	3.2	(8%)
Statistical, MC samples	0.7	(4%)	0.4	(12%)	2.0	(5%)

Table 5. Expected background event yields and dominant systematic uncertainties on background estimates in the A-type (inclusive), B-type and C-type (inclusive) regions. Individual uncertainties can be correlated, and do not necessarily add up quadratically to the total background uncertainty. The percentages show the size of the uncertainty relative to the total expected background.

variations of factorisation and renormalisation scales in the ME. The latter have been evaluated using 7 point-variations, changing the renormalisation and factorisation scales up and down by factors 0.5 and 2, such that when one scale is up the other is down, and vice-versa.

For the SUSY signal processes, both the experimental and theoretical uncertainties in the expected signal yield are considered. Experimental uncertainties are found to be 6–36% across the mass plane with fixed LSP mass for A-type SRs, and 4–40% for C-type SRs. For models where $\Delta m(\tilde{\chi}_2^0, \tilde{\chi}_1^0) = 130\,\text{GeV}$ is assumed, scenarios where SRB is relevant have uncertainties of 11–37%.

In all SRs, the dominant uncertainty on the signal yields is found to be from the b-tagging efficiency.

Theoretical uncertainties in the approximate NNLO+NNLL cross-section are calculated for each SUSY signal scenario, and are dominated by the uncertainties in the renormalisation and factorisation scales, followed by the uncertainty in the PDFs. These are 7–17% for bottom-squark masses in the range between 400 GeV and 1500 GeV. Additional uncertainties in the acceptance and efficiency due to the modelling of ISR and CKKW scale variations in SUSY signal MC samples are also taken into account, and contribute up to ∼10%.

8 Results and interpretation

The event yields for all SRs are reported in table 6. The SM background expectations resulting from background-only fits are also reported showing statistical plus systematic uncertainties. The largest background contribution in A-type and B-type SRs arises from $t\bar{t}$ production, whilst the contribution from $Z \to \nu\bar{\nu}$ production in association with b-quarks is largest in the C-type SRs, with sub-dominant contributions from the $t\bar{t}$ and single-top processes. Other background sources are $t\bar{t}+W/Z$, $t\bar{t}+h$, diboson and W+jets production. The results are also summarised in figure 6, where the significances for each of the SRs are also presented. No significant deviations are observed between expected and observed yields in all signal regions considered.

JHEP12(2019)060

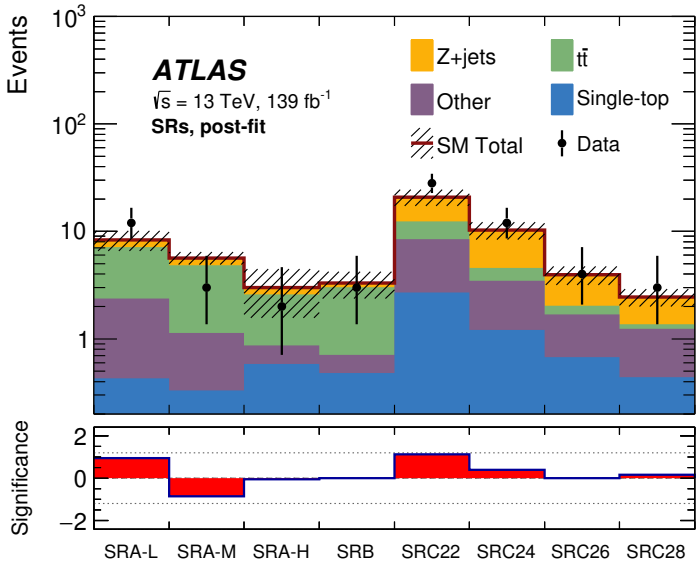

Figure 6. Results of the background-only fit extrapolated to all SRs. The normalisation of the backgrounds is obtained from the fit to the CRs. The upper panel shows the observed number of events and the predicted background yields. The backgrounds which contribute only a small amount (diboson, W+jets and $t\bar{t}$ +$W/Z/h$) are grouped and labelled as "Other". All uncertainties defined in section 7 are included in the uncertainty band. The lower panel shows the significance in each SR. The significance calculation is performed as described in ref. [91].

Figure 7 shows comparisons between the observed data and the post-fit SM predictions for some relevant kinematic distributions for the inclusive SRA, SRB and SRC selections before selection requirements are applied on the quantity shown. The expected distributions for scenarios with different bottom squark, $\tilde{\chi}_2^0$ and $\tilde{\chi}_1^0$ masses (depending on the SR considered) are shown for illustrative purposes.

The $\mathrm{CL_s}$ technique [95] is used to place 95% Confidence Level (CL) upper limits on event yields from physics beyond the SM (BSM) for each signal region. The profile-likelihood-ratio test statistic is used to exclude the signal-plus-background hypothesis for specific signal models. When normalised to the integrated luminosity of the data sample, results can be interpreted as corresponding upper limits on the visible cross-section, σ_{vis}, defined as the product of the BSM production cross-section, the acceptance and the selection efficiency of a BSM signal. When calculating the model-independent upper limits of the A- and C-type regions, only the inclusive SR selection is used. Table 7 summarises the observed (S_{obs}^{95}) and expected (S_{exp}^{95}) 95% CL upper limits on the number of BSM events and on σ_{vis} for all SRs. The p_0-values, which represent the probability of the SM background to fluctuate to the observed number of events or higher, are also provided and are capped at $p_0 = 0.5$; the associated significance is provided in parentheses.

Model-dependent exclusion limits are obtained assuming the two types of SUSY particle mass hierarchies described in section 1. The lightest bottom squark decays exclusively via $\tilde{b}_1 \to b\tilde{\chi}_2^0$ with subsequent decay $\tilde{\chi}_2^0 \to h\tilde{\chi}_1^0$. The expected limits from the SRs are

JHEP12(2019)060

	SRA	SRA-L	SRA-M	SRA-H	SRB
Observed events	17	12	3	2	3
Fitted SM bkg events	17.1 ± 2.8	8.4 ± 1.7	5.7 ± 0.8	3.0 ± 1.5	3.3 ± 0.9
$t\bar{t}$	10.1 ± 2.5	4.7 ± 1.5	3.7 ± 0.6	1.7 ± 1.4	2.3 ± 0.8
Z+jets	2.6 ± 0.4	1.3 ± 0.2	0.9 ± 0.2	0.4 ± 0.1	0.3 ± 0.1
Single-top	1.4 ± 0.3	0.4 ± 0.1	0.3 ± 0.1	0.6 ± 0.2	0.5 ± 0.1
$t\bar{t}+W/Z$	1.2 ± 0.3	0.7 ± 0.1	0.3 ± 0.1	0.1 ± 0.0	0.07 ± 0.02
$t\bar{t}+h$	1.1 ± 0.2	0.7 ± 0.1	0.3 ± 0.1	0.1 ± 0.0	0.13 ± 0.02
W+jets	0.4 ± 0.1	0.2 ± 0.1	0.1 ± 0.0	–	0.02 ± 0.01
Diboson	0.4 ± 0.1	0.3 ± 0.1	–	–	–
$m(\tilde{b}_1,\tilde{\chi}_2^0,\tilde{\chi}_1^0)=(1100,330,200)$ GeV	13.7 ± 0.3	0.7 ± 0.1	6.3 ± 0.2	6.6 ± 0.2	0.3 ± 0.1
$m(\tilde{b}_1,\tilde{\chi}_2^0,\tilde{\chi}_1^0)=(700,680,550)$ GeV	1.3 ± 0.6	0.2 ± 0.1	0.5 ± 0.4	0.6 ± 0.4	7.4 ± 1.2
$m(\tilde{b}_1,\tilde{\chi}_2^0,\tilde{\chi}_1^0)=(1200,1150,60)$ GeV	8.7 ± 0.2	1.4 ± 0.1	3.4 ± 0.1	3.8 ± 0.1	0.6 ± 0.1
	SRC	SRC22	SRC24	SRC26	SRC28
Observed events	47	28	12	4	3
Fitted SM bkg events	37.9 ± 6.2	21.2 ± 4.1	10.6 ± 2.3	3.7 ± 0.9	2.4 ± 0.6
$t\bar{t}$	5.4 ± 2.6	3.9 ± 2.3	1.1 ± 0.6	0.3 ± 0.3	0.1 ± 0.1
Z+jets	17.6 ± 4.7	8.8 ± 2.5	6.0 ± 1.8	1.7 ± 0.7	1.1 ± 0.4
Single-top	5.0 ± 1.5	2.7 ± 1.0	1.2 ± 0.3	0.7 ± 0.2	0.4 ± 0.1
$t\bar{t}+W/Z$	4.3 ± 0.6	2.5 ± 0.4	1.1 ± 0.2	0.5 ± 0.1	0.2 ± 0.1
$t\bar{t}+h$	0.2 ± 0.0	0.2 ± 0.0	—	0.1 ± 0.0	0.0 ± 0.0
W+jets	3.5 ± 0.8	2.2 ± 0.5	0.6 ± 0.2	0.2 ± 0.1	0.4 ± 0.1
Diboson	1.8 ± 0.3	0.9 ± 0.2	0.6 ± 0.1	0.2 ± 0.0	0.1 ± 0.1
$m(\tilde{b}_1,\tilde{\chi}_2^0,\tilde{\chi}_1^0)=(1100,330,200)$ GeV	0.4 ± 0.1	0.3 ± 0.1	0.1 ± 0.0	0.03 ± 0.02	0.03 ± 0.01
$m(\tilde{b}_1,\tilde{\chi}_2^0,\tilde{\chi}_1^0)=(700,680,550)$ GeV	1.2 ± 0.5	0.5 ± 0.2	0.7 ± 0.4	—	—
$m(\tilde{b}_1,\tilde{\chi}_2^0,\tilde{\chi}_1^0)=(1200,1150,60)$ GeV	26.7 ± 0.3	6.3 ± 0.2	6.4 ± 0.2	5.8 ± 0.2	8.3 ± 0.2

Table 6. Background-only fit results for the A- and B-type regions (top table) and C-type regions (bottom table) performed using 139 $\text{fb}^{-1}$of data. The quoted uncertainties on the fitted SM background include both the statistical and systematic uncertainties.

Signal channel	σ_{vis}[fb]	S_{obs}^{95}	S_{exp}^{95}	CL_B	p_0 (Z)
SRA	0.06	9.0	$10.1^{+4.7}_{-3.1}$	0.38	0.50 (0.00)
SRB	0.04	4.9	$5.1^{+2.8}_{-1.7}$	0.45	0.50 (0.00)
SRC	0.19	26.0	$20.8^{+7.0}_{-5.5}$	0.80	0.17 (0.97)

Table 7. From left to right, observed 95% CL upper limits on the visible cross sections σ_{vis}, the observed (S_{obs}^{95}) and expected (S_{exp}^{95}) 95% CL upper limits on the number of signal events with ± 1 σ excursions of the expectation, the CL of the background-only hypothesis, CL_B, the discovery p-value (p_0), truncated at 0.5, and the associated significance (in parentheses).

JHEP12(2019)060

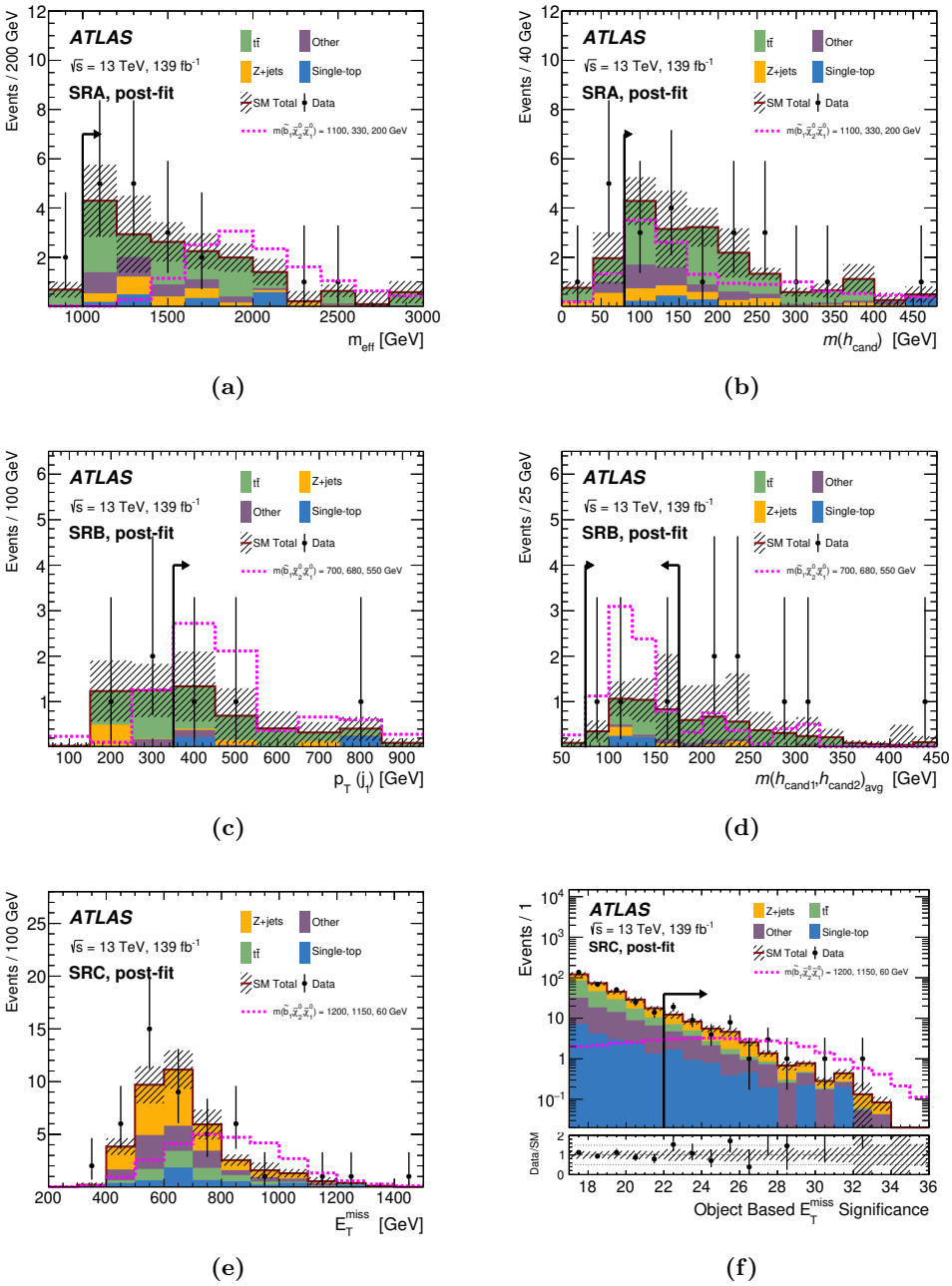

Figure 7. Post-fit distributions of (a) the m_{eff} and (b) the $m(h_{\text{cand}})$ in the inclusive SRA region; (c) the leading jet p_{T} and (d) the $m(h_{\text{cand1}}, h_{\text{cand2}})_{\text{avg}}$ for the Higgs candidates in the SRB region; (e) $E_{\text{T}}^{\text{miss}}$ and (f) $\mathcal{S}$ for SRC regions. All SR selections are applied except for the selection on the variable shown, where the selection on the variable under consideration is denoted by an arrow, except in the case of (e), where the full SRC selection is applied. All uncertainties as defined in section 7 are included in the uncertainty band. The minor backgrounds (diboson, W+jets and $t\bar{t}$ +$W/Z/h$) are grouped and labelled as "Other". For illustration, contributions expected for scenarios with different bottom-squark, $\tilde{\chi}_2^0$ and $\tilde{\chi}_1^0$ masses depending on the SR considered are superimposed. Overflow events which do not fall into the axis range are placed into the right-most bin.

JHEP12(2019)060

compared for each set of scenarios and the observed limits are obtained by choosing the SR with the best expected sensitivity for each SUSY model. The fit procedure takes into account correlations in the yield predictions between control and signal regions due to common background normalisation parameters and systematic uncertainties. The experimental systematic uncertainties in the signal are taken into account for the calculation and are assumed to be fully correlated with those in the SM background.

Figures 8a and 8b show the observed (solid line) and expected (dashed line) exclusion contours at 95% CL in the $\tilde{b}_1$–$\tilde{\chi}_2^0$ mass planes for the two types of SUSY scenarios considered. For the scenarios where the mass of the neutralino is assumed to be 60 GeV, the sensitivity to models with the largest mass difference between the $\tilde{b}_1$ and the $\tilde{\chi}_2^0$ is achieved with the combination of the A-type SRs. Sensitivity to scenarios with small mass differences is obtained with the dedicated C-type SRs. For scenarios with $\Delta m(\tilde{\chi}_2^0, \tilde{\chi}_1^0) = 130$ GeV, the sensitivity of the A-type SRs is complemented by the B-type SR in the case of small mass difference between the $\tilde{b}_1$ and the $\tilde{\chi}_2^0$.

Bottom-squark masses up to 1.5 TeV are excluded for models with fixed $m_{\tilde{\chi}_1^0} = 60$ GeV and $\tilde{\chi}_2^0$ masses $\in [0.5, 1.1]$ TeV. In case of $\Delta m(\tilde{\chi}_2^0, \tilde{\chi}_1^0) = 130$ GeV, bottom-squark masses up to 1.3 TeV are excluded for $\tilde{\chi}_2^0$ masses up to 750 GeV. The losses in sensitivity for models where $\tilde{\chi}_2^0$ masses are below 190 GeV are due to the stringent requirements on $E_{\mathrm{T}}^{\mathrm{miss}}$.

The results constitute a large improvement upon previous Run-1 searches and significantly strengthen the constraints on bottom squark masses; they are also complementary to other searches where bottom squarks are assumed to decay directly to a bottom-quark and a neutralino or to a top-quark and a chargino [96].

JHEP12(2019)060

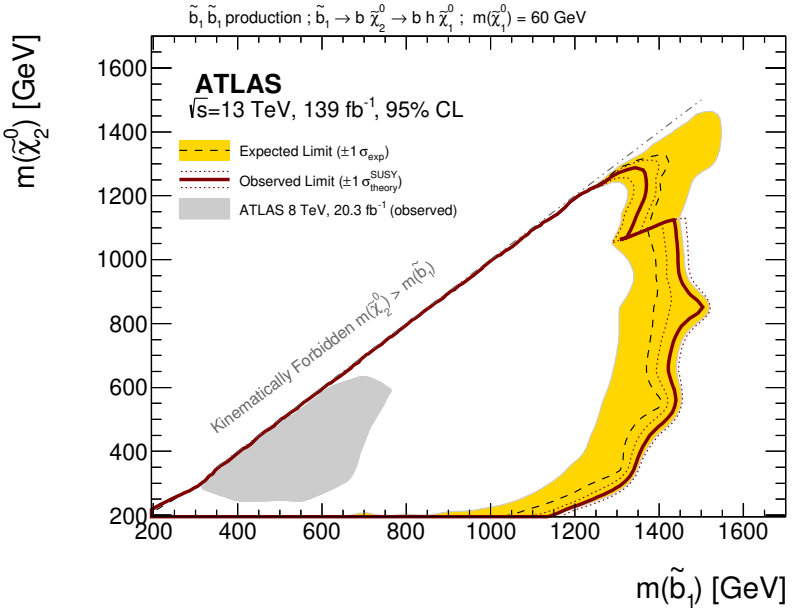

(a)

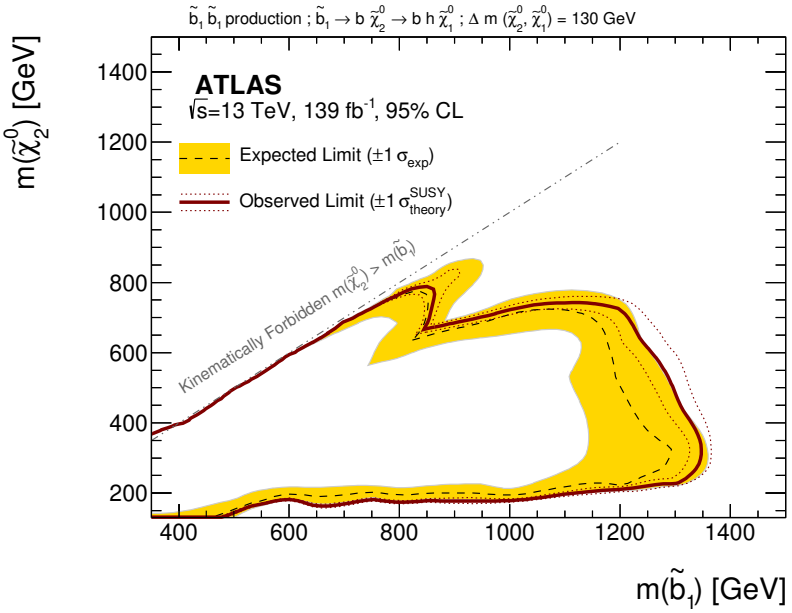

(b)

Figure 8. Exclusion contour at the 95% CL in the $m(\tilde{b}_1, \tilde{\chi}_2^0)$ phase space for (a) the $m(\tilde{\chi}_1^0) = 60\,\text{GeV}$ signal scenario, ATLAS Run 1 limit taken from ref. [27] and (b) the $\Delta m(\tilde{\chi}_2^0, \tilde{\chi}_1^0) = 130\,\text{GeV}$ signal scenario, using the SR with the best-expected sensitivity. The theory uncertainty band contains the systematic uncertainties on the signal model under consideration and the uncertainty in the signal cross section.

JHEP12(2019)060

9 Conclusion

The result of a search for pair production of bottom squarks is reported. The analysis uses 139 fb^{-1} of pp collisions at $\sqrt{s} = 13$ TeV collected by the ATLAS experiment at the LHC between 2015 and 2018. R-parity-conserving SUSY scenarios where bottom squarks decay into a b-quark and the second-lightest neutralino, $\tilde{b}_1 \to b + \tilde{\chi}_2^0$, with $\tilde{\chi}_2^0$ subsequently decaying into a Higgs boson like the one in the SM and the lightest neutralino, are considered. The search investigates final states containing large missing transverse momentum and three or more b-jets. No significant excess of events above the expected Standard Model background is found and exclusion limits at the 95% confidence level are placed on the visible cross-section and on the mass of the bottom squark for various assumptions about the mass hierarchy of the $\tilde{b}_1$, $\tilde{\chi}_2^0$ and $\tilde{\chi}_1^0$. Bottom-squark masses up to 1.5 (1.3) TeV are excluded for $\tilde{\chi}_2^0$ masses up to 1100 (750) GeV in models with fixed $m(\tilde{\chi}_1^0) = 60$ GeV ($\Delta m(\tilde{\chi}_2^0, \tilde{\chi}_1^0) = 130$ GeV). As the first search for such scenarios carried out by ATLAS in Run 2, these results are a significant improvement upon the previous Run-1 result, considerably tightening the constraints on bottom-squark production.

Acknowledgments

We thank CERN for the very successful operation of the LHC, as well as the support staff from our institutions without whom ATLAS could not be operated efficiently.

We acknowledge the support of ANPCyT, Argentina; YerPhI, Armenia; ARC, Australia; BMWFW and FWF, Austria; ANAS, Azerbaijan; SSTC, Belarus; CNPq and FAPESP, Brazil; NSERC, NRC and CFI, Canada; CERN; CONICYT, Chile; CAS, MOST and NSFC, China; COLCIENCIAS, Colombia; MSMT CR, MPO CR and VSC CR, Czech Republic; DNRF and DNSRC, Denmark; IN2P3-CNRS, CEA-DRF/IRFU, France; SRNSFG, Georgia; BMBF, HGF, and MPG, Germany; GSRT, Greece; RGC, Hong Kong SAR, China; ISF and Benoziyo Center, Israel; INFN, Italy; MEXT and JSPS, Japan; CNRST, Morocco; NWO, Netherlands; RCN, Norway; MNiSW and NCN, Poland; FCT, Portugal; MNE/IFA, Romania; MES of Russia and NRC KI, Russian Federation; JINR; MESTD, Serbia; MSSR, Slovakia; ARRS and MIZŠ, Slovenia; DST/NRF, South Africa; MINECO, Spain; SRC and Wallenberg Foundation, Sweden; SERI, SNSF and Cantons of Bern and Geneva, Switzerland; MOST, Taiwan; TAEK, Turkey; STFC, United Kingdom; DOE and NSF, United States of America. In addition, individual groups and members have received support from BCKDF, CANARIE, CRC and Compute Canada, Canada; COST, ERC, ERDF, Horizon 2020, and Marie Skłodowska-Curie Actions, European Union; Investissements d' Avenir Labex and Idex, ANR, France; DFG and AvH Foundation, Germany; Herakleitos, Thales and Aristeia programmes co-financed by EU-ESF and the Greek NSRF, Greece; BSF-NSF and GIF, Israel; CERCA Programme Generalitat de Catalunya, Spain; The Royal Society and Leverhulme Trust, United Kingdom.

The crucial computing support from all WLCG partners is acknowledged gratefully, in particular from CERN, the ATLAS Tier-1 facilities at TRIUMF (Canada), NDGF (Denmark, Norway, Sweden), CC-IN2P3 (France), KIT/GridKA (Germany), INFN-CNAF

JHEP12(2019)060

(Italy), NL-T1 (Netherlands), PIC (Spain), ASGC (Taiwan), RAL (U.K.) and BNL (U.S.A.), the Tier-2 facilities worldwide and large non-WLCG resource providers. Major contributors of computing resources are listed in ref. [97].

References

[1] Yu.A. Golfand and E.P. Likhtman, *Extension of the algebra of Poincaré group generators and violation of p invariance*, *JETP Lett.* **13** (1971) 323 [*Pisma Zh. Eksp. Teor. Fiz.* **13** (1971) 452] [INSPIRE].

[2] D.V. Volkov and V.P. Akulov, *Is the neutrino a Goldstone particle?*, *Phys. Lett.* **B 46** (1973) 109 [INSPIRE].

[3] J. Wess and B. Zumino, *Supergauge transformations in four-dimensions*, *Nucl. Phys.* **B 70** (1974) 39 [INSPIRE].

[4] J. Wess and B. Zumino, *Supergauge invariant extension of quantum electrodynamics*, *Nucl. Phys.* **B 78** (1974) 1 [INSPIRE].

[5] S. Ferrara and B. Zumino, *Supergauge invariant Yang-Mills theories*, *Nucl. Phys.* **B 79** (1974) 413 [INSPIRE].

[6] A. Salam and J.A. Strathdee, *Supersymmetry and non-Abelian gauges*, *Phys. Lett.* **B 51** (1974) 353 [INSPIRE].

[7] N. Sakai, *Naturalness in supersymmetric GUTs*, *Z. Phys.* **C 11** (1981) 153 [INSPIRE].

[8] S. Dimopoulos, S. Raby and F. Wilczek, *Supersymmetry and the scale of unification*, *Phys. Rev.* **D 24** (1981) 1681 [INSPIRE].

[9] L.E. Ibáñez and G.G. Ross, *Low-energy predictions in supersymmetric Grand Unified Theories*, *Phys. Lett.* **B 105** (1981) 439 [INSPIRE].

[10] S. Dimopoulos and H. Georgi, *Softly broken supersymmetry and* SU(5), *Nucl. Phys.* **B 193** (1981) 150 [INSPIRE].

[11] G.R. Farrar and P. Fayet, *Phenomenology of the production, decay and detection of new hadronic states associated with supersymmetry*, *Phys. Lett.* **B 76** (1978) 575 [INSPIRE].

[12] H. Goldberg, *Constraint on the photino mass from cosmology*, *Phys. Rev. Lett.* **50** (1983) 1419 [*Erratum ibid.* **103** (2009) 099905] [INSPIRE].

[13] J.R. Ellis, J.S. Hagelin, D.V. Nanopoulos, K.A. Olive and M. Srednicki, *Supersymmetric relics from the big bang*, *Nucl. Phys.* **B 238** (1984) 453 [INSPIRE].

[14] R. Barbieri and G.F. Giudice, *Upper bounds on supersymmetric particle masses*, *Nucl. Phys.* **B 306** (1988) 63 [INSPIRE].

[15] B. de Carlos and J.A. Casas, *One loop analysis of the electroweak breaking in supersymmetric models and the fine tuning problem*, *Phys. Lett.* **B 309** (1993) 320 [hep-ph/9303291] [INSPIRE].

[16] P. Fayet, *Supersymmetry and weak, electromagnetic and strong interactions*, *Phys. Lett.* **B 64** (1976) 159 [INSPIRE].

JHEP12(2019)060

[17] P. Fayet, *Spontaneously broken supersymmetric theories of weak, electromagnetic and strong interactions*, *Phys. Lett.* **B 69** (1977) 489 [INSPIRE].

[18] ATLAS collaboration, *Search for supersymmetry in events with b-tagged jets and missing transverse momentum in pp collisions at $\sqrt{s} = 13$ TeV with the ATLAS detector*, *JHEP* **11** (2017) 195 [arXiv:1708.09266] [INSPIRE].

[19] CMS collaboration, *Search for new phenomena with the M_{T2} variable in the all-hadronic final state produced in proton-proton collisions at $\sqrt{s} = 13$ TeV*, *Eur. Phys. J.* **C 77** (2017) 710 [arXiv:1705.04650] [INSPIRE].

[20] ATLAS collaboration, *Search for supersymmetry in final states with two same-sign or three leptons and jets using 36 fb^{-1} of $\sqrt{s} = 13$ TeV pp collision data with the ATLAS detector*, *JHEP* **09** (2017) 084 [*Erratum ibid.* **08** (2019) 121] [arXiv:1706.03731] [INSPIRE].

[21] CMS collaboration, *Search for physics beyond the Standard Model in events with two leptons of same sign, missing transverse momentum and jets in proton-proton collisions at $\sqrt{s} = 13$ TeV*, *Eur. Phys. J.* **C 77** (2017) 578 [arXiv:1704.07323] [INSPIRE].

[22] CMS collaboration, *Search for supersymmetry in events with at least three electrons or muons, jets and missing transverse momentum in proton-proton collisions at $\sqrt{s} = 13$ TeV*, *JHEP* **02** (2018) 067 [arXiv:1710.09154] [INSPIRE].

[23] ATLAS collaboration, *Observation of $H \to b\bar{b}$ decays and VH production with the ATLAS detector*, *Phys. Lett.* **B 786** (2018) 59 [arXiv:1808.08238] [INSPIRE].

[24] LHC Higgs Cross Section Working Group collaboration, *Handbook of LHC Higgs cross sections: 4. Deciphering the nature of the Higgs sector*, arXiv:1610.07922 [INSPIRE].

[25] J. Alwall, M.-P. Le, M. Lisanti and J.G. Wacker, *Searching for directly decaying gluinos at the Tevatron*, *Phys. Lett.* **B 666** (2008) 34 [arXiv:0803.0019] [INSPIRE].

[26] J. Alwall, P. Schuster and N. Toro, *Simplified models for a first characterization of new physics at the LHC*, *Phys. Rev.* **D 79** (2009) 075020 [arXiv:0810.3921] [INSPIRE].

[27] ATLAS collaboration, *ATLAS run 1 searches for direct pair production of third-generation squarks at the Large Hadron Collider*, *Eur. Phys. J.* **C 75** (2015) 510 [*Erratum ibid.* **C 76** (2016) 153] [arXiv:1506.08616] [INSPIRE].

[28] M. Escudero, A. Berlin, D. Hooper and M.-X. Lin, *Toward (finally!) ruling out Z and Higgs mediated dark matter models*, *JCAP* **12** (2016) 029 [arXiv:1609.09079] [INSPIRE].

[29] CMS collaboration, *Search for supersymmetry using Higgs boson to diphoton decays at $\sqrt{s} = 13$ TeV*, arXiv:1908.08500 [INSPIRE].

[30] ATLAS collaboration, *The ATLAS experiment at the CERN Large Hadron Collider*, 2008 *JINST* **3** S08003 [INSPIRE].

[31] ATLAS collaboration, *ATLAS insertable B-layer technical design report*, ATLAS-TDR-19, CERN, Geneva, Switzerland (2010).

[32] ATLAS IBL collaboration, *Production and integration of the ATLAS insertable B-layer*, 2018 *JINST* **13** T05008 [arXiv:1803.00844] [INSPIRE].

[33] ATLAS collaboration, *Performance of the ATLAS trigger system in* 2015, *Eur. Phys. J.* **C 77** (2017) 317 [arXiv:1611.09661] [INSPIRE].

[34] ATLAS collaboration, *Luminosity determination in pp collisions at $\sqrt{s} = 13$ TeV using the ATLAS detector at the LHC*, ATLAS-CONF-2019-021, CERN, Geneva, Switzerland (2019).

JHEP12(2019)060

[35] G. Avoni et al., *The new LUCID-2 detector for luminosity measurement and monitoring in ATLAS*, 2018 *JINST* **13** P07017 [INSPIRE].

[36] ATLAS collaboration, 2015 *start-up trigger menu and initial performance assessment of the ATLAS trigger using run-2 data*, ATL-DAQ-PUB-2016-001, CERN, Geneva, Switzerland (2016).

[37] ATLAS collaboration, *The ATLAS simulation infrastructure*, *Eur. Phys. J.* **C 70** (2010) 823 [arXiv:1005.4568] [INSPIRE].

[38] GEANT4 collaboration, *GEANT4: a simulation toolkit*, *Nucl. Instrum. Meth.* **A 506** (2003) 250 [INSPIRE].

[39] J. Alwall et al., *The automated computation of tree-level and next-to-leading order differential cross sections and their matching to parton shower simulations*, *JHEP* **07** (2014) 079 [arXiv:1405.0301] [INSPIRE].

[40] T. Sjöstrand et al., *An introduction to PYTHIA* 8.2, *Comput. Phys. Commun.* **191** (2015) 159 [arXiv:1410.3012] [INSPIRE].

[41] ATLAS collaboration, *ATLAS run* 1 *PYTHIA*8 *tunes*, ATL-PHYS-PUB-2014-021, CERN, Geneva, Switzerland (2014).

[42] L. Lönnblad and S. Prestel, *Merging multi-leg NLO matrix elements with parton showers*, *JHEP* **03** (2013) 166 [arXiv:1211.7278] [INSPIRE].

[43] R.D. Ball et al., *Parton distributions with LHC data*, *Nucl. Phys.* **B 867** (2013) 244 [arXiv:1207.1303] [INSPIRE].

[44] W. Beenakker, C. Borschensky, M. Krämer, A. Kulesza and E. Laenen, *NNLL-fast: predictions for coloured supersymmetric particle production at the LHC with threshold and Coulomb resummation*, *JHEP* **12** (2016) 133 [arXiv:1607.07741] [INSPIRE].

[45] W. Beenakker, R. Höpker, M. Spira and P.M. Zerwas, *Squark and gluino production at hadron colliders*, *Nucl. Phys.* **B 492** (1997) 51 [hep-ph/9610490] [INSPIRE].

[46] W. Beenakker, S. Brensing, M. Krämer, A. Kulesza, E. Laenen and I. Niessen, *Supersymmetric top and bottom squark production at hadron colliders*, *JHEP* **08** (2010) 098 [arXiv:1006.4771] [INSPIRE].

[47] W. Beenakker, C. Borschensky, R. Heger, M. Krämer, A. Kulesza and E. Laenen, *NNLL resummation for stop pair-production at the LHC*, *JHEP* **05** (2016) 153 [arXiv:1601.02954] [INSPIRE].

[48] J. Butterworth et al., *PDF4LHC recommendations for LHC run II*, *J. Phys.* **G 43** (2016) 023001 [arXiv:1510.03865] [INSPIRE].

[49] S. Frixione, P. Nason and G. Ridolfi, *A positive-weight next-to-leading-order Monte Carlo for heavy flavour hadroproduction*, *JHEP* **09** (2007) 126 [arXiv:0707.3088] [INSPIRE].

[50] P. Nason, *A new method for combining NLO QCD with shower Monte Carlo algorithms*, *JHEP* **11** (2004) 040 [hep-ph/0409146] [INSPIRE].

[51] S. Frixione, P. Nason and C. Oleari, *Matching NLO QCD computations with parton shower simulations: the POWHEG method*, *JHEP* **11** (2007) 070 [arXiv:0709.2092] [INSPIRE].

[52] S. Alioli, P. Nason, C. Oleari and E. Re, *A general framework for implementing NLO calculations in shower Monte Carlo programs: the POWHEG BOX*, *JHEP* **06** (2010) 043 [arXiv:1002.2581] [INSPIRE].

JHEP12(2019)060

[53] ATLAS collaboration, *Further studies on simulation of top-quark production for the ATLAS experiment at* $\sqrt{s} = 13$ *TeV*, ATL-PHYS-PUB-2016-016, CERN, Geneva, Switzerland (2016).

[54] E. Re, *Single-top Wt-channel production matched with parton showers using the POWHEG method*, *Eur. Phys. J.* **C 71** (2011) 1547 [arXiv:1009.2450] [INSPIRE].

[55] T. Gleisberg et al., *Event generation with SHERPA* 1.1, *JHEP* **02** (2009) 007 [arXiv:0811.4622] [INSPIRE].

[56] T. Gleisberg and S. Höche, *Comix, a new matrix element generator*, *JHEP* **12** (2008) 039 [arXiv:0808.3674] [INSPIRE].

[57] F. Cascioli, P. Maierhöfer and S. Pozzorini, *Scattering amplitudes with open loops*, *Phys. Rev. Lett.* **108** (2012) 111601 [arXiv:1111.5206] [INSPIRE].

[58] S. Schumann and F. Krauss, *A parton shower algorithm based on Catani-Seymour dipole factorisation*, *JHEP* **03** (2008) 038 [arXiv:0709.1027] [INSPIRE].

[59] S. Höche, F. Krauss, M. Schönherr and F. Siegert, *QCD matrix elements + parton showers: the NLO case*, *JHEP* **04** (2013) 027 [arXiv:1207.5030] [INSPIRE].

[60] ATLAS collaboration, *Search for squarks and gluinos with the ATLAS detector in final states with jets and missing transverse momentum using* $4.7\,fb^{-1}$ *of* $\sqrt{s} = 7$ *TeV proton-proton collision data*, *Phys. Rev.* **D 87** (2013) 012008 [arXiv:1208.0949] [INSPIRE].

[61] M. Beneke, P. Falgari, S. Klein and C. Schwinn, *Hadronic top-quark pair production with NNLL threshold resummation*, *Nucl. Phys.* **B 855** (2012) 695 [arXiv:1109.1536] [INSPIRE].

[62] M. Cacciari, M. Czakon, M. Mangano, A. Mitov and P. Nason, *Top-pair production at hadron colliders with next-to-next-to-leading logarithmic soft-gluon resummation*, *Phys. Lett.* **B 710** (2012) 612 [arXiv:1111.5869] [INSPIRE].

[63] P. Bärnreuther, M. Czakon and A. Mitov, *Percent level precision physics at the Tevatron: first genuine NNLO QCD corrections to* $q\bar{q} \to t\bar{t} + X$, *Phys. Rev. Lett.* **109** (2012) 132001 [arXiv:1204.5201] [INSPIRE].

[64] M. Czakon and A. Mitov, *NNLO corrections to top-pair production at hadron colliders: the all-fermionic scattering channels*, *JHEP* **12** (2012) 054 [arXiv:1207.0236] [INSPIRE].

[65] M. Czakon and A. Mitov, *NNLO corrections to top pair production at hadron colliders: the quark-gluon reaction*, *JHEP* **01** (2013) 080 [arXiv:1210.6832] [INSPIRE].

[66] M. Czakon, P. Fiedler and A. Mitov, *Total top-quark pair-production cross section at hadron colliders through* $O(\alpha_S^4)$, *Phys. Rev. Lett.* **110** (2013) 252004 [arXiv:1303.6254] [INSPIRE].

[67] M. Czakon and A. Mitov, *Top++: a program for the calculation of the top-pair cross-section at hadron colliders*, *Comput. Phys. Commun.* **185** (2014) 2930 [arXiv:1112.5675] [INSPIRE].

[68] N. Kidonakis, *Next-to-next-to-leading-order collinear and soft gluon corrections for t-channel single top quark production*, *Phys. Rev.* **D 83** (2011) 091503 [arXiv:1103.2792] [INSPIRE].

[69] N. Kidonakis, *NNLL resummation for s-channel single top quark production*, *Phys. Rev.* **D 81** (2010) 054028 [arXiv:1001.5034] [INSPIRE].

[70] N. Kidonakis, *Two-loop soft anomalous dimensions for single top quark associated production with a* W^- *or* H^-, *Phys. Rev.* **D 82** (2010) 054018 [arXiv:1005.4451] [INSPIRE].

[71] D.J. Lange, *The EvtGen particle decay simulation package*, *Nucl. Instrum. Meth.* **A 462** (2001) 152 [INSPIRE].

JHEP12(2019)060

[72] ATLAS collaboration, *A study of the PYTHIA 8 description of ATLAS minimum bias measurements with the Donnachie-Landshoff diffractive model*, ATL-PHYS-PUB-2016-017, CERN, Geneva, Switzerland (2016).

[73] ATLAS collaboration, *Vertex reconstruction performance of the ATLAS detector at* $\sqrt{s} = 13$ *TeV*, ATL-PHYS-PUB-2015-026, CERN, Geneva, Switzerland (2015).

[74] ATLAS collaboration, *Topological cell clustering in the ATLAS calorimeters and its performance in LHC run* 1, *Eur. Phys. J.* **C 77** (2017) 490 [arXiv:1603.02934] [INSPIRE].

[75] M. Cacciari, G.P. Salam and G. Soyez, *The anti-*k_t *jet clustering algorithm*, *JHEP* **04** (2008) 063 [arXiv:0802.1189] [INSPIRE].

[76] M. Cacciari, G.P. Salam and G. Soyez, *FastJet user manual*, *Eur. Phys. J.* **C 72** (2012) 1896 [arXiv:1111.6097] [INSPIRE].

[77] ATLAS collaboration, *Jet energy scale measurements and their systematic uncertainties in proton-proton collisions at* $\sqrt{s} = 13$ *TeV with the ATLAS detector*, *Phys. Rev.* **D 96** (2017) 072002 [arXiv:1703.09665] [INSPIRE].

[78] ATLAS collaboration, *Selection of jets produced in* 13 *TeV proton-proton collisions with the ATLAS detector*, ATLAS-CONF-2015-029, CERN, Geneva, Switzerland (2015).

[79] ATLAS collaboration, *Tagging and suppression of pileup jets with the ATLAS detector*, ATLAS-CONF-2014-018, CERN, Geneva, Switzerland (2014).

[80] ATLAS collaboration, *Constituent-level pile-up mitigation techniques in ATLAS*, ATLAS-CONF-2017-065, CERN, Geneva, Switzerland (2017).

[81] ATLAS collaboration, *ATLAS b-jet identification performance and efficiency measurement with* $t\bar{t}$ *events in pp collisions at* $\sqrt{s} = 13$ *TeV*, *Eur. Phys. J.* **C 79** (2019) 970 [arXiv:1907.05120] [INSPIRE].

[82] ATLAS collaboration, *Electron and photon performance measurements with the ATLAS detector using the* 2015–2017 *LHC proton-proton collision data*, arXiv:1908.00005 [INSPIRE].

[83] ATLAS collaboration, *Muon reconstruction performance of the ATLAS detector in proton-proton collision data at* $\sqrt{s} = 13$ *TeV*, *Eur. Phys. J.* **C 76** (2016) 292 [arXiv:1603.05598] [INSPIRE].

[84] ATLAS collaboration, *Measurement of the* $t\bar{t}$ *production cross-section using* $e\mu$ *events with b-tagged jets in pp collisions at* $\sqrt{s} = 13$ *TeV with the ATLAS detector*, *Phys. Lett.* **B 761** (2016) 136 [*Erratum ibid.* **B 772** (2017) 879] [arXiv:1606.02699] [INSPIRE].

[85] ATLAS collaboration, *Performance of missing transverse momentum reconstruction with the ATLAS detector using proton-proton collisions at* $\sqrt{s} = 13$ *TeV*, *Eur. Phys. J.* **C 78** (2018) 903 [arXiv:1802.08168] [INSPIRE].

[86] ATLAS collaboration, *Performance of algorithms that reconstruct missing transverse momentum in* $\sqrt{s} = 8$ *TeV proton-proton collisions in the ATLAS detector*, *Eur. Phys. J.* **C 77** (2017) 241 [arXiv:1609.09324] [INSPIRE].

[87] ATLAS collaboration, *Jet energy measurement with the ATLAS detector in proton-proton collisions at* $\sqrt{s} = 7$ *TeV*, *Eur. Phys. J.* **C 73** (2013) 2304 [arXiv:1112.6426] [INSPIRE].

[88] I. Hinchliffe, F.E. Paige, M.D. Shapiro, J. Söderqvist and W. Yao, *Precision SUSY measurements at CERN LHC*, *Phys. Rev.* **D 55** (1997) 5520 [hep-ph/9610544] [INSPIRE].

JHEP12(2019)060

[89] ATLAS collaboration, *Object-based missing transverse momentum significance in the ATLAS detector*, ATLAS-CONF-2018-038, CERN, Geneva, Switzerland (2018).

[90] M. Baak, G.J. Besjes, D. Côte, A. Koutsman, J. Lorenz and D. Short, *HistFitter software framework for statistical data analysis*, *Eur. Phys. J.* **C 75** (2015) 153 [arXiv:1410.1280] [INSPIRE].

[91] G. Choudalakis and D. Casadei, *Plotting the differences between data and expectation*, *Eur. Phys. J. Plus* **127** (2012) 25 [arXiv:1111.2062] [INSPIRE].

[92] ATLAS collaboration, *Jet energy resolution in proton-proton collisions at $\sqrt{s} = 7$ TeV recorded in* 2010 *with the ATLAS detector*, *Eur. Phys. J.* **C 73** (2013) 2306 [arXiv:1210.6210] [INSPIRE].

[93] M. Bähr et al., *HERWIG++ physics and manual*, *Eur. Phys. J.* **C 58** (2008) 639 [arXiv:0803.0883] [INSPIRE].

[94] J. Bellm et al., *HERWIG* 7.0*/HERWIG++* 3.0 *release note*, *Eur. Phys. J.* **C 76** (2016) 196 [arXiv:1512.01178] [INSPIRE].

[95] A.L. Read, *Presentation of search results: the CL_s technique*, *J. Phys.* **G 28** (2002) 2693 [INSPIRE].

[96] ATLAS collaboration, *Search for supersymmetry in events with b-tagged jets and missing transverse momentum in pp collisions at $\sqrt{s} = 13$ TeV with the ATLAS detector*, *JHEP* **11** (2017) 195 [arXiv:1708.09266] [INSPIRE].

[97] ATLAS collaboration, *ATLAS computing acknowledgements*, ATL-GEN-PUB-2016-002, CERN, Geneva, Switzerland (2016).

JHEP12(2019)060

The ATLAS collaboration

G. Aad[101], B. Abbott[128], D.C. Abbott[102], O. Abdinov[13,*], A. Abed Abud[70a,70b], K. Abeling[53], D.K. Abhayasinghe[93], S.H. Abidi[167], O.S. AbouZeid[40], N.L. Abraham[156], H. Abramowicz[161], H. Abreu[160], Y. Abulaiti[6], B.S. Acharya[66a,66b,p], B. Achkar[53], S. Adachi[163], L. Adam[99], C. Adam Bourdarios[132], L. Adamczyk[83a], L. Adamek[167], J. Adelman[121], M. Adersberger[114], A. Adiguzel[12c,al], S. Adorni[54], T. Adye[144], A.A. Affolder[146], Y. Afik[160], C. Agapopoulou[132], M.N. Agaras[38], A. Aggarwal[119], C. Agheorghiesei[27c], J.A. Aguilar-Saavedra[140f,140a,ak], F. Ahmadov[79], W.S. Ahmed[103], X. Ai[18], G. Aielli[73a,73b], S. Akatsuka[85], T.P.A. Åkesson[96], E. Akilli[54], A.V. Akimov[110], K. Al Khoury[132], G.L. Alberghi[23b,23a], J. Albert[176], M.J. Alconada Verzini[161], S. Alderweireldt[36], M. Aleksa[36], I.N. Aleksandrov[79], C. Alexa[27b], D. Alexandre[19], T. Alexopoulos[10], A. Alfonsi[120], M. Alhroob[128], B. Ali[142], G. Alimonti[68a], J. Alison[37], S.P. Alkire[148], C. Allaire[132], B.M.M. Allbrooke[156], B.W. Allen[131], P.P. Allport[21], A. Aloisio[69a,69b], A. Alonso[40], F. Alonso[88], C. Alpigiani[148], A.A. Alshehri[57], M. Alvarez Estevez[98], D. Álvarez Piqueras[174], M.G. Alviggi[69a,69b], Y. Amaral Coutinho[80b], A. Ambler[103], L. Ambroz[135], C. Amelung[26], D. Amidei[105], S.P. Amor Dos Santos[140a], S. Amoroso[46], C.S. Amrouche[54], F. An[78], C. Anastopoulos[149], N. Andari[145], T. Andeen[11], C.F. Anders[61b], J.K. Anders[20], A. Andreazza[68a,68b], V. Andrei[61a], C.R. Anelli[176], S. Angelidakis[38], A. Angerami[39], A.V. Anisenkov[122b,122a], A. Annovi[71a], C. Antel[61a], M.T. Anthony[149], M. Antonelli[51], D.J.A. Antrim[171], F. Anulli[72a], M. Aoki[81], J.A. Aparisi Pozo[174], L. Aperio Bella[36], G. Arabidze[106], J.P. Araque[140a], V. Araujo Ferraz[80b], R. Araujo Pereira[80b], C. Arcangeletti[51], A.T.H. Arce[49], F.A. Arduh[88], J-F. Arguin[109], S. Argyropoulos[77], J.-H. Arling[46], A.J. Armbruster[36], A. Armstrong[171], O. Arnaez[167], H. Arnold[120], A. Artamonov[111,*], G. Artoni[135], S. Artz[99], S. Asai[163], N. Asbah[59], E.M. Asimakopoulou[172], L. Asquith[156], K. Assamagan[29], R. Astalos[28a], R.J. Atkin[33a], M. Atkinson[173], N.B. Atlay[19], H. Atmani[132], K. Augsten[142], G. Avolio[36], R. Avramidou[60a], M.K. Ayoub[15a], A.M. Azoulay[168b], G. Azuelos[109,ba], M.J. Baca[21], H. Bachacou[145], K. Bachas[67a,67b], M. Backes[135], F. Backman[45a,45b], P. Bagnaia[72a,72b], M. Bahmani[84], H. Bahrasemani[152], A.J. Bailey[174], V.R. Bailey[173], J.T. Baines[144], M. Bajic[40], C. Bakalis[10], O.K. Baker[183], P.J. Bakker[120], D. Bakshi Gupta[8], S. Balaji[157], E.M. Baldin[122b,122a], P. Balek[180], F. Balli[145], W.K. Balunas[135], J. Balz[99], E. Banas[84], A. Bandyopadhyay[24], Sw. Banerjee[181,j], A.A.E. Bannoura[182], L. Barak[161], W.M. Barbe[38], E.L. Barberio[104], D. Barberis[55b,55a], M. Barbero[101], T. Barillari[115], M-S. Barisits[36], J. Barkeloo[131], T. Barklow[153], R. Barnea[160], S.L. Barnes[60c], B.M. Barnett[144], R.M. Barnett[18], Z. Barnovska-Blenessy[60a], A. Baroncelli[60a], G. Barone[29], A.J. Barr[135], L. Barranco Navarro[45a,45b], F. Barreiro[98], J. Barreiro Guimarães da Costa[15a], S. Barsov[138], R. Bartoldus[153], G. Bartolini[101], A.E. Barton[89], P. Bartos[28a], A. Basalaev[46], A. Bassalat[132,at], R.L. Bates[57], S.J. Batista[167], S. Batlamous[35e], J.R. Batley[32], B. Batool[151], M. Battaglia[146], M. Bauce[72a,72b], F. Bauer[145], K.T. Bauer[171], H.S. Bawa[31,n], J.B. Beacham[49], T. Beau[136], P.H. Beauchemin[170], F. Becherer[52], P. Bechtle[24], H.C. Beck[53], H.P. Beck[20,t], K. Becker[52], M. Becker[99], C. Becot[46], A. Beddall[12d], A.J. Beddall[12a], V.A. Bednyakov[79], M. Bedognetti[120], C.P. Bee[155], T.A. Beermann[76], M. Begalli[80b], M. Begel[29], A. Behera[155], J.K. Behr[46], F. Beisiegel[24], A.S. Bell[94], G. Bella[161], L. Bellagamba[23b], A. Bellerive[34], P. Bellos[9], K. Beloborodov[122b,122a], K. Belotskiy[112], N.L. Belyaev[112], D. Benchekroun[35a], N. Benekos[10], Y. Benhammou[161], D.P. Benjamin[6], M. Benoit[54], J.R. Bensinger[26], S. Bentvelsen[120], L. Beresford[135], M. Beretta[51], D. Berge[46], E. Bergeaas Kuutmann[172], N. Berger[5], B. Bergmann[142], L.J. Bergsten[26], J. Beringer[18], S. Berlendis[7], N.R. Bernard[102], G. Bernardi[136], C. Bernius[153], T. Berry[93], P. Berta[99], C. Bertella[15a], I.A. Bertram[89], G.J. Besjes[40], O. Bessidskaia Bylund[182], N. Besson[145], A. Bethani[100], S. Bethke[115], A. Betti[24], A.J. Bevan[92],

JHEP12(2019)060

J. Beyer[115], R. Bi[139], R.M. Bianchi[139], O. Biebel[114], D. Biedermann[19], R. Bielski[36], K. Bierwagen[99], N.V. Biesuz[71a,71b], M. Biglietti[74a], T.R.V. Billoud[109], M. Bindi[53], A. Bingul[12d], C. Bini[72a,72b], S. Biondi[23b,23a], M. Birman[180], T. Bisanz[53], J.P. Biswal[161], A. Bitadze[100], C. Bittrich[48], K. Bjørke[134], K.M. Black[25], T. Blazek[28a], I. Bloch[46], C. Blocker[26], A. Blue[57], U. Blumenschein[92], G.J. Bobbink[120], V.S. Bobrovnikov[122b,122a], S.S. Bocchetta[96], A. Bocci[49], D. Boerner[46], D. Bogavac[14], A.G. Bogdanchikov[122b,122a], C. Bohm[45a], V. Boisvert[93], P. Bokan[53,172], T. Bold[83a], A.S. Boldyrev[113], A.E. Bolz[61b], M. Bomben[136], M. Bona[92], J.S. Bonilla[131], M. Boonekamp[145], H.M. Borecka-Bielska[90], A. Borisov[123], G. Borissov[89], J. Bortfeldt[36], D. Bortoletto[135], V. Bortolotto[73a,73b], D. Boscherini[23b], M. Bosman[14], J.D. Bossio Sola[103], K. Bouaouda[35a], J. Boudreau[139], E.V. Bouhova-Thacker[89], D. Boumediene[38], S.K. Boutle[57], A. Boveia[126], J. Boyd[36], D. Boye[33b,au], I.R. Boyko[79], A.J. Bozson[93], J. Bracinik[21], N. Brahimi[101], G. Brandt[182], O. Brandt[61a], F. Braren[46], B. Brau[102], J.E. Brau[131], W.D. Breaden Madden[57], K. Brendlinger[46], L. Brenner[46], R. Brenner[172], S. Bressler[180], B. Brickwedde[99], D.L. Briglin[21], D. Britton[57], D. Britzger[115], I. Brock[24], R. Brock[106], G. Brooijmans[39], W.K. Brooks[147c], E. Brost[121], J.H Broughton[21], P.A. Bruckman de Renstrom[84], D. Bruncko[28b], A. Bruni[23b], G. Bruni[23b], L.S. Bruni[120], S. Bruno[73a,73b], B.H. Brunt[32], M. Bruschi[23b], N. Bruscino[139], P. Bryant[37], L. Bryngemark[96], T. Buanes[17], Q. Buat[36], P. Buchholz[151], A.G. Buckley[57], I.A. Budagov[79], M.K. Bugge[134], F. Bührer[52], O. Bulekov[112], T.J. Burch[121], S. Burdin[90], C.D. Burgard[120], A.M. Burger[129], B. Burghgrave[8], J.T.P. Burr[46], J.C. Burzynski[102], V. Büscher[99], E. Buschmann[53], P.J. Bussey[57], J.M. Butler[25], C.M. Buttar[57], J.M. Butterworth[94], P. Butti[36], W. Buttinger[36], A. Buzatu[158], A.R. Buzykaev[122b,122a], G. Cabras[23b,23a], S. Cabrera Urbán[174], D. Caforio[56], H. Cai[173], V.M.M. Cairo[153], O. Cakir[4a], N. Calace[36], P. Calafiura[18], A. Calandri[101], G. Calderini[136], P. Calfayan[65], G. Callea[57], L.P. Caloba[80b], S. Calvente Lopez[98], D. Calvet[38], S. Calvet[38], T.P. Calvet[155], M. Calvetti[71a,71b], R. Camacho Toro[136], S. Camarda[36], D. Camarero Munoz[98], P. Camarri[73a,73b], D. Cameron[134], R. Caminal Armadans[102], C. Camincher[36], S. Campana[36], M. Campanelli[94], A. Camplani[40], A. Campoverde[151], V. Canale[69a,69b], A. Canesse[103], M. Cano Bret[60c], J. Cantero[129], T. Cao[161], Y. Cao[173], M.D.M. Capeans Garrido[36], M. Capua[41b,41a], R. Cardarelli[73a], F. Cardillo[149], G. Carducci[41b,41a], I. Carli[143], T. Carli[36], G. Carlino[69a], B.T. Carlson[139], L. Carminati[68a,68b], R.M.D. Carney[45a,45b], S. Caron[119], E. Carquin[147c], S. Carrá[46], J.W.S. Carter[167], M.P. Casado[14,e], A.F. Casha[167], D.W. Casper[171], R. Castelijn[120], F.L. Castillo[174], V. Castillo Gimenez[174], N.F. Castro[140a,140e], A. Catinaccio[36], J.R. Catmore[134], A. Cattai[36], J. Caudron[24], V. Cavaliere[29], E. Cavallaro[14], M. Cavalli-Sforza[14], V. Cavasinni[71a,71b], E. Celebi[12b], F. Ceradini[74a,74b], L. Cerda Alberich[174], K. Cerny[130], A.S. Cerqueira[80a], A. Cerri[156], L. Cerrito[73a,73b], F. Cerutti[18], A. Cervelli[23b,23a], S.A. Cetin[12b], Z. Chadi[35a], D. Chakraborty[121], S.K. Chan[59], W.S. Chan[120], W.Y. Chan[90], J.D. Chapman[32], B. Chargeishvili[159b], D.G. Charlton[21], T.P. Charman[92], C.C. Chau[34], S. Che[126], A. Chegwidden[106], S. Chekanov[6], S.V. Chekulaev[168a], G.A. Chelkov[79,az], M.A. Chelstowska[36], B. Chen[78], C. Chen[60a], C.H. Chen[78], H. Chen[29], J. Chen[60a], J. Chen[39], S. Chen[137], S.J. Chen[15c], X. Chen[15b,ay], Y. Chen[82], Y-H. Chen[46], H.C. Cheng[63a], H.J. Cheng[15a,15d], A. Cheplakov[79], E. Cheremushkina[123], R. Cherkaoui El Moursli[35e], E. Cheu[7], K. Cheung[64], T.J.A. Chevalérias[145], L. Chevalier[145], V. Chiarella[51], G. Chiarelli[71a], G. Chiodini[67a], A.S. Chisholm[36,21], A. Chitan[27b], I. Chiu[163], Y.H. Chiu[176], M.V. Chizhov[79], K. Choi[65], A.R. Chomont[72a,72b], S. Chouridou[162], Y.S. Chow[120], M.C. Chu[63a], X. Chu[15a], J. Chudoba[141], A.J. Chuinard[103], J.J. Chwastowski[84], L. Chytka[130], K.M. Ciesla[84], D. Cinca[47], V. Cindro[91], I.A. Cioară[27b], A. Ciocio[18], F. Cirotto[69a,69b], Z.H. Citron[180,l], M. Citterio[68a], D.A. Ciubotaru[27b], B.M. Ciungu[167], A. Clark[54], M.R. Clark[39], P.J. Clark[50], C. Clement[45a,45b], Y. Coadou[101], M. Cobal[66a,66c], A. Coccaro[55b], J. Cochran[78], H. Cohen[161], A.E.C. Coimbra[36], L. Colasurdo[119], B. Cole[39], A.P. Colijn[120], J. Collot[58], P. Conde Muiño[140a,f], E. Coniavitis[52],

JHEP12(2019)060

S.H. Connell[33b], I.A. Connelly[57], S. Constantinescu[27b], F. Conventi[69a,bb], A.M. Cooper-Sarkar[135], F. Cormier[175], K.J.R. Cormier[167], L.D. Corpe[94], M. Corradi[72a,72b], E.E. Corrigan[96], F. Corriveau[103,ag], A. Cortes-Gonzalez[36], M.J. Costa[174], F. Costanza[5], D. Costanzo[149], G. Cowan[93], J.W. Cowley[32], J. Crane[100], K. Cranmer[124], S.J. Crawley[57], R.A. Creager[137], S. Crépé-Renaudin[58], F. Crescioli[136], M. Cristinziani[24], V. Croft[120], G. Crosetti[41b,41a], A. Cueto[5], T. Cuhadar Donszelmann[149], A.R. Cukierman[153], S. Czekierda[84], P. Czodrowski[36], M.J. Da Cunha Sargedas De Sousa[60b], J.V. Da Fonseca Pinto[80b], C. Da Via[100], W. Dabrowski[83a], T. Dado[28a], S. Dahbi[35e], T. Dai[105], C. Dallapiccola[102], M. Dam[40], G. D'amen[23b,23a], V. D'Amico[74a,74b], J. Damp[99], J.R. Dandoy[137], M.F. Daneri[30], N.P. Dang[181,j], N.S. Dann[100], M. Danninger[175], V. Dao[36], G. Darbo[55b], O. Dartsi[5], A. Dattagupta[131], T. Daubney[46], S. D'Auria[68a,68b], W. Davey[24], C. David[46], T. Davidek[143], D.R. Davis[49], I. Dawson[149], K. De[8], R. De Asmundis[69a], M. De Beurs[120], S. De Castro[23b,23a], S. De Cecco[72a,72b], N. De Groot[119], P. de Jong[120], H. De la Torre[106], A. De Maria[15c], D. De Pedis[72a], A. De Salvo[72a], U. De Sanctis[73a,73b], M. De Santis[73a,73b], A. De Santo[156], K. De Vasconcelos Corga[101], J.B. De Vivie De Regie[132], C. Debenedetti[146], D.V. Dedovich[79], A.M. Deiana[42], M. Del Gaudio[41b,41a], J. Del Peso[98], Y. Delabat Diaz[46], D. Delgove[132], F. Deliot[145,s], C.M. Delitzsch[7], M. Della Pietra[69a,69b], D. Della Volpe[54], A. Dell'Acqua[36], L. Dell'Asta[73a,73b], M. Delmastro[5], C. Delporte[132], P.A. Delsart[58], D.A. DeMarco[167], S. Demers[183], M. Demichev[79], G. Demontigny[109], S.P. Denisov[123], D. Denysiuk[120], L. D'Eramo[136], D. Derendarz[84], J.E. Derkaoui[35d], F. Derue[136], P. Dervan[90], K. Desch[24], C. Deterre[46], K. Dette[167], C. Deutsch[24], M.R. Devesa[30], P.O. Deviveiros[36], A. Dewhurst[144], S. Dhaliwal[26], F.A. Di Bello[54], A. Di Ciaccio[73a,73b], L. Di Ciaccio[5], W.K. Di Clemente[137], C. Di Donato[69a,69b], A. Di Girolamo[36], G. Di Gregorio[71a,71b], B. Di Micco[74a,74b], R. Di Nardo[102], K.F. Di Petrillo[59], R. Di Sipio[167], D. Di Valentino[34], C. Diaconu[101], F.A. Dias[40], T. Dias Do Vale[140a], M.A. Diaz[147a], J. Dickinson[18], E.B. Diehl[105], J. Dietrich[19], S. Díez Cornell[46], A. Dimitrievska[18], W. Ding[15b], J. Dingfelder[24], F. Dittus[36], F. Djama[101], T. Djobava[159b], J.I. Djuvsland[17], M.A.B. Do Vale[80c], M. Dobre[27b], D. Dodsworth[26], C. Doglioni[96], J. Dolejsi[143], Z. Dolezal[143], M. Donadelli[80d], B. Dong[60c], J. Donini[38], A. D'onofrio[92], M. D'Onofrio[90], J. Dopke[144], A. Doria[69a], M.T. Dova[88], A.T. Doyle[57], E. Drechsler[152], E. Dreyer[152], T. Dreyer[53], A.S. Drobac[170], Y. Duan[60b], F. Dubinin[110], M. Dubovsky[28a], A. Dubreuil[54], E. Duchovni[180], G. Duckeck[114], A. Ducourthial[136], O.A. Ducu[109], D. Duda[115], A. Dudarev[36], A.C. Dudder[99], E.M. Duffield[18], L. Duflot[132], M. Dührssen[36], C. Dülsen[182], M. Dumancic[180], A.E. Dumitriu[27b], A.K. Duncan[57], M. Dunford[61a], A. Duperrin[101], H. Duran Yildiz[4a], M. Düren[56], A. Durglishvili[159b], D. Duschinger[48], B. Dutta[46], D. Duvnjak[1], G.I. Dyckes[137], M. Dyndal[36], S. Dysch[100], B.S. Dziedzic[84], K.M. Ecker[115], R.C. Edgar[105], M.G. Eggleston[49], T. Eifert[36], G. Eigen[17], K. Einsweiler[18], T. Ekelof[172], H. El Jarrari[35e], M. El Kacimi[35c], R. El Kosseifi[101], V. Ellajosyula[172], M. Ellert[172], F. Ellinghaus[182], A.A. Elliot[92], N. Ellis[36], J. Elmsheuser[29], M. Elsing[36], D. Emeliyanov[144], A. Emerman[39], Y. Enari[163], M.B. Epland[49], J. Erdmann[47], A. Ereditato[20], M. Errenst[36], M. Escalier[132], C. Escobar[174], O. Estrada Pastor[174], E. Etzion[161], H. Evans[65], A. Ezhilov[138], F. Fabbri[57], L. Fabbri[23b,23a], V. Fabiani[119], G. Facini[94], R.M. Faisca Rodrigues Pereira[140a], R.M. Fakhrutdinov[123], S. Falciano[72a], P.J. Falke[5], S. Falke[5], J. Faltova[143], Y. Fang[15a], Y. Fang[15a], G. Fanourakis[44], M. Fanti[68a,68b], M. Faraj[66a,66c,v], A. Farbin[8], A. Farilla[74a], E.M. Farina[70a,70b], T. Farooque[106], S. Farrell[18], S.M. Farrington[50], P. Farthouat[36], F. Fassi[35e], P. Fassnacht[36], D. Fassouliotis[9], M. Faucci Giannelli[50], W.J. Fawcett[32], L. Fayard[132], O.L. Fedin[138,q], W. Fedorko[175], M. Feickert[42], S. Feigl[134], L. Feligioni[101], A. Fell[149], C. Feng[60b], E.J. Feng[36], M. Feng[49], M.J. Fenton[57], A.B. Fenyuk[123], J. Ferrando[46], A. Ferrante[173], A. Ferrari[172], P. Ferrari[120], R. Ferrari[70a], D.E. Ferreira de Lima[61b], A. Ferrer[174], D. Ferrere[54], C. Ferretti[105], F. Fiedler[99], A. Filipčič[91], F. Filthaut[119], K.D. Finelli[25], M.C.N. Fiolhais[140a,140c,a],

JHEP12(2019)060

L. Fiorini[174], F. Fischer[114], W.C. Fisher[106], I. Fleck[151], P. Fleischmann[105], R.R.M. Fletcher[137], T. Flick[182], B.M. Flierl[114], L. Flores[137], L.R. Flores Castillo[63a], F.M. Follega[75a,75b], N. Fomin[17], J.H. Foo[167], G.T. Forcolin[75a,75b], A. Formica[145], F.A. Förster[14], A.C. Forti[100], A.G. Foster[21], M.G. Foti[135], D. Fournier[132], H. Fox[89], P. Francavilla[71a,71b], S. Francescato[72a,72b], M. Franchini[23b,23a], S. Franchino[61a], D. Francis[36], L. Franconi[20], M. Franklin[59], A.N. Fray[92], B. Freund[109], W.S. Freund[80b], E.M. Freundlich[47], D.C. Frizzell[128], D. Froidevaux[36], J.A. Frost[135], C. Fukunaga[164], E. Fullana Torregrosa[174], E. Fumagalli[55b,55a], T. Fusayasu[116], J. Fuster[174], A. Gabrielli[23b,23a], A. Gabrielli[18], G.P. Gach[83a], S. Gadatsch[54], P. Gadow[115], G. Gagliardi[55b,55a], L.G. Gagnon[109], C. Galea[27b], B. Galhardo[140a], G.E. Gallardo[135], E.J. Gallas[135], B.J. Gallop[144], G. Galster[40], R. Gamboa Goni[92], K.K. Gan[126], S. Ganguly[180], J. Gao[60a], Y. Gao[50], Y.S. Gao[31,n], C. García[174], J.E. García Navarro[174], J.A. García Pascual[15a], C. Garcia-Argos[52], M. Garcia-Sciveres[18], R.W. Gardner[37], N. Garelli[153], S. Gargiulo[52], V. Garonne[134], A. Gaudiello[55b,55a], G. Gaudio[70a], I.L. Gavrilenko[110], A. Gavrilyuk[111], C. Gay[175], G. Gaycken[46], E.N. Gazis[10], A.A. Geanta[27b], C.N.P. Gee[144], J. Geisen[53], M. Geisen[99], M.P. Geisler[61a], C. Gemme[55b], M.H. Genest[58], C. Geng[105], S. Gentile[72a,72b], S. George[93], T. Geralis[44], L.O. Gerlach[53], P. Gessinger-Befurt[99], G. Gessner[47], S. Ghasemi[151], M. Ghasemi Bostanabad[176], A. Ghosh[132], A. Ghosh[77], B. Giacobbe[23b], S. Giagu[72a,72b], N. Giangiacomi[23b,23a], P. Giannetti[71a], A. Giannini[69a,69b], S.M. Gibson[93], M. Gignac[146], D. Gillberg[34], G. Gilles[182], D.M. Gingrich[3,ba], M.P. Giordani[66a,66c], F.M. Giorgi[23b], P.F. Giraud[145], G. Giugliarelli[66a,66c], D. Giugni[68a], F. Giuli[73a,73b], S. Gkaitatzis[162], I. Gkialas[9,h], E.L. Gkougkousis[14], P. Gkountoumis[10], L.K. Gladilin[113], C. Glasman[98], J. Glatzer[14], P.C.F. Glaysher[46], A. Glazov[46], M. Goblirsch-Kolb[26], S. Goldfarb[104], T. Golling[54], D. Golubkov[123], A. Gomes[140a,140b], R. Goncalves Gama[53], R. Gonçalo[140a,140b], G. Gonella[52], L. Gonella[21], A. Gongadze[79], F. Gonnella[21], J.L. Gonski[59], S. González de la Hoz[174], S. Gonzalez-Sevilla[54], G.R. Gonzalvo Rodriguez[174], L. Goossens[36], P.A. Gorbounov[111], H.A. Gordon[29], B. Gorini[36], E. Gorini[67a,67b], A. Gorišek[91], A.T. Goshaw[49], M.I. Gostkin[79], C.A. Gottardo[119], M. Gouighri[35b], D. Goujdami[35c], A.G. Goussiou[148], N. Govender[33b], C. Goy[5], E. Gozani[160], I. Grabowska-Bold[83a], E.C. Graham[90], J. Gramling[171], E. Gramstad[134], S. Grancagnolo[19], M. Grandi[156], V. Gratchev[138], P.M. Gravila[27f], F.G. Gravili[67a,67b], C. Gray[57], H.M. Gray[18], C. Grefe[24], K. Gregersen[96], I.M. Gregor[46], P. Grenier[153], K. Grevtsov[46], C. Grieco[14], N.A. Grieser[128], J. Griffiths[8], A.A. Grillo[146], K. Grimm[31,m], S. Grinstein[14,aa], J.-F. Grivaz[132], S. Groh[99], E. Gross[180], J. Grosse-Knetter[53], Z.J. Grout[94], C. Grud[105], A. Grummer[118], L. Guan[105], W. Guan[181], J. Guenther[36], A. Guerguichon[132], J.G.R. Guerrero Rojas[174], F. Guescini[115], D. Guest[171], R. Gugel[52], T. Guillemin[5], S. Guindon[36], U. Gul[57], J. Guo[60c], W. Guo[105], Y. Guo[60a,u], Z. Guo[101], R. Gupta[46], S. Gurbuz[12c], G. Gustavino[128], P. Gutierrez[128], C. Gutschow[94], C. Guyot[145], C. Gwenlan[135], C.B. Gwilliam[90], A. Haas[124], C. Haber[18], H.K. Hadavand[8], N. Haddad[35e], A. Hadef[60a], S. Hageböck[36], M. Hagihara[169], M. Haleem[177], J. Haley[129], G. Halladjian[106], G.D. Hallewell[101], K. Hamacher[182], P. Hamal[130], K. Hamano[176], H. Hamdaoui[35e], G.N. Hamity[149], K. Han[60a,an], L. Han[60a], S. Han[15a,15d], K. Hanagaki[81,y], M. Hance[146], D.M. Handl[114], B. Haney[137], R. Hankache[136], E. Hansen[96], J.B. Hansen[40], J.D. Hansen[40], M.C. Hansen[24], P.H. Hansen[40], E.C. Hanson[100], K. Hara[169], A.S. Hard[181], T. Harenberg[182], S. Harkusha[107], P.F. Harrison[178], N.M. Hartmann[114], Y. Hasegawa[150], A. Hasib[50], S. Hassani[145], S. Haug[20], R. Hauser[106], L.B. Havener[39], M. Havranek[142], C.M. Hawkes[21], R.J. Hawkings[36], D. Hayden[106], C. Hayes[155], R.L. Hayes[175], C.P. Hays[135], J.M. Hays[92], H.S. Hayward[90], S.J. Haywood[144], F. He[60a], M.P. Heath[50], V. Hedberg[96], L. Heelan[8], S. Heer[24], K.K. Heidegger[52], W.D. Heidorn[78], J. Heilman[34], S. Heim[46], T. Heim[18], B. Heinemann[46,av], J.J. Heinrich[131], L. Heinrich[36], C. Heinz[56], J. Hejbal[141], L. Helary[61b], A. Held[175], S. Hellesund[134], C.M. Helling[146], S. Hellman[45a,45b], C. Helsens[36],

JHEP12(2019)060

R.C.W. Henderson[89], Y. Heng[181], S. Henkelmann[175], A.M. Henriques Correia[36], G.H. Herbert[19], H. Herde[26], V. Herget[177], Y. Hernández Jiménez[33c], H. Herr[99], M.G. Herrmann[114], T. Herrmann[48], G. Herten[52], R. Hertenberger[114], L. Hervas[36], T.C. Herwig[137], G.G. Hesketh[94], N.P. Hessey[168a], A. Higashida[163], S. Higashino[81], E. Higón-Rodriguez[174], K. Hildebrand[37], E. Hill[176], J.C. Hill[32], K.K. Hill[29], K.H. Hiller[46], S.J. Hillier[21], M. Hils[48], I. Hinchliffe[18], F. Hinterkeuser[24], M. Hirose[133], S. Hirose[52], D. Hirschbuehl[182], B. Hiti[91], O. Hladik[141], D.R. Hlaluku[33c], X. Hoad[50], J. Hobbs[155], N. Hod[180], M.C. Hodgkinson[149], A. Hoecker[36], F. Hoenig[114], D. Hohn[52], D. Hohov[132], T.R. Holmes[37], M. Holzbock[114], L.B.A.H Hommels[32], S. Honda[169], T. Honda[81], T.M. Hong[139], A. Hönle[115], B.H. Hooberman[173], W.H. Hopkins[6], Y. Horii[117], P. Horn[48], L.A. Horyn[37], A. Hostiuc[148], S. Hou[158], A. Hoummada[35a], J. Howarth[100], J. Hoya[88], M. Hrabovsky[130], J. Hrdinka[76], I. Hristova[19], J. Hrivnac[132], A. Hrynevich[108], T. Hryn'ova[5], P.J. Hsu[64], S.-C. Hsu[148], Q. Hu[29], S. Hu[60c], Y. Huang[15a], Z. Hubacek[142], F. Hubaut[101], M. Huebner[24], F. Huegging[24], T.B. Huffman[135], M. Huhtinen[36], R.F.H. Hunter[34], P. Huo[155], A.M. Hupe[34], N. Huseynov[79,ai], J. Huston[106], J. Huth[59], R. Hyneman[105], S. Hyrych[28a], G. Iacobucci[54], G. Iakovidis[29], I. Ibragimov[151], L. Iconomidou-Fayard[132], Z. Idrissi[35e], P. Iengo[36], R. Ignazzi[40], O. Igonkina[120,ac,*], R. Iguchi[163], T. Iizawa[54], Y. Ikegami[81], M. Ikeno[81], D. Iliadis[162], N. Ilic[119,167,ag], F. Iltzsche[48], G. Introzzi[70a,70b], M. Iodice[74a], K. Iordanidou[168a], V. Ippolito[72a,72b], M.F. Isacson[172], M. Ishino[163], M. Ishitsuka[165], W. Islam[129], C. Issever[135], S. Istin[160], F. Ito[169], J.M. Iturbe Ponce[63a], R. Iuppa[75a,75b], A. Ivina[180], H. Iwasaki[81], J.M. Izen[43], V. Izzo[69a], P. Jacka[141], P. Jackson[1], R.M. Jacobs[24], B.P. Jaeger[152], V. Jain[2], G. Jäkel[182], K.B. Jakobi[99], K. Jakobs[52], S. Jakobsen[76], T. Jakoubek[141], J. Jamieson[57], K.W. Janas[83a], R. Jansky[54], J. Janssen[24], M. Janus[53], P.A. Janus[83a], G. Jarlskog[96], N. Javadov[79,ai], T. Javůrek[36], M. Javurkova[52], F. Jeanneau[145], L. Jeanty[131], J. Jejelava[159a,aj], A. Jelinskas[178], P. Jenni[52,b], J. Jeong[46], N. Jeong[46], S. Jézéquel[5], H. Ji[181], J. Jia[155], H. Jiang[78], Y. Jiang[60a], Z. Jiang[153,r], S. Jiggins[52], F.A. Jimenez Morales[38], J. Jimenez Pena[115], S. Jin[15c], A. Jinaru[27b], O. Jinnouchi[165], H. Jivan[33c], P. Johansson[149], K.A. Johns[7], C.A. Johnson[65], K. Jon-And[45a,45b], R.W.L. Jones[89], S.D. Jones[156], S. Jones[7], T.J. Jones[90], J. Jongmanns[61a], P.M. Jorge[140a], J. Jovicevic[36], X. Ju[18], J.J. Junggeburth[115], A. Juste Rozas[14,aa], A. Kaczmarska[84], M. Kado[72a,72b], H. Kagan[126], M. Kagan[153], C. Kahra[99], T. Kaji[179], E. Kajomovitz[160], C.W. Kalderon[96], A. Kaluza[99], A. Kamenshchikov[123], L. Kanjir[91], Y. Kano[163], V.A. Kantserov[112], J. Kanzaki[81], L.S. Kaplan[181], D. Kar[33c], M.J. Kareem[168b], S.N. Karpov[79], Z.M. Karpova[79], V. Kartvelishvili[89], A.N. Karyukhin[123], L. Kashif[181], R.D. Kass[126], A. Kastanas[45a,45b], Y. Kataoka[163], C. Kato[60d,60c], J. Katzy[46], K. Kawade[82], K. Kawagoe[87], T. Kawaguchi[117], T. Kawamoto[163], G. Kawamura[53], E.F. Kay[176], V.F. Kazanin[122b,122a], R. Keeler[176], R. Kehoe[42], J.S. Keller[34], E. Kellermann[96], D. Kelsey[156], J.J. Kempster[21], J. Kendrick[21], O. Kepka[141], S. Kersten[182], B.P. Kerševan[91], S. Ketabchi Haghighat[167], M. Khader[173], F. Khalil-Zada[13], M. Khandoga[145], A. Khanov[129], A.G. Kharlamov[122b,122a], T. Kharlamova[122b,122a], E.E. Khoda[175], A. Khodinov[166], T.J. Khoo[54], E. Khramov[79], J. Khubua[159b], S. Kido[82], M. Kiehn[54], C.R. Kilby[93], Y.K. Kim[37], N. Kimura[94], O.M. Kind[19], B.T. King[90,*], D. Kirchmeier[48], J. Kirk[144], A.E. Kiryunin[115], T. Kishimoto[163], D.P. Kisliuk[167], V. Kitali[46], O. Kivernyk[5], E. Kladiva[28b,*], T. Klapdor-Kleingrothaus[52], M. Klassen[61a], M.H. Klein[105], M. Klein[90], U. Klein[90], K. Kleinknecht[99], P. Klimek[121], A. Klimentov[29], T. Klingl[24], T. Klioutchnikova[36], F.F. Klitzner[114], P. Kluit[120], S. Kluth[115], E. Kneringer[76], E.B.F.G. Knoops[101], A. Knue[52], D. Kobayashi[87], T. Kobayashi[163], M. Kobel[48], M. Kocian[153], P. Kodys[143], P.T. Koenig[24], T. Koffas[34], N.M. Köhler[36], T. Koi[153], M. Kolb[61b], I. Koletsou[5], T. Komarek[130], T. Kondo[81], N. Kondrashova[60c], K. Köneke[52], A.C. König[119], T. Kono[125], R. Konoplich[124,aq], V. Konstantinides[94], N. Konstantinidis[94], B. Konya[96], R. Kopeliansky[65], S. Koperny[83a], K. Korcyl[84], K. Kordas[162], G. Koren[161], A. Korn[94], I. Korolkov[14], E.V. Korolkova[149], N. Korotkova[113], O. Kortner[115], S. Kortner[115], T. Kosek[143],

JHEP12(2019)060

V.V. Kostyukhin[24], A. Kotwal[49], A. Koulouris[10], A. Kourkoumeli-Charalampidi[70a,70b], C. Kourkoumelis[9], E. Kourlitis[149], V. Kouskoura[29], A.B. Kowalewska[84], R. Kowalewski[176], C. Kozakai[163], W. Kozanecki[145], A.S. Kozhin[123], V.A. Kramarenko[113], G. Kramberger[91], D. Krasnopevtsev[60a], M.W. Krasny[136], A. Krasznahorkay[36], D. Krauss[115], J.A. Kremer[83a], J. Kretzschmar[90], P. Krieger[167], F. Krieter[114], A. Krishnan[61b], K. Krizka[18], K. Kroeninger[47], H. Kroha[115], J. Kroll[141], J. Kroll[137], J. Krstic[16], U. Kruchonak[79], H. Krüger[24], N. Krumnack[78], M.C. Kruse[49], J.A. Krzysiak[84], T. Kubota[104], O. Kuchinskaia[166], S. Kuday[4b], J.T. Kuechler[46], S. Kuehn[36], A. Kugel[61a], T. Kuhl[46], V. Kukhtin[79], R. Kukla[101], Y. Kulchitsky[107,am], S. Kuleshov[147c], Y.P. Kulinich[173], M. Kuna[58], T. Kunigo[85], A. Kupco[141], T. Kupfer[47], O. Kuprash[52], H. Kurashige[82], L.L. Kurchaninov[168a], Y.A. Kurochkin[107], A. Kurova[112], M.G. Kurth[15a,15d], E.S. Kuwertz[36], M. Kuze[165], A.K. Kvam[148], J. Kvita[130], T. Kwan[103], A. La Rosa[115], L. La Rotonda[41b,41a], F. La Ruffa[41b,41a], C. Lacasta[174], F. Lacava[72a,72b], D.P.J. Lack[100], H. Lacker[19], D. Lacour[136], E. Ladygin[79], R. Lafaye[5], B. Laforge[136], T. Lagouri[33c], S. Lai[53], S. Lammers[65], W. Lampl[7], C. Lampoudis[162], E. Lançon[29], U. Landgraf[52], M.P.J. Landon[92], M.C. Lanfermann[54], V.S. Lang[46], J.C. Lange[53], R.J. Langenberg[36], A.J. Lankford[171], F. Lanni[29], K. Lantzsch[24], A. Lanza[70a], A. Lapertosa[55b,55a], S. Laplace[136], J.F. Laporte[145], T. Lari[68a], F. Lasagni Manghi[23b,23a], M. Lassnig[36], T.S. Lau[63a], A. Laudrain[132], A. Laurier[34], M. Lavorgna[69a,69b], M. Lazzaroni[68a,68b], B. Le[104], E. Le Guirriec[101], M. LeBlanc[7], T. LeCompte[6], F. Ledroit-Guillon[58], C.A. Lee[29], G.R. Lee[17], L. Lee[59], S.C. Lee[158], S.J. Lee[34], B. Lefebvre[168a], M. Lefebvre[176], F. Legger[114], C. Leggett[18], K. Lehmann[152], N. Lehmann[182], G. Lehmann Miotto[36], W.A. Leight[46], A. Leisos[162,z], M.A.L. Leite[80d], C.E. Leitgeb[114], R. Leitner[143], D. Lellouch[180,*], K.J.C. Leney[42], T. Lenz[24], B. Lenzi[36], R. Leone[7], S. Leone[71a], C. Leonidopoulos[50], A. Leopold[136], G. Lerner[156], C. Leroy[109], R. Les[167], C.G. Lester[32], M. Levchenko[138], J. Levêque[5], D. Levin[105], L.J. Levinson[180], D.J. Lewis[21], B. Li[15b], B. Li[105], C-Q. Li[60a], F. Li[60c], H. Li[60a], H. Li[60b], J. Li[60c], K. Li[153], L. Li[60c], M. Li[15a], Q. Li[15a,15d], Q.Y. Li[60a], S. Li[60d,60c], X. Li[46], Y. Li[46], Z. Li[60b], Z. Liang[15a], B. Liberti[73a], A. Liblong[167], K. Lie[63c], S. Liem[120], C.Y. Lin[32], K. Lin[106], T.H. Lin[99], R.A. Linck[65], J.H. Lindon[21], A.L. Lionti[54], E. Lipeles[137], A. Lipniacka[17], M. Lisovyi[61b], T.M. Liss[173,ax], A. Lister[175], A.M. Litke[146], J.D. Little[8], B. Liu[78,af], B.L Liu[6], H.B. Liu[29], H. Liu[105], J.B. Liu[60a], J.K.K. Liu[135], K. Liu[136], M. Liu[60a], P. Liu[18], Y. Liu[15a,15d], Y.L. Liu[105], Y.W. Liu[60a], M. Livan[70a,70b], A. Lleres[58], J. Llorente Merino[15a], S.L. Lloyd[92], C.Y. Lo[63b], F. Lo Sterzo[42], E.M. Lobodzinska[46], P. Loch[7], S. Loffredo[73a,73b], T. Lohse[19], K. Lohwasser[149], M. Lokajicek[141], J.D. Long[173], R.E. Long[89], L. Longo[36], K.A. Looper[126], J.A. Lopez[147c], I. Lopez Paz[100], A. Lopez Solis[149], J. Lorenz[114], N. Lorenzo Martinez[5], M. Losada[22], P.J. Lösel[114], A. Lösle[52], X. Lou[46], X. Lou[15a], A. Lounis[132], J. Love[6], P.A. Love[89], J.J. Lozano Bahilo[174], M. Lu[60a], Y.J. Lu[64], H.J. Lubatti[148], C. Luci[72a,72b], A. Lucotte[58], C. Luedtke[52], F. Luehring[65], I. Luise[136], L. Luminari[72a], B. Lund-Jensen[154], M.S. Lutz[102], D. Lynn[29], R. Lysak[141], E. Lytken[96], F. Lyu[15a], V. Lyubushkin[79], T. Lyubushkina[79], H. Ma[29], L.L. Ma[60b], Y. Ma[60b], G. Maccarrone[51], A. Macchiolo[115], C.M. Macdonald[149], J. Machado Miguens[137], D. Madaffari[174], R. Madar[38], W.F. Mader[48], N. Madysa[48], J. Maeda[82], K. Maekawa[163], S. Maeland[17], T. Maeno[29], M. Maerker[48], A.S. Maevskiy[113], V. Magerl[52], N. Magini[78], D.J. Mahon[39], C. Maidantchik[80b], T. Maier[114], A. Maio[140a,140b,140d], K. Maj[84], O. Majersky[28a], S. Majewski[131], Y. Makida[81], N. Makovec[132], B. Malaescu[136], Pa. Malecki[84], V.P. Maleev[138], F. Malek[58], U. Mallik[77], D. Malon[6], C. Malone[32], S. Maltezos[10], S. Malyukov[79], J. Mamuzic[174], G. Mancini[51], I. Mandić[91], L. Manhaes de Andrade Filho[80a], I.M. Maniatis[162], J. Manjarres Ramos[48], K.H. Mankinen[96], A. Mann[114], A. Manousos[76], B. Mansoulie[145], I. Manthos[162], S. Manzoni[120], A. Marantis[162], G. Marceca[30], L. Marchese[135], G. Marchiori[136], M. Marcisovsky[141], C. Marcon[96], C.A. Marin Tobon[36], M. Marjanovic[38], Z. Marshall[18], M.U.F Martensson[172], S. Marti-Garcia[174],

JHEP12(2019)060

C.B. Martin[126], T.A. Martin[178], V.J. Martin[50], B. Martin dit Latour[17], L. Martinelli[74a,74b], M. Martinez[14,aa], V.I. Martinez Outschoorn[102], S. Martin-Haugh[144], V.S. Martoiu[27b], A.C. Martyniuk[94], A. Marzin[36], S.R. Maschek[115], L. Masetti[99], T. Mashimo[163], R. Mashinistov[110], J. Masik[100], A.L. Maslennikov[122b,122a], L.H. Mason[104], L. Massa[73a,73b], P. Massarotti[69a,69b], P. Mastrandrea[71a,71b], A. Mastroberardino[41b,41a], T. Masubuchi[163], D. Matakias[10], A. Matic[114], P. Mättig[24], J. Maurer[27b], B. Maček[91], D.A. Maximov[122b,122a], R. Mazini[158], I. Maznas[162], S.M. Mazza[146], S.P. Mc Kee[105], T.G. McCarthy[115], L.I. McClymont[94], W.P. McCormack[18], E.F. McDonald[104], J.A. Mcfayden[36], M.A. McKay[42], K.D. McLean[176], S.J. McMahon[144], P.C. McNamara[104], C.J. McNicol[178], R.A. McPherson[176,ag], J.E. Mdhluli[33c], Z.A. Meadows[102], S. Meehan[148], T. Megy[52], S. Mehlhase[114], A. Mehta[90], T. Meideck[58], B. Meirose[43], D. Melini[174], B.R. Mellado Garcia[33c], J.D. Mellenthin[53], M. Melo[28a], F. Meloni[46], A. Melzer[24], S.B. Menary[100], E.D. Mendes Gouveia[140a,140e], L. Meng[36], X.T. Meng[105], S. Menke[115], E. Meoni[41b,41a], S. Mergelmeyer[19], S.A.M. Merkt[139], C. Merlassino[20], P. Mermod[54], L. Merola[69a,69b], C. Meroni[68a], O. Meshkov[113,110], J.K.R. Meshreki[151], A. Messina[72a,72b], J. Metcalfe[6], A.S. Mete[171], C. Meyer[65], J. Meyer[160], J-P. Meyer[145], H. Meyer Zu Theenhausen[61a], F. Miano[156], M. Michetti[19], R.P. Middleton[144], L. Mijović[50], G. Mikenberg[180], M. Mikestikova[141], M. Mikuž[91], H. Mildner[149], M. Milesi[104], A. Milic[167], D.A. Millar[92], D.W. Miller[37], A. Milov[180], D.A. Milstead[45a,45b], R.A. Mina[153,r], A.A. Minaenko[123], M. Miñano Moya[174], I.A. Minashvili[159b], A.I. Mincer[124], B. Mindur[83a], M. Mineev[79], Y. Minegishi[163], Y. Ming[181], L.M. Mir[14], A. Mirto[67a,67b], K.P. Mistry[137], T. Mitani[179], J. Mitrevski[114], V.A. Mitsou[174], M. Mittal[60c], O. Miu[167], A. Miucci[20], P.S. Miyagawa[149], A. Mizukami[81], J.U. Mjörnmark[96], T. Mkrtchyan[184], M. Mlynarikova[143], T. Moa[45a,45b], K. Mochizuki[109], P. Mogg[52], S. Mohapatra[39], R. Moles-Valls[24], M.C. Mondragon[106], K. Mönig[46], J. Monk[40], E. Monnier[101], A. Montalbano[152], J. Montejo Berlingen[36], M. Montella[94], F. Monticelli[88], S. Monzani[68a], N. Morange[132], D. Moreno[22], M. Moreno Llácer[36], C. Moreno Martinez[14], P. Morettini[55b], M. Morgenstern[120], S. Morgenstern[48], D. Mori[152], M. Morii[59], M. Morinaga[179], V. Morisbak[134], A.K. Morley[36], G. Mornacchi[36], A.P. Morris[94], L. Morvaj[155], P. Moschovakos[36], B. Moser[120], M. Mosidze[159b], T. Moskalets[145], H.J. Moss[149], J. Moss[31,o], K. Motohashi[165], E. Mountricha[36], E.J.W. Moyse[102], S. Muanza[101], J. Mueller[139], R.S.P. Mueller[114], D. Muenstermann[89], G.A. Mullier[96], J.L. Munoz Martinez[14], F.J. Munoz Sanchez[100], P. Murin[28b], W.J. Murray[178,144], A. Murrone[68a,68b], M. Muškinja[18], C. Mwewa[33a], A.G. Myagkov[123,ar], J. Myers[131], M. Myska[142], B.P. Nachman[18], O. Nackenhorst[47], A.Nag Nag[48], K. Nagai[135], K. Nagano[81], Y. Nagasaka[62], M. Nagel[52], E. Nagy[101], A.M. Nairz[36], Y. Nakahama[117], K. Nakamura[81], T. Nakamura[163], I. Nakano[127], H. Nanjo[133], F. Napolitano[61a], R.F. Naranjo Garcia[46], R. Narayan[42], I. Naryshkin[138], T. Naumann[46], G. Navarro[22], H.A. Neal[105,*], P.Y. Nechaeva[110], F. Nechansky[46], T.J. Neep[21], A. Negri[70a,70b], M. Negrini[23b], C. Nellist[53], M.E. Nelson[135], S. Nemecek[141], P. Nemethy[124], M. Nessi[36,d], M.S. Neubauer[173], M. Neumann[182], P.R. Newman[21], Y.S. Ng[19], Y.W.Y. Ng[171], H.D.N. Nguyen[101], T. Nguyen Manh[109], E. Nibigira[38], R.B. Nickerson[135], R. Nicolaidou[145], D.S. Nielsen[40], J. Nielsen[146], N. Nikiforou[11], V. Nikolaenko[123,ar], I. Nikolic-Audit[136], K. Nikolopoulos[21], P. Nilsson[29], H.R. Nindhito[54], Y. Ninomiya[81], A. Nisati[72a], N. Nishu[60c], R. Nisius[115], I. Nitsche[47], T. Nitta[179], T. Nobe[163], Y. Noguchi[85], I. Nomidis[136], M.A. Nomura[29], M. Nordberg[36], N. Norjoharuddeen[135], T. Novak[91], O. Novgorodova[48], R. Novotny[142], L. Nozka[130], K. Ntekas[171], E. Nurse[94], F.G. Oakham[34,ba], H. Oberlack[115], J. Ocariz[136], A. Ochi[82], I. Ochoa[39], J.P. Ochoa-Ricoux[147a], K. O'Connor[26], S. Oda[87], S. Odaka[81], S. Oerdek[53], A. Ogrodnik[83a], A. Oh[100], S.H. Oh[49], C.C. Ohm[154], H. Oide[55b,55a], M.L. Ojeda[167], H. Okawa[169], Y. Okazaki[85], Y. Okumura[163], T. Okuyama[81], A. Olariu[27b], L.F. Oleiro Seabra[140a], S.A. Olivares Pino[147a], D. Oliveira Damazio[29], J.L. Oliver[1], M.J.R. Olsson[171], A. Olszewski[84], J. Olszowska[84], D.C. O'Neil[152], A. Onofre[140a,140e], K. Onogi[117], P.U.E. Onyisi[11], H. Oppen[134],

JHEP12(2019)060

M.J. Oreglia[37], G.E. Orellana[88], D. Orestano[74a,74b], N. Orlando[14], R.S. Orr[167], V. O'Shea[57], R. Ospanov[60a], G. Otero y Garzon[30], H. Otono[87], P.S. Ott[61a], M. Ouchrif[35d], J. Ouellette[29], F. Ould-Saada[134], A. Ouraou[145], Q. Ouyang[15a], M. Owen[57], R.E. Owen[21], V.E. Ozcan[12c], N. Ozturk[8], J. Pacalt[130], H.A. Pacey[32], K. Pachal[49], A. Pacheco Pages[14], C. Padilla Aranda[14], S. Pagan Griso[18], M. Paganini[183], G. Palacino[65], S. Palazzo[50], S. Palestini[36], M. Palka[83b], D. Pallin[38], I. Panagoulias[10], C.E. Pandini[36], J.G. Panduro Vazquez[93], P. Pani[46], G. Panizzo[66a,66c], L. Paolozzi[54], C. Papadatos[109], K. Papageorgiou[9,h], A. Paramonov[6], D. Paredes Hernandez[63b], S.R. Paredes Saenz[135], B. Parida[166], T.H. Park[167], A.J. Parker[89], M.A. Parker[32], F. Parodi[55b,55a], E.W.P. Parrish[121], J.A. Parsons[39], U. Parzefall[52], L. Pascual Dominguez[136], V.R. Pascuzzi[167], J.M.P. Pasner[146], E. Pasqualucci[72a], S. Passaggio[55b], F. Pastore[93], P. Pasuwan[45a,45b], S. Pataraia[99], J.R. Pater[100], A. Pathak[181], T. Pauly[36], B. Pearson[115], M. Pedersen[134], L. Pedraza Diaz[119], R. Pedro[140a], T. Peiffer[53], S.V. Peleganchuk[122b,122a], O. Penc[141], H. Peng[60a], B.S. Peralva[80a], M.M. Perego[132], A.P. Pereira Peixoto[140a], D.V. Perepelitsa[29], F. Peri[19], L. Perini[68a,68b], H. Pernegger[36], S. Perrella[69a,69b], K. Peters[46], R.F.Y. Peters[100], B.A. Petersen[36], T.C. Petersen[40], E. Petit[101], A. Petridis[1], C. Petridou[162], P. Petroff[132], M. Petrov[135], F. Petrucci[74a,74b], M. Pettee[183], N.E. Pettersson[102], K. Petukhova[143], A. Peyaud[145], R. Pezoa[147c], L. Pezzotti[70a,70b], T. Pham[104], F.H. Phillips[106], P.W. Phillips[144], M.W. Phipps[173], G. Piacquadio[155], E. Pianori[18], A. Picazio[102], R.H. Pickles[100], R. Piegaia[30], D. Pietreanu[27b], J.E. Pilcher[37], A.D. Pilkington[100], M. Pinamonti[73a,73b], J.L. Pinfold[3], M. Pitt[180], L. Pizzimento[73a,73b], M.-A. Pleier[29], V. Pleskot[143], E. Plotnikova[79], P. Podberezko[122b,122a], R. Poettgen[96], R. Poggi[54], L. Poggioli[132], I. Pogrebnyak[106], D. Pohl[24], I. Pokharel[53], G. Polesello[70a], A. Poley[18], A. Policicchio[72a,72b], R. Polifka[143], A. Polini[23b], C.S. Pollard[46], V. Polychronakos[29], D. Ponomarenko[112], L. Pontecorvo[36], S. Popa[27a], G.A. Popeneciu[27d], D.M. Portillo Quintero[58], S. Pospisil[142], K. Potamianos[46], I.N. Potrap[79], C.J. Potter[32], H. Potti[11], T. Poulsen[96], J. Poveda[36], T.D. Powell[149], G. Pownall[46], M.E. Pozo Astigarraga[36], P. Pralavorio[101], S. Prell[78], D. Price[100], M. Primavera[67a], S. Prince[103], M.L. Proffitt[148], N. Proklova[112], K. Prokofiev[63c], F. Prokoshin[79], S. Protopopescu[29], J. Proudfoot[6], M. Przybycien[83a], D. Pudzha[138], A. Puri[173], P. Puzo[132], J. Qian[105], Y. Qin[100], A. Quadt[53], M. Queitsch-Maitland[46], A. Qureshi[1], P. Rados[104], F. Ragusa[68a,68b], G. Rahal[97], J.A. Raine[54], S. Rajagopalan[29], A. Ramirez Morales[92], K. Ran[15a,15d], T. Rashid[132], S. Raspopov[5], D.M. Rauch[46], F. Rauscher[114], S. Rave[99], B. Ravina[149], I. Ravinovich[180], J.H. Rawling[100], M. Raymond[36], A.L. Read[134], N.P. Readioff[58], M. Reale[67a,67b], D.M. Rebuzzi[70a,70b], A. Redelbach[177], G. Redlinger[29], K. Reeves[43], L. Rehnisch[19], J. Reichert[137], D. Reikher[161], A. Reiss[99], A. Rej[151], C. Rembser[36], M. Renda[27b], M. Rescigno[72a], S. Resconi[68a], E.D. Resseguie[137], S. Rettie[175], E. Reynolds[21], O.L. Rezanova[122b,122a], P. Reznicek[143], E. Ricci[75a,75b], R. Richter[115], S. Richter[46], E. Richter-Was[83b], O. Ricken[24], M. Ridel[136], P. Rieck[115], C.J. Riegel[182], O. Rifki[46], M. Rijssenbeek[155], A. Rimoldi[70a,70b], M. Rimoldi[46], L. Rinaldi[23b], G. Ripellino[154], B. Ristić[89], I. Riu[14], J.C. Rivera Vergara[176], F. Rizatdinova[129], E. Rizvi[92], C. Rizzi[36], R.T. Roberts[100], S.H. Robertson[103,ag], M. Robin[46], D. Robinson[32], J.E.M. Robinson[46], C.M. Robles Gajardo[147c], A. Robson[57], E. Rocco[99], C. Roda[71a,71b], S. Rodriguez Bosca[174], A. Rodriguez Perez[14], D. Rodriguez Rodriguez[174], A.M. Rodríguez Vera[168b], S. Roe[36], O. Røhne[134], R. Röhrig[115], C.P.A. Roland[65], J. Roloff[59], A. Romaniouk[112], M. Romano[23b,23a], N. Rompotis[90], M. Ronzani[124], L. Roos[136], S. Rosati[72a], K. Rosbach[52], G. Rosin[102], B.J. Rosser[137], E. Rossi[46], E. Rossi[74a,74b], E. Rossi[69a,69b], L.P. Rossi[55b], L. Rossini[68a,68b], R. Rosten[14], M. Rotaru[27b], J. Rothberg[148], D. Rousseau[132], G. Rovelli[70a,70b], A. Roy[11], D. Roy[33c], A. Rozanov[101], Y. Rozen[160], X. Ruan[33c], F. Rubbo[153], F. Rühr[52], A. Ruiz-Martinez[174], A. Rummler[36], Z. Rurikova[52], N.A. Rusakovich[79], H.L. Russell[103], L. Rustige[38,47], J.P. Rutherfoord[7],

JHEP12(2019)060

E.M. Rüttinger[46,k], M. Rybar[39], G. Rybkin[132], E.B. Rye[134], A. Ryzhov[123], G.F. Rzehorz[53], P. Sabatini[53], G. Sabato[120], S. Sacerdoti[132], H.F-W. Sadrozinski[146], R. Sadykov[79], F. Safai Tehrani[72a], B. Safarzadeh Samani[156], P. Saha[121], S. Saha[103], M. Sahinsoy[61a], A. Sahu[182], M. Saimpert[46], M. Saito[163], T. Saito[163], H. Sakamoto[163], A. Sakharov[124,aq], D. Salamani[54], G. Salamanna[74a,74b], J.E. Salazar Loyola[147c], P.H. Sales De Bruin[172], A. Salnikov[153], J. Salt[174], D. Salvatore[41b,41a], F. Salvatore[156], A. Salvucci[63a,63b,63c], A. Salzburger[36], J. Samarati[36], D. Sammel[52], D. Sampsonidis[162], D. Sampsonidou[162], J. Sánchez[174], A. Sanchez Pineda[66a,66c], H. Sandaker[134], C.O. Sander[46], I.G. Sanderswood[89], M. Sandhoff[182], C. Sandoval[22], D.P.C. Sankey[144], M. Sannino[55b,55a], Y. Sano[117], A. Sansoni[51], C. Santoni[38], H. Santos[140a,140b], S.N. Santpur[18], A. Santra[174], A. Sapronov[79], J.G. Saraiva[140a,140d], O. Sasaki[81], K. Sato[169], E. Sauvan[5], P. Savard[167,ba], N. Savic[115], R. Sawada[163], C. Sawyer[144], L. Sawyer[95,ao], C. Sbarra[23b], A. Sbrizzi[23a], T. Scanlon[94], J. Schaarschmidt[148], P. Schacht[115], B.M. Schachtner[114], D. Schaefer[37], L. Schaefer[137], J. Schaeffer[99], S. Schaepe[36], U. Schäfer[99], A.C. Schaffer[132], D. Schaile[114], R.D. Schamberger[155], N. Scharmberg[100], V.A. Schegelsky[138], D. Scheirich[143], F. Schenck[19], M. Schernau[171], C. Schiavi[55b,55a], S. Schier[146], L.K. Schildgen[24], Z.M. Schillaci[26], E.J. Schioppa[36], M. Schioppa[41b,41a], K.E. Schleicher[52], S. Schlenker[36], K.R. Schmidt-Sommerfeld[115], K. Schmieden[36], C. Schmitt[99], S. Schmitt[46], S. Schmitz[99], J.C. Schmoeckel[46], U. Schnoor[52], L. Schoeffel[145], A. Schoening[61b], P.G. Scholer[52], E. Schopf[135], M. Schott[99], J.F.P. Schouwenberg[119], J. Schovancova[36], S. Schramm[54], F. Schroeder[182], A. Schulte[99], H-C. Schultz-Coulon[61a], M. Schumacher[52], B.A. Schumm[146], Ph. Schune[145], A. Schwartzman[153], T.A. Schwarz[105], Ph. Schwemling[145], R. Schwienhorst[106], A. Sciandra[146], G. Sciolla[26], M. Scodeggio[46], M. Scornajenghi[41b,41a], F. Scuri[71a], F. Scutti[104], L.M. Scyboz[115], C.D. Sebastiani[72a,72b], P. Seema[19], S.C. Seidel[118], A. Seiden[146], T. Seiss[37], J.M. Seixas[80b], G. Sekhniaidze[69a], K. Sekhon[105], S.J. Sekula[42], N. Semprini-Cesari[23b,23a], S. Sen[49], S. Senkin[38], C. Serfon[76], L. Serin[132], L. Serkin[66a,66b], M. Sessa[60a], H. Severini[128], T. Šfiligoj[91], F. Sforza[170], A. Sfyrla[54], E. Shabalina[53], J.D. Shahinian[146], N.W. Shaikh[45a,45b], D. Shaked Renous[180], L.Y. Shan[15a], R. Shang[173], J.T. Shank[25], M. Shapiro[18], A. Sharma[135], A.S. Sharma[1], P.B. Shatalov[111], K. Shaw[156], S.M. Shaw[100], A. Shcherbakova[138], Y. Shen[128], N. Sherafati[34], A.D. Sherman[25], P. Sherwood[94], L. Shi[158,aw], S. Shimizu[81], C.O. Shimmin[183], Y. Shimogama[179], M. Shimojima[116], I.P.J. Shipsey[135], S. Shirabe[87], M. Shiyakova[79,ad], J. Shlomi[180], A. Shmeleva[110], M.J. Shochet[37], J. Shojaii[104], D.R. Shope[128], S. Shrestha[126], E.M. Shrif[33c], E. Shulga[180], P. Sicho[141], A.M. Sickles[173], P.E. Sidebo[154], E. Sideras Haddad[33c], O. Sidiropoulou[36], A. Sidoti[23b,23a], F. Siegert[48], Dj. Sijacki[16], M.Jr. Silva[181], M.V. Silva Oliveira[80a], S.B. Silverstein[45a], S. Simion[132], E. Simioni[99], R. Simoniello[99], S. Simsek[12b], P. Sinervo[167], V. Sinetckii[113,110], N.B. Sinev[131], M. Sioli[23b,23a], I. Siral[105], S.Yu. Sivoklokov[113], J. Sjölin[45a,45b], E. Skorda[96], P. Skubic[128], M. Slawinska[84], K. Sliwa[170], R. Slovak[143], V. Smakhtin[180], B.H. Smart[144], J. Smiesko[28a], N. Smirnov[112], S.Yu. Smirnov[112], Y. Smirnov[112], L.N. Smirnova[113,w], O. Smirnova[96], J.W. Smith[53], M. Smizanska[89], K. Smolek[142], A. Smykiewicz[84], A.A. Snesarev[110], H.L. Snoek[120], I.M. Snyder[131], S. Snyder[29], R. Sobie[176,ag], A.M. Soffa[171], A. Soffer[161], A. Søgaard[50], F. Sohns[53], C.A. Solans Sanchez[36], E.Yu. Soldatov[112], U. Soldevila[174], A.A. Solodkov[123], A. Soloshenko[79], O.V. Solovyanov[123], V. Solovyev[138], P. Sommer[149], H. Son[170], W. Song[144], W.Y. Song[168b], A. Sopczak[142], F. Sopkova[28b], C.L. Sotiropoulou[71a,71b], S. Sottocornola[70a,70b], R. Soualah[66a,66c,g], A.M. Soukharev[122b,122a], D. South[46], S. Spagnolo[67a,67b], M. Spalla[115], M. Spangenberg[178], F. Spanò[93], D. Sperlich[52], T.M. Spieker[61a], R. Spighi[23b], G. Spigo[36], M. Spina[156], D.P. Spiteri[57], M. Spousta[143], A. Stabile[68a,68b], B.L. Stamas[121], R. Stamen[61a], M. Stamenkovic[120], E. Stanecka[84], R.W. Stanek[6], B. Stanislaus[135], M.M. Stanitzki[46], M. Stankaityte[135], B. Stapf[120], E.A. Starchenko[123], G.H. Stark[146], J. Stark[58], S.H. Stark[40], P. Staroba[141], P. Starovoitov[61a],

JHEP12(2019)060

S. Stärz[103], R. Staszewski[84], G. Stavropoulos[44], M. Stegler[46], P. Steinberg[29], A.L. Steinhebel[131], B. Stelzer[152], H.J. Stelzer[139], O. Stelzer-Chilton[168a], H. Stenzel[56], T.J. Stevenson[156], G.A. Stewart[36], M.C. Stockton[36], G. Stoicea[27b], M. Stolarski[140a], P. Stolte[53], S. Stonjek[115], A. Straessner[48], J. Strandberg[154], S. Strandberg[45a,45b], M. Strauss[128], P. Strizenec[28b], R. Ströhmer[177], D.M. Strom[131], R. Stroynowski[42], A. Strubig[50], S.A. Stucci[29], B. Stugu[17], J. Stupak[128], N.A. Styles[46], D. Su[153], S. Suchek[61a], V.V. Sulin[110], M.J. Sullivan[90], D.M.S. Sultan[54], S. Sultansoy[4c], T. Sumida[85], S. Sun[105], X. Sun[3], K. Suruliz[156], C.J.E. Suster[157], M.R. Sutton[156], S. Suzuki[81], M. Svatos[141], M. Swiatlowski[37], S.P. Swift[2], T. Swirski[177], A. Sydorenko[99], I. Sykora[28a], M. Sykora[143], T. Sykora[143], D. Ta[99], K. Tackmann[46,ab], J. Taenzer[161], A. Taffard[171], R. Tafirout[168a], H. Takai[29], R. Takashima[86], K. Takeda[82], T. Takeshita[150], E.P. Takeva[50], Y. Takubo[81], M. Talby[101], A.A. Talyshev[122b,122a], N.M. Tamir[161], J. Tanaka[163], M. Tanaka[165], R. Tanaka[132], S. Tapia Araya[173], S. Tapprogge[99], A. Tarek Abouelfadl Mohamed[136], S. Tarem[160], G. Tarna[27b,c], G.F. Tartarelli[68a], P. Tas[143], M. Tasevsky[141], T. Tashiro[85], E. Tassi[41b,41a], A. Tavares Delgado[140a,140b], Y. Tayalati[35e], A.J. Taylor[50], G.N. Taylor[104], W. Taylor[168b], H. Teagle[90], A.S. Tee[89], R. Teixeira De Lima[153], P. Teixeira-Dias[93], H. Ten Kate[36], J.J. Teoh[120], S. Terada[81], K. Terashi[163], J. Terron[98], S. Terzo[14], M. Testa[51], R.J. Teuscher[167,ag], S.J. Thais[183], T. Theveneaux-Pelzer[46], F. Thiele[40], D.W. Thomas[93], J.O. Thomas[42], J.P. Thomas[21], A.S. Thompson[57], P.D. Thompson[21], L.A. Thomsen[183], E. Thomson[137], E.J. Thorpe[92], Y. Tian[39], R.E. Ticse Torres[53], V.O. Tikhomirov[110,as], Yu.A. Tikhonov[122b,122a], S. Timoshenko[112], P. Tipton[183], S. Tisserant[101], K. Todome[23b,23a], S. Todorova-Nova[5], S. Todt[48], J. Tojo[87], S. Tokár[28a], K. Tokushuku[81], E. Tolley[126], K.G. Tomiwa[33c], M. Tomoto[117], L. Tompkins[153,r], B. Tong[59], P. Tornambe[102], E. Torrence[131], H. Torres[48], E. Torró Pastor[148], C. Tosciri[135], J. Toth[101,ae], D.R. Tovey[149], A. Traeet[17], C.J. Treado[124], T. Trefzger[177], F. Tresoldi[156], A. Tricoli[29], I.M. Trigger[168a], S. Trincaz-Duvoid[136], W. Trischuk[167], B. Trocmé[58], A. Trofymov[145], C. Troncon[68a], M. Trovatelli[176], F. Trovato[156], L. Truong[33b], M. Trzebinski[84], A. Trzupek[84], F. Tsai[46], J.C-L. Tseng[135], P.V. Tsiareshka[107,am], A. Tsirigotis[162], N. Tsirintanis[9], V. Tsiskaridze[155], E.G. Tskhadadze[159a], M. Tsopoulou[162], I.I. Tsukerman[111], V. Tsulaia[18], S. Tsuno[81], D. Tsybychev[155], Y. Tu[63b], A. Tudorache[27b], V. Tudorache[27b], T.T. Tulbure[27a], A.N. Tuna[59], S. Turchikhin[79], D. Turgeman[180], I. Turk Cakir[4b,x], R.J. Turner[21], R.T. Turra[68a], P.M. Tuts[39], S. Tzamarias[162], E. Tzovara[99], G. Ucchielli[47], K. Uchida[163], I. Ueda[81], M. Ughetto[45a,45b], F. Ukegawa[169], G. Unal[36], A. Undrus[29], G. Unel[171], F.C. Ungaro[104], Y. Unno[81], K. Uno[163], J. Urban[28b], P. Urquijo[104], G. Usai[8], J. Usui[81], Z. Uysal[12d], L. Vacavant[101], V. Vacek[142], B. Vachon[103], K.O.H. Vadla[134], A. Vaidya[94], C. Valderanis[114], E. Valdes Santurio[45a,45b], M. Valente[54], S. Valentinetti[23b,23a], A. Valero[174], L. Valéry[46], R.A. Vallance[21], A. Vallier[36], J.A. Valls Ferrer[174], T.R. Van Daalen[14], P. Van Gemmeren[6], I. Van Vulpen[120], M. Vanadia[73a,73b], W. Vandelli[36], A. Vaniachine[166], D. Vannicola[72a,72b], R. Vari[72a], E.W. Varnes[7], C. Varni[55b,55a], T. Varol[42], D. Varouchas[132], K.E. Varvell[157], M.E. Vasile[27b], G.A. Vasquez[176], J.G. Vasquez[183], F. Vazeille[38], D. Vazquez Furelos[14], T. Vazquez Schroeder[36], J. Veatch[53], V. Vecchio[74a,74b], M.J. Veen[120], L.M. Veloce[167], F. Veloso[140a,140c], S. Veneziano[72a], A. Ventura[67a,67b], N. Venturi[36], A. Verbytskyi[115], V. Vercesi[70a], M. Verducci[71a,71b], C.M. Vergel Infante[78], C. Vergis[24], W. Verkerke[120], A.T. Vermeulen[120], J.C. Vermeulen[120], M.C. Vetterli[152,ba], N. Viaux Maira[147c], M. Vicente Barreto Pinto[54], T. Vickey[149], O.E. Vickey Boeriu[149], G.H.A. Viehhauser[135], L. Vigani[61b], M. Villa[23b,23a], M. Villaplana Perez[68a,68b], E. Vilucchi[51], M.G. Vincter[34], V.B. Vinogradov[79], A. Vishwakarma[46], C. Vittori[23b,23a], I. Vivarelli[156], M. Vogel[182], P. Vokac[142], S.E. von Buddenbrock[33c], E. Von Toerne[24], V. Vorobel[143], K. Vorobev[112], M. Vos[174], J.H. Vossebeld[90], M. Vozak[100], N. Vranjes[16], M. Vranjes Milosavljevic[16], V. Vrba[142], M. Vreeswijk[120], R. Vuillermet[36], I. Vukotic[37], P. Wagner[24], W. Wagner[182], J. Wagner-Kuhr[114],

JHEP12(2019)060

S. Wahdan[182], H. Wahlberg[88], K. Wakamiya[82], V.M. Walbrecht[115], J. Walder[89], R. Walker[114], S.D. Walker[93], W. Walkowiak[151], V. Wallangen[45a,45b], A.M. Wang[59], C. Wang[60c], C. Wang[60b], F. Wang[181], H. Wang[18], H. Wang[3], J. Wang[157], J. Wang[61b], P. Wang[42], Q. Wang[128], R.-J. Wang[99], R. Wang[60a], R. Wang[6], S.M. Wang[158], W.T. Wang[60a], W. Wang[15c,ah], W.X. Wang[60a,ah], Y. Wang[60a,ap], Z. Wang[60c], C. Wanotayaroj[46], A. Warburton[103], C.P. Ward[32], D.R. Wardrope[94], N. Warrack[57], A. Washbrook[50], A.T. Watson[21], M.F. Watson[21], G. Watts[148], B.M. Waugh[94], A.F. Webb[11], S. Webb[99], C. Weber[183], M.S. Weber[20], S.A. Weber[34], S.M. Weber[61a], A.R. Weidberg[135], J. Weingarten[47], M. Weirich[99], C. Weiser[52], P.S. Wells[36], T. Wenaus[29], T. Wengler[36], S. Wenig[36], N. Wermes[24], M.D. Werner[78], M. Wessels[61a], T.D. Weston[20], K. Whalen[131], N.L. Whallon[148], A.M. Wharton[89], A.S. White[105], A. White[8], M.J. White[1], D. Whiteson[171], B.W. Whitmore[89], W. Wiedenmann[181], M. Wielers[144], N. Wieseotte[99], C. Wiglesworth[40], L.A.M. Wiik-Fuchs[52], F. Wilk[100], H.G. Wilkens[36], L.J. Wilkins[93], H.H. Williams[137], S. Williams[32], C. Willis[106], S. Willocq[102], J.A. Wilson[21], I. Wingerter-Seez[5], E. Winkels[156], F. Winklmeier[131], O.J. Winston[156], B.T. Winter[52], M. Wittgen[153], M. Wobisch[95], A. Wolf[99], T.M.H. Wolf[120], R. Wolff[101], R.W. Wölker[135], J. Wollrath[52], M.W. Wolter[84], H. Wolters[140a,140c], V.W.S. Wong[175], N.L. Woods[146], S.D. Worm[21], B.K. Wosiek[84], K.W. Woźniak[84], K. Wraight[57], S.L. Wu[181], X. Wu[54], Y. Wu[60a], T.R. Wyatt[100], B.M. Wynne[50], S. Xella[40], Z. Xi[105], L. Xia[178], D. Xu[15a], H. Xu[60a,c], L. Xu[29], T. Xu[145], W. Xu[105], Z. Xu[60b], Z. Xu[153], B. Yabsley[157], S. Yacoob[33a], K. Yajima[133], D.P. Yallup[94], D. Yamaguchi[165], Y. Yamaguchi[165], A. Yamamoto[81], F. Yamane[82], M. Yamatani[163], T. Yamazaki[163], Y. Yamazaki[82], Z. Yan[25], H.J. Yang[60c,60d], H.T. Yang[18], S. Yang[77], X. Yang[60b,58], Y. Yang[163], W-M. Yao[18], Y.C. Yap[46], Y. Yasu[81], E. Yatsenko[60c,60d], J. Ye[42], S. Ye[29], I. Yeletskikh[79], M.R. Yexley[89], E. Yigitbasi[25], K. Yorita[179], K. Yoshihara[137], C.J.S. Young[36], C. Young[153], J. Yu[78], R. Yuan[60b,i], X. Yue[61a], S.P.Y. Yuen[24], B. Zabinski[84], G. Zacharis[10], E. Zaffaroni[54], J. Zahreddine[136], A.M. Zaitsev[123,ar], T. Zakareishvili[159b], N. Zakharchuk[34], S. Zambito[59], D. Zanzi[36], D.R. Zaripovas[57], S.V. Zeißner[47], C. Zeitnitz[182], G. Zemaityte[135], J.C. Zeng[173], O. Zenin[123], T. Ženiš[28a], D. Zerwas[132], M. Zgubič[135], D.F. Zhang[15b], F. Zhang[181], G. Zhang[15b], H. Zhang[15c], J. Zhang[6], L. Zhang[15c], L. Zhang[60a], M. Zhang[173], R. Zhang[24], X. Zhang[60b], Y. Zhang[15a,15d], Z. Zhang[63a], Z. Zhang[132], P. Zhao[49], Y. Zhao[60b], Z. Zhao[60a], A. Zhemchugov[79], Z. Zheng[105], D. Zhong[173], B. Zhou[105], C. Zhou[181], M.S. Zhou[15a,15d], M. Zhou[155], N. Zhou[60c], Y. Zhou[7], C.G. Zhu[60b], H.L. Zhu[60a], H. Zhu[15a], J. Zhu[105], Y. Zhu[60a], X. Zhuang[15a], K. Zhukov[110], V. Zhulanov[122b,122a], D. Zieminska[65], N.I. Zimine[79], S. Zimmermann[52], Z. Zinonos[115], M. Ziolkowski[151], L. Živković[16], G. Zobernig[181], A. Zoccoli[23b,23a], K. Zoch[53], T.G. Zorbas[149], R. Zou[37] and L. Zwalinski[36]

[1] *Department of Physics, University of Adelaide, Adelaide; Australia*
[2] *Physics Department, SUNY Albany, Albany NY; United States of America*
[3] *Department of Physics, University of Alberta, Edmonton AB; Canada*
[4] [(a)] *Department of Physics, Ankara University, Ankara;* [(b)] *Istanbul Aydin University, Istanbul;* [(c)] *Division of Physics, TOBB University of Economics and Technology, Ankara; Turkey*
[5] *LAPP, Université Grenoble Alpes, Université Savoie Mont Blanc, CNRS/IN2P3, Annecy; France*
[6] *High Energy Physics Division, Argonne National Laboratory, Argonne IL; United States of America*
[7] *Department of Physics, University of Arizona, Tucson AZ; United States of America*
[8] *Department of Physics, University of Texas at Arlington, Arlington TX; United States of America*
[9] *Physics Department, National and Kapodistrian University of Athens, Athens; Greece*
[10] *Physics Department, National Technical University of Athens, Zografou; Greece*
[11] *Department of Physics, University of Texas at Austin, Austin TX; United States of America*
[12] [(a)] *Bahcesehir University, Faculty of Engineering and Natural Sciences, Istanbul;* [(b)] *Istanbul Bilgi University, Faculty of Engineering and Natural Sciences, Istanbul;* [(c)] *Department of Physics,*

JHEP12(2019)060

Bogazici University, Istanbul;[(d)] *Department of Physics Engineering, Gaziantep University, Gaziantep; Turkey*

[13] *Institute of Physics, Azerbaijan Academy of Sciences, Baku; Azerbaijan*

[14] *Institut de Física d'Altes Energies (IFAE), Barcelona Institute of Science and Technology, Barcelona; Spain*

[15] [(a)] *Institute of High Energy Physics, Chinese Academy of Sciences, Beijing;*[(b)] *Physics Department, Tsinghua University, Beijing;*[(c)] *Department of Physics, Nanjing University, Nanjing;*[(d)] *University of Chinese Academy of Science (UCAS), Beijing; China*

[16] *Institute of Physics, University of Belgrade, Belgrade; Serbia*

[17] *Department for Physics and Technology, University of Bergen, Bergen; Norway*

[18] *Physics Division, Lawrence Berkeley National Laboratory and University of California, Berkeley CA; United States of America*

[19] *Institut für Physik, Humboldt Universität zu Berlin, Berlin; Germany*

[20] *Albert Einstein Center for Fundamental Physics and Laboratory for High Energy Physics, University of Bern, Bern; Switzerland*

[21] *School of Physics and Astronomy, University of Birmingham, Birmingham; United Kingdom*

[22] *Facultad de Ciencias y Centro de Investigaciónes, Universidad Antonio Nariño, Bogota; Colombia*

[23] [(a)] *INFN Bologna and Universita' di Bologna, Dipartimento di Fisica;*[(b)] *INFN Sezione di Bologna; Italy*

[24] *Physikalisches Institut, Universität Bonn, Bonn; Germany*

[25] *Department of Physics, Boston University, Boston MA; United States of America*

[26] *Department of Physics, Brandeis University, Waltham MA; United States of America*

[27] [(a)] *Transilvania University of Brasov, Brasov;*[(b)] *Horia Hulubei National Institute of Physics and Nuclear Engineering, Bucharest;*[(c)] *Department of Physics, Alexandru Ioan Cuza University of Iasi, Iasi;*[(d)] *National Institute for Research and Development of Isotopic and Molecular Technologies, Physics Department, Cluj-Napoca;*[(e)] *University Politehnica Bucharest, Bucharest;*[(f)] *West University in Timisoara, Timisoara; Romania*

[28] [(a)] *Faculty of Mathematics, Physics and Informatics, Comenius University, Bratislava;*[(b)] *Department of Subnuclear Physics, Institute of Experimental Physics of the Slovak Academy of Sciences, Kosice; Slovak Republic*

[29] *Physics Department, Brookhaven National Laboratory, Upton NY; United States of America*

[30] *Departamento de Física, Universidad de Buenos Aires, Buenos Aires; Argentina*

[31] *California State University, CA; United States of America*

[32] *Cavendish Laboratory, University of Cambridge, Cambridge; United Kingdom*

[33] [(a)] *Department of Physics, University of Cape Town, Cape Town;*[(b)] *Department of Mechanical Engineering Science, University of Johannesburg, Johannesburg;*[(c)] *School of Physics, University of the Witwatersrand, Johannesburg; South Africa*

[34] *Department of Physics, Carleton University, Ottawa ON; Canada*

[35] [(a)] *Faculté des Sciences Ain Chock, Réseau Universitaire de Physique des Hautes Energies — Université Hassan II, Casablanca;*[(b)] *Faculté des Sciences, Université Ibn-Tofail, Kénitra;*[(c)] *Faculté des Sciences Semlalia, Université Cadi Ayyad, LPHEA-Marrakech;*[(d)] *Faculté des Sciences, Université Mohamed Premier and LPTPM, Oujda;*[(e)] *Faculté des sciences, Université Mohammed V, Rabat; Morocco*

[36] *CERN, Geneva; Switzerland*

[37] *Enrico Fermi Institute, University of Chicago, Chicago IL; United States of America*

[38] *LPC, Université Clermont Auvergne, CNRS/IN2P3, Clermont-Ferrand; France*

[39] *Nevis Laboratory, Columbia University, Irvington NY; United States of America*

[40] *Niels Bohr Institute, University of Copenhagen, Copenhagen; Denmark*

[41] [(a)] *Dipartimento di Fisica, Università della Calabria, Rende;*[(b)] *INFN Gruppo Collegato di Cosenza, Laboratori Nazionali di Frascati; Italy*

[42] *Physics Department, Southern Methodist University, Dallas TX; United States of America*

[43] *Physics Department, University of Texas at Dallas, Richardson TX; United States of America*

JHEP12(2019)060

[44] National Centre for Scientific Research "Demokritos", Agia Paraskevi; Greece
[45] [(a)] Department of Physics, Stockholm University; [(b)] Oskar Klein Centre, Stockholm; Sweden
[46] Deutsches Elektronen-Synchrotron DESY, Hamburg and Zeuthen; Germany
[47] Lehrstuhl für Experimentelle Physik IV, Technische Universität Dortmund, Dortmund; Germany
[48] Institut für Kern- und Teilchenphysik, Technische Universität Dresden, Dresden; Germany
[49] Department of Physics, Duke University, Durham NC; United States of America
[50] SUPA — School of Physics and Astronomy, University of Edinburgh, Edinburgh; United Kingdom
[51] INFN e Laboratori Nazionali di Frascati, Frascati; Italy
[52] Physikalisches Institut, Albert-Ludwigs-Universität Freiburg, Freiburg; Germany
[53] II. Physikalisches Institut, Georg-August-Universität Göttingen, Göttingen; Germany
[54] Département de Physique Nucléaire et Corpusculaire, Université de Genève, Genève; Switzerland
[55] [(a)] Dipartimento di Fisica, Università di Genova, Genova; [(b)] INFN Sezione di Genova; Italy
[56] II. Physikalisches Institut, Justus-Liebig-Universität Giessen, Giessen; Germany
[57] SUPA — School of Physics and Astronomy, University of Glasgow, Glasgow; United Kingdom
[58] LPSC, Université Grenoble Alpes, CNRS/IN2P3, Grenoble INP, Grenoble; France
[59] Laboratory for Particle Physics and Cosmology, Harvard University, Cambridge MA; United States of America
[60] [(a)] Department of Modern Physics and State Key Laboratory of Particle Detection and Electronics, University of Science and Technology of China, Hefei; [(b)] Institute of Frontier and Interdisciplinary Science and Key Laboratory of Particle Physics and Particle Irradiation (MOE), Shandong University, Qingdao; [(c)] School of Physics and Astronomy, Shanghai Jiao Tong University, KLPPAC-MoE, SKLPPC, Shanghai; [(d)] Tsung-Dao Lee Institute, Shanghai; China
[61] [(a)] Kirchhoff-Institut für Physik, Ruprecht-Karls-Universität Heidelberg, Heidelberg; [(b)] Physikalisches Institut, Ruprecht-Karls-Universität Heidelberg, Heidelberg; Germany
[62] Faculty of Applied Information Science, Hiroshima Institute of Technology, Hiroshima; Japan
[63] [(a)] Department of Physics, Chinese University of Hong Kong, Shatin, N.T., Hong Kong; [(b)] Department of Physics, University of Hong Kong, Hong Kong; [(c)] Department of Physics and Institute for Advanced Study, Hong Kong University of Science and Technology, Clear Water Bay, Kowloon, Hong Kong; China
[64] Department of Physics, National Tsing Hua University, Hsinchu; Taiwan
[65] Department of Physics, Indiana University, Bloomington IN; United States of America
[66] [(a)] INFN Gruppo Collegato di Udine, Sezione di Trieste, Udine; [(b)] ICTP, Trieste; [(c)] Dipartimento Politecnico di Ingegneria e Architettura, Università di Udine, Udine; Italy
[67] [(a)] INFN Sezione di Lecce; [(b)] Dipartimento di Matematica e Fisica, Università del Salento, Lecce; Italy
[68] [(a)] INFN Sezione di Milano; [(b)] Dipartimento di Fisica, Università di Milano, Milano; Italy
[69] [(a)] INFN Sezione di Napoli; [(b)] Dipartimento di Fisica, Università di Napoli, Napoli; Italy
[70] [(a)] INFN Sezione di Pavia; [(b)] Dipartimento di Fisica, Università di Pavia, Pavia; Italy
[71] [(a)] INFN Sezione di Pisa; [(b)] Dipartimento di Fisica E. Fermi, Università di Pisa, Pisa; Italy
[72] [(a)] INFN Sezione di Roma; [(b)] Dipartimento di Fisica, Sapienza Università di Roma, Roma; Italy
[73] [(a)] INFN Sezione di Roma Tor Vergata; [(b)] Dipartimento di Fisica, Università di Roma Tor Vergata, Roma; Italy
[74] [(a)] INFN Sezione di Roma Tre; [(b)] Dipartimento di Matematica e Fisica, Università Roma Tre, Roma; Italy
[75] [(a)] INFN-TIFPA; [(b)] Università degli Studi di Trento, Trento; Italy
[76] Institut für Astro- und Teilchenphysik, Leopold-Franzens-Universität, Innsbruck; Austria
[77] University of Iowa, Iowa City IA; United States of America
[78] Department of Physics and Astronomy, Iowa State University, Ames IA; United States of America
[79] Joint Institute for Nuclear Research, Dubna; Russia
[80] [(a)] Departamento de Engenharia Elétrica, Universidade Federal de Juiz de Fora (UFJF), Juiz de Fora; [(b)] Universidade Federal do Rio De Janeiro COPPE/EE/IF, Rio de Janeiro; [(c)] Universidade Federal de São João del Rei (UFSJ), São João del Rei; [(d)] Instituto de Física, Universidade de São

JHEP12(2019)060

Paulo, São Paulo; Brazil
[81] *KEK, High Energy Accelerator Research Organization, Tsukuba; Japan*
[82] *Graduate School of Science, Kobe University, Kobe; Japan*
[83] [(a)] *AGH University of Science and Technology, Faculty of Physics and Applied Computer Science, Krakow;*[(b)] *Marian Smoluchowski Institute of Physics, Jagiellonian University, Krakow; Poland*
[84] *Institute of Nuclear Physics Polish Academy of Sciences, Krakow; Poland*
[85] *Faculty of Science, Kyoto University, Kyoto; Japan*
[86] *Kyoto University of Education, Kyoto; Japan*
[87] *Research Center for Advanced Particle Physics and Department of Physics, Kyushu University, Fukuoka; Japan*
[88] *Instituto de Física La Plata, Universidad Nacional de La Plata and CONICET, La Plata; Argentina*
[89] *Physics Department, Lancaster University, Lancaster; United Kingdom*
[90] *Oliver Lodge Laboratory, University of Liverpool, Liverpool; United Kingdom*
[91] *Department of Experimental Particle Physics, Jožef Stefan Institute and Department of Physics, University of Ljubljana, Ljubljana; Slovenia*
[92] *School of Physics and Astronomy, Queen Mary University of London, London; United Kingdom*
[93] *Department of Physics, Royal Holloway University of London, Egham; United Kingdom*
[94] *Department of Physics and Astronomy, University College London, London; United Kingdom*
[95] *Louisiana Tech University, Ruston LA; United States of America*
[96] *Fysiska institutionen, Lunds universitet, Lund; Sweden*
[97] *Centre de Calcul de l'Institut National de Physique Nucléaire et de Physique des Particules (IN2P3), Villeurbanne; France*
[98] *Departamento de Física Teorica C-15 and CIAFF, Universidad Autónoma de Madrid, Madrid; Spain*
[99] *Institut für Physik, Universität Mainz, Mainz; Germany*
[100] *School of Physics and Astronomy, University of Manchester, Manchester; United Kingdom*
[101] *CPPM, Aix-Marseille Université, CNRS/IN2P3, Marseille; France*
[102] *Department of Physics, University of Massachusetts, Amherst MA; United States of America*
[103] *Department of Physics, McGill University, Montreal QC; Canada*
[104] *School of Physics, University of Melbourne, Victoria; Australia*
[105] *Department of Physics, University of Michigan, Ann Arbor MI; United States of America*
[106] *Department of Physics and Astronomy, Michigan State University, East Lansing MI; United States of America*
[107] *B.I. Stepanov Institute of Physics, National Academy of Sciences of Belarus, Minsk; Belarus*
[108] *Research Institute for Nuclear Problems of Byelorussian State University, Minsk; Belarus*
[109] *Group of Particle Physics, University of Montreal, Montreal QC; Canada*
[110] *P.N. Lebedev Physical Institute of the Russian Academy of Sciences, Moscow; Russia*
[111] *Institute for Theoretical and Experimental Physics of the National Research Centre Kurchatov Institute, Moscow; Russia*
[112] *National Research Nuclear University MEPhI, Moscow; Russia*
[113] *D.V. Skobeltsyn Institute of Nuclear Physics, M.V. Lomonosov Moscow State University, Moscow; Russia*
[114] *Fakultät für Physik, Ludwig-Maximilians-Universität München, München; Germany*
[115] *Max-Planck-Institut für Physik (Werner-Heisenberg-Institut), München; Germany*
[116] *Nagasaki Institute of Applied Science, Nagasaki; Japan*
[117] *Graduate School of Science and Kobayashi-Maskawa Institute, Nagoya University, Nagoya; Japan*
[118] *Department of Physics and Astronomy, University of New Mexico, Albuquerque NM; United States of America*
[119] *Institute for Mathematics, Astrophysics and Particle Physics, Radboud University Nijmegen/Nikhef, Nijmegen; Netherlands*
[120] *Nikhef National Institute for Subatomic Physics and University of Amsterdam, Amsterdam; Netherlands*

JHEP12(2019)060

[121] Department of Physics, Northern Illinois University, DeKalb IL; United States of America
[122] [(a)] Budker Institute of Nuclear Physics and NSU, SB RAS, Novosibirsk;[(b)] Novosibirsk State University Novosibirsk; Russia
[123] Institute for High Energy Physics of the National Research Centre Kurchatov Institute, Protvino; Russia
[124] Department of Physics, New York University, New York NY; United States of America
[125] Ochanomizu University, Otsuka, Bunkyo-ku, Tokyo; Japan
[126] Ohio State University, Columbus OH; United States of America
[127] Faculty of Science, Okayama University, Okayama; Japan
[128] Homer L. Dodge Department of Physics and Astronomy, University of Oklahoma, Norman OK; United States of America
[129] Department of Physics, Oklahoma State University, Stillwater OK; United States of America
[130] Palacký University, RCPTM, Joint Laboratory of Optics, Olomouc; Czech Republic
[131] Center for High Energy Physics, University of Oregon, Eugene OR; United States of America
[132] LAL, Université Paris-Sud, CNRS/IN2P3, Université Paris-Saclay, Orsay; France
[133] Graduate School of Science, Osaka University, Osaka; Japan
[134] Department of Physics, University of Oslo, Oslo; Norway
[135] Department of Physics, Oxford University, Oxford; United Kingdom
[136] LPNHE, Sorbonne Université, Université de Paris, CNRS/IN2P3, Paris; France
[137] Department of Physics, University of Pennsylvania, Philadelphia PA; United States of America
[138] Konstantinov Nuclear Physics Institute of National Research Centre "Kurchatov Institute", PNPI, St. Petersburg; Russia
[139] Department of Physics and Astronomy, University of Pittsburgh, Pittsburgh PA; United States of America
[140] [(a)] Laboratório de Instrumentação e Física Experimental de Partículas — LIP, Lisboa;[(b)] Departamento de Física, Faculdade de Ciências, Universidade de Lisboa, Lisboa;[(c)] Departamento de Física, Universidade de Coimbra, Coimbra;[(d)] Centro de Física Nuclear da Universidade de Lisboa, Lisboa;[(e)] Departamento de Física, Universidade do Minho, Braga;[(f)] Universidad de Granada, Granada (Spain);[(g)] Dep Física and CEFITEC of Faculdade de Ciências e Tecnologia, Universidade Nova de Lisboa, Caparica;[(h)] Instituto Superior Técnico, Universidade de Lisboa, Lisboa; Portugal
[141] Institute of Physics of the Czech Academy of Sciences, Prague; Czech Republic
[142] Czech Technical University in Prague, Prague; Czech Republic
[143] Charles University, Faculty of Mathematics and Physics, Prague; Czech Republic
[144] Particle Physics Department, Rutherford Appleton Laboratory, Didcot; United Kingdom
[145] IRFU, CEA, Université Paris-Saclay, Gif-sur-Yvette; France
[146] Santa Cruz Institute for Particle Physics, University of California Santa Cruz, Santa Cruz CA; United States of America
[147] [(a)] Departamento de Física, Pontificia Universidad Católica de Chile, Santiago;[(b)] Universidad Andres Bello, Department of Physics, Santiago;[(c)] Departamento de Física, Universidad Técnica Federico Santa María, Valparaíso; Chile
[148] Department of Physics, University of Washington, Seattle WA; United States of America
[149] Department of Physics and Astronomy, University of Sheffield, Sheffield; United Kingdom
[150] Department of Physics, Shinshu University, Nagano; Japan
[151] Department Physik, Universität Siegen, Siegen; Germany
[152] Department of Physics, Simon Fraser University, Burnaby BC; Canada
[153] SLAC National Accelerator Laboratory, Stanford CA; United States of America
[154] Physics Department, Royal Institute of Technology, Stockholm; Sweden
[155] Departments of Physics and Astronomy, Stony Brook University, Stony Brook NY; United States of America
[156] Department of Physics and Astronomy, University of Sussex, Brighton; United Kingdom
[157] School of Physics, University of Sydney, Sydney; Australia

JHEP12(2019)060

[158] Institute of Physics, Academia Sinica, Taipei; Taiwan
[159] [(a)] E. Andronikashvili Institute of Physics, Iv. Javakhishvili Tbilisi State University, Tbilisi;[(b)] High Energy Physics Institute, Tbilisi State University, Tbilisi; Georgia
[160] Department of Physics, Technion, Israel Institute of Technology, Haifa; Israel
[161] Raymond and Beverly Sackler School of Physics and Astronomy, Tel Aviv University, Tel Aviv; Israel
[162] Department of Physics, Aristotle University of Thessaloniki, Thessaloniki; Greece
[163] International Center for Elementary Particle Physics and Department of Physics, University of Tokyo, Tokyo; Japan
[164] Graduate School of Science and Technology, Tokyo Metropolitan University, Tokyo; Japan
[165] Department of Physics, Tokyo Institute of Technology, Tokyo; Japan
[166] Tomsk State University, Tomsk; Russia
[167] Department of Physics, University of Toronto, Toronto ON; Canada
[168] [(a)] TRIUMF, Vancouver BC;[(b)] Department of Physics and Astronomy, York University, Toronto ON; Canada
[169] Division of Physics and Tomonaga Center for the History of the Universe, Faculty of Pure and Applied Sciences, University of Tsukuba, Tsukuba; Japan
[170] Department of Physics and Astronomy, Tufts University, Medford MA; United States of America
[171] Department of Physics and Astronomy, University of California Irvine, Irvine CA; United States of America
[172] Department of Physics and Astronomy, University of Uppsala, Uppsala; Sweden
[173] Department of Physics, University of Illinois, Urbana IL; United States of America
[174] Instituto de Física Corpuscular (IFIC), Centro Mixto Universidad de Valencia — CSIC, Valencia; Spain
[175] Department of Physics, University of British Columbia, Vancouver BC; Canada
[176] Department of Physics and Astronomy, University of Victoria, Victoria BC; Canada
[177] Fakultät für Physik und Astronomie, Julius-Maximilians-Universität Würzburg, Würzburg; Germany
[178] Department of Physics, University of Warwick, Coventry; United Kingdom
[179] Waseda University, Tokyo; Japan
[180] Department of Particle Physics, Weizmann Institute of Science, Rehovot; Israel
[181] Department of Physics, University of Wisconsin, Madison WI; United States of America
[182] Fakultät für Mathematik und Naturwissenschaften, Fachgruppe Physik, Bergische Universität Wuppertal, Wuppertal; Germany
[183] Department of Physics, Yale University, New Haven CT; United States of America
[184] Yerevan Physics Institute, Yerevan; Armenia

[a] Also at Borough of Manhattan Community College, City University of New York, New York NY; United States of America
[b] Also at CERN, Geneva; Switzerland
[c] Also at CPPM, Aix-Marseille Université, CNRS/IN2P3, Marseille; France
[d] Also at Département de Physique Nucléaire et Corpusculaire, Université de Genève, Genève; Switzerland
[e] Also at Departament de Fisica de la Universitat Autonoma de Barcelona, Barcelona; Spain
[f] Also at Departamento de Física, Instituto Superior Técnico, Universidade de Lisboa, Lisboa; Portugal
[g] Also at Department of Applied Physics and Astronomy, University of Sharjah, Sharjah; United Arab Emirates
[h] Also at Department of Financial and Management Engineering, University of the Aegean, Chios; Greece
[i] Also at Department of Physics and Astronomy, Michigan State University, East Lansing MI; United States of America

JHEP12(2019)060

[j] Also at Department of Physics and Astronomy, University of Louisville, Louisville, KY; United States of America
[k] Also at Department of Physics and Astronomy, University of Sheffield, Sheffield; United Kingdom
[l] Also at Department of Physics, Ben Gurion University of the Negev, Beer Sheva; Israel
[m] Also at Department of Physics, California State University, East Bay; United States of America
[n] Also at Department of Physics, California State University, Fresno; United States of America
[o] Also at Department of Physics, California State University, Sacramento; United States of America
[p] Also at Department of Physics, King's College London, London; United Kingdom
[q] Also at Department of Physics, St. Petersburg State Polytechnical University, St. Petersburg; Russia
[r] Also at Department of Physics, Stanford University, Stanford CA; United States of America
[s] Also at Department of Physics, University of Adelaide, Adelaide; Australia
[t] Also at Department of Physics, University of Fribourg, Fribourg; Switzerland
[u] Also at Department of Physics, University of Michigan, Ann Arbor MI; United States of America
[v] Also at Dipartimento di Matematica, Informatica e Fisica, Università di Udine, Udine; Italy
[w] Also at Faculty of Physics, M.V. Lomonosov Moscow State University, Moscow; Russia
[x] Also at Giresun University, Faculty of Engineering, Giresun; Turkey
[y] Also at Graduate School of Science, Osaka University, Osaka; Japan
[z] Also at Hellenic Open University, Patras; Greece
[aa] Also at Institucio Catalana de Recerca i Estudis Avancats, ICREA, Barcelona; Spain
[ab] Also at Institut für Experimentalphysik, Universität Hamburg, Hamburg; Germany
[ac] Also at Institute for Mathematics, Astrophysics and Particle Physics, Radboud University Nijmegen/Nikhef, Nijmegen; Netherlands
[ad] Also at Institute for Nuclear Research and Nuclear Energy (INRNE) of the Bulgarian Academy of Sciences, Sofia; Bulgaria
[ae] Also at Institute for Particle and Nuclear Physics, Wigner Research Centre for Physics, Budapest; Hungary
[af] Also at Institute of High Energy Physics, Chinese Academy of Sciences, Beijing; China
[ag] Also at Institute of Particle Physics (IPP), Vancouver; Canada
[ah] Also at Institute of Physics, Academia Sinica, Taipei; Taiwan
[ai] Also at Institute of Physics, Azerbaijan Academy of Sciences, Baku; Azerbaijan
[aj] Also at Institute of Theoretical Physics, Ilia State University, Tbilisi; Georgia
[ak] Also at Instituto de Fisica Teorica, IFT-UAM/CSIC, Madrid; Spain
[al] Also at Istanbul University, Dept. of Physics, Istanbul; Turkey
[am] Also at Joint Institute for Nuclear Research, Dubna; Russia
[an] Also at LAL, Université Paris-Sud, CNRS/IN2P3, Université Paris-Saclay, Orsay; France
[ao] Also at Louisiana Tech University, Ruston LA; United States of America
[ap] Also at LPNHE, Sorbonne Université, Université de Paris, CNRS/IN2P3, Paris; France
[aq] Also at Manhattan College, New York NY; United States of America
[ar] Also at Moscow Institute of Physics and Technology State University, Dolgoprudny; Russia
[as] Also at National Research Nuclear University MEPhI, Moscow; Russia
[at] Also at Physics Department, An-Najah National University, Nablus; Palestine
[au] Also at Physics Dept, University of South Africa, Pretoria; South Africa
[av] Also at Physikalisches Institut, Albert-Ludwigs-Universität Freiburg, Freiburg; Germany
[aw] Also at School of Physics, Sun Yat-sen University, Guangzhou; China
[ax] Also at The City College of New York, New York NY; United States of America
[ay] Also at The Collaborative Innovation Center of Quantum Matter (CICQM), Beijing; China
[az] Also at Tomsk State University, Tomsk, and Moscow Institute of Physics and Technology State University, Dolgoprudny; Russia
[ba] Also at TRIUMF, Vancouver BC; Canada
[bb] Also at Universita di Napoli Parthenope, Napoli; Italy * Deceased

JHEP12(2019)060